LA-UR-21-28167

Approved for public release; distribution is unlimited.

Title:	Proof that Combining the Forced-collision and DXTRAN Monte Carlo Variance-reduction Techniques is Fair
Author(s):	Pearson, Eric John Kulesza, Joel A.
Intended for:	Report
Issued:	2021-08-16

Proof that Combining the Forced-collision and DXTRAN Monte Carlo Variance-reduction Techniques is Fair

Eric J. Pearson and Joel A. Kulesza

August 12, 2021

1 Introduction and Background

This report provides mathematical proof that the MCNP DXTRAN (also known in other codes as forced-flight [1]) and forced-collision variance-reduction techniques [2] do not bias the expected value of Monte Carlo simulation estimates when combined. Proof is also provided that the techniques are unbiased when used independently. To prove that the techniques are unbiased, this report derives the first History Score Moment Equation (HSME) for non-multiplying media employing only forced collisions, only DXTRAN, and then both the variance-reduction techniques combined, as defined next. The HSMEs are found by forming the History Score Probability Density Functions (HSPDFs) and then taking the first score moment. Following its derivation, each HSME with a variance-reduction technique employed is reduced to the HSME for an analog simulation. Because the HSME represents the expected contribution to estimators in the simulation, reducing the HSME with variance reduction to the analog HSME shows that the simulation is unbiased despite the variance-reduction technique considered in the HSME. Analysis regarding higher-score moments of each technique is the subject of prior work [3–6] and is not addressed herein.

Throughout this work, the phase space $\boldsymbol{p}$ is defined to be the particle position $\boldsymbol{x}$, direction-of-flight unit vector $\hat{\boldsymbol{\Omega}}$, energy E, and statistical weight w,

$$\boldsymbol{p} \equiv (\boldsymbol{x}, \hat{\boldsymbol{\Omega}}, E, w). \tag{1}$$

A reduced phase-space excluding the statistical weight of the particle,

$$\boldsymbol{r} \equiv (\boldsymbol{x}, \hat{\boldsymbol{\Omega}}, E), \tag{2}$$

is also used.

1.1 Forced-Collision Technique

For simplicity, the forced-collision technique is defined here not in combination with either the weight-cutoff or weight-window technique. This definition corresponds to a negative entry on the forced-collision card in the MCNP® code [2, Sec. 2.7.B.9]. In this case, transport is only modified when a particle enters a cell with forced collisions specified in it. Upon entering a cell with the technique in play at position $\boldsymbol{x}$ with energy E, a portion of the statistical weight of the particle w_0 is transmitted along the direction of the particle $\hat{\boldsymbol{\Omega}}$ to the surface across the cell and the remainder of the statistical weight of the particle is forced to undergo a collision in the cell at some point along the streaming path. The position of the forced collision is sampled from a truncated exponential distribution as given in Eq. 191. This splits the computational particle into two separate particles. A representative image of a particle undergoing the forced-collision technique is given in Fig. 1.

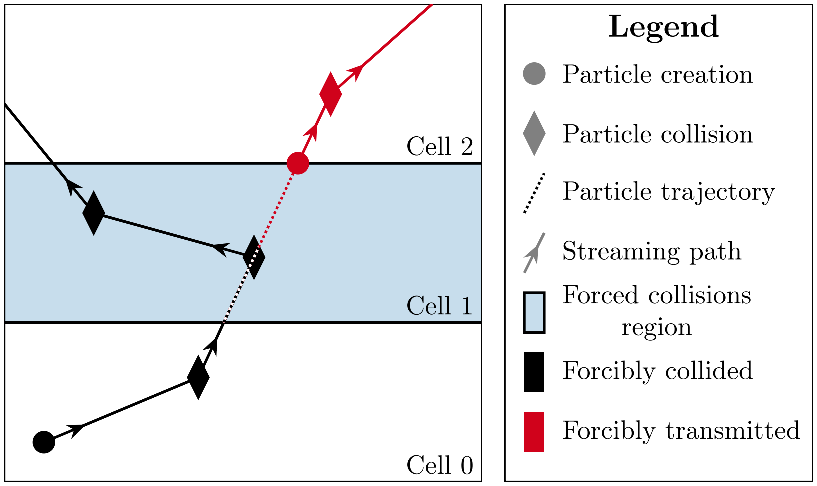

Figure 1: Representative portion of a history in which the forced-collision variance-reduction technique is applied. Different colors distinguish parts of the history following intervention from forced collisions.

The weight of the transmitted particle is given as the product of the weight of the incident particle and the probability of free flight through the cell,

$$w_t = w_0 \exp\Big(-\ell(\boldsymbol{x}, \boldsymbol{x}_S(\boldsymbol{x}, \hat{\boldsymbol{\Omega}}))\Big), \tag{3}$$

where $\boldsymbol{x}_S(\boldsymbol{x}, \hat{\boldsymbol{\Omega}})$ is the first point of intersection between the ray from $\boldsymbol{x}$ along $\hat{\boldsymbol{\Omega}}$ and a surface bounding the current cell and $\ell(\boldsymbol{x}, \boldsymbol{x}_S)$ is the optical thickness between positions $\boldsymbol{x}$ and $\boldsymbol{x}_S$ defined as

$$\ell(\boldsymbol{x}, \boldsymbol{x}') \equiv \int_0^{\|\boldsymbol{x}'-\boldsymbol{x}\|} \Sigma_t\left(\boldsymbol{x} + a\frac{\boldsymbol{x}'-\boldsymbol{x}}{\|\boldsymbol{x}'-\boldsymbol{x}\|}\right) da. \tag{4}$$

The weight of the collided particle is the remainder,

$$w_c = w_0 - w_t. \tag{5}$$

Following transmission or collision, both particles are transported without modification as a result of forced collisions until they enter another cell with forced collisions specified, which may be immediate in the case of the transmitted particle. This technique may be interpreted as cleaving a computational particle into a particle that next undergoes a collision in the current cell and a particle that does not and simulating both.

1.2 DXTRAN Technique

Again for simplicity, the DXTRAN technique is defined here for a single spherical DXTRAN region without preference to any portion of that region, identical to the definition given in Ref. [2, Sec. 2.7.B.12] with one radius specified. Additionally, the technique is defined without any auxiliary techniques, such as those specified in Ref. [2, Sec. 2.7.B.12.7], in play. In this case, following the construction of a particle from the source or the emergence of a particle from a collision at any position outside the DXTRAN region, traveling in any direction $\hat{\boldsymbol{\Omega}}$, and at any energy E, a DXTRAN particle is created on the surface of the DXTRAN region[1] and non-DXTRAN particles are killed if they attempt to enter a DXTRAN region. A representation of a particle that undergoes the DXTRAN technique is given in Fig. 2.

The weight of the inciting particle w_0 is unmodified and the weight of the DXTRAN particle is given as the product of the inciting particle weight, the ratio of the analog to biased probability of exiting the inciting

[1] Care must be taken to not create DXTRAN particles from streaming paths that intersect regions of zero importance when combining DXTRAN with cell-based importance splitting and Russian-roulette variance-reduction techniques.

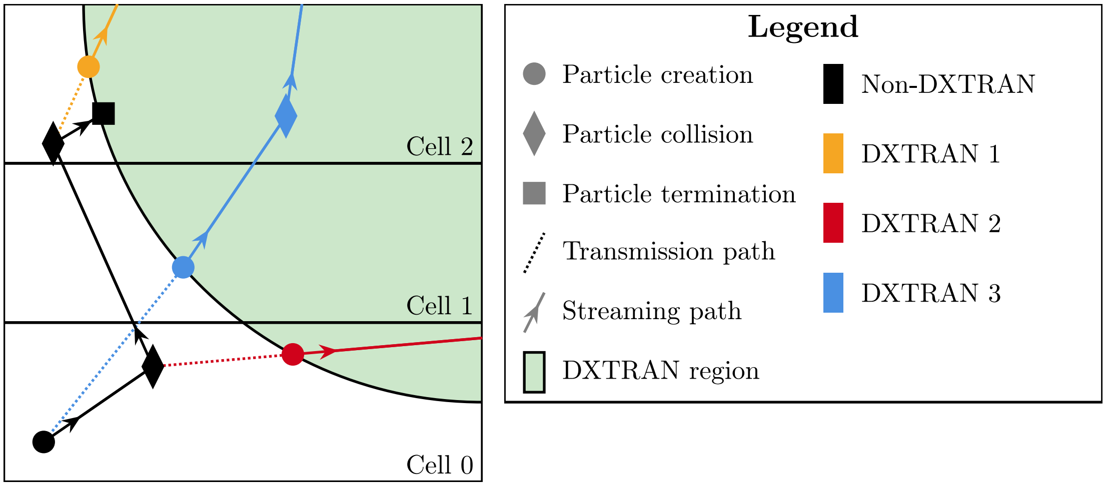

Figure 2: Representative portion of a history in which the DXTRAN variance-reduction technique is applied. Different colors distinguish parts of the history following intervention from the DXTRAN technique.

event directed towards the DXTRAN region, and the probability of free flight from the inciting event to the DXTRAN region,

$$w_{DX} = w_0 \frac{f(\boldsymbol{x}, \hat{\boldsymbol{\Omega}} \to \hat{\boldsymbol{\Omega}}', E \to E')}{f_{DX}(\boldsymbol{x}, \hat{\boldsymbol{\Omega}} \to \hat{\boldsymbol{\Omega}}', E \to E')} \exp\Big(-\ell(\boldsymbol{x}, \boldsymbol{x}_{DX}(\boldsymbol{x}, \hat{\boldsymbol{\Omega}}'))\Big), \tag{6}$$

where $f(\boldsymbol{x}, \hat{\boldsymbol{\Omega}} \to \hat{\boldsymbol{\Omega}}', E \to E')$ is the analog probability density function (PDF) governing the outgoing angle and energy of the inciting event, $f_{DX}(\boldsymbol{x}, \hat{\boldsymbol{\Omega}} \to \hat{\boldsymbol{\Omega}}', E \to E')$ is the biased PDF governing the outgoing angle and energy of the inciting event that only considers outgoing angles directed towards the DXTRAN region, $\boldsymbol{x}_{DX}(\boldsymbol{x}, \hat{\boldsymbol{\Omega}}')$ is the position on the surface of the DXTRAN region that the ray traveling towards the DXTRAN region from $\boldsymbol{x}$ along $\hat{\boldsymbol{\Omega}}'$ first intersects, and $\ell(\boldsymbol{x}, \boldsymbol{x}_{DX}(\boldsymbol{x}, \hat{\boldsymbol{\Omega}}'))$ is the optical thickness between the inciting event and the intersection of the biased outgoing angle and the DXTRAN region defined in Eq. 4. To conserve statistical weight, non-DXTRAN particles are terminated if they reach the DXTRAN region during normal transport. This technique may be interpreted as cleaving the computational particle into a particle that next enters the DXTRAN region and a particle that does not and simulating both.

1.3 Combined Forced-Collision and DXTRAN Techniques

When both forced-collision and DXTRAN variance-reduction techniques are specified for the same simulation, they may interact in different ways depending on where the DXTRAN region is placed and which cells have forced collisions specified. If all cells with forced collisions specified are located entirely outside of the DXTRAN region, the techniques combine in a straightforward way. As described in Sec. 1.2, following particle construction from a source or a collision, forced or otherwise, a DXTRAN particle is created on the DXTRAN surface and any non-DXTRAN particle, forcibly transmitted or otherwise, that attempts to enter the DXTRAN region is killed. The only interactions between the techniques in this case is the creation of DXTRAN particles due to forced collisions. Similarly, if all cells with forced collisions specified are located entirely inside the DXTRAN region, the techniques do not influence each other at all as the DXTRAN technique does not alter transport inside the DXTRAN region and the forced-collision technique does not alter transport outside of cells where it is specified.

The more complicated case to consider when combining techniques is that in which forced collisions are specified for a cell that contains a portion or the entirety of the DXTRAN region. Behavior in such a cell may be further subdivided into two subcases. If the direction of the particle that is to undergo a forced collision is directed away from the portion of the DXTRAN region within the cell, then behavior is identical to the

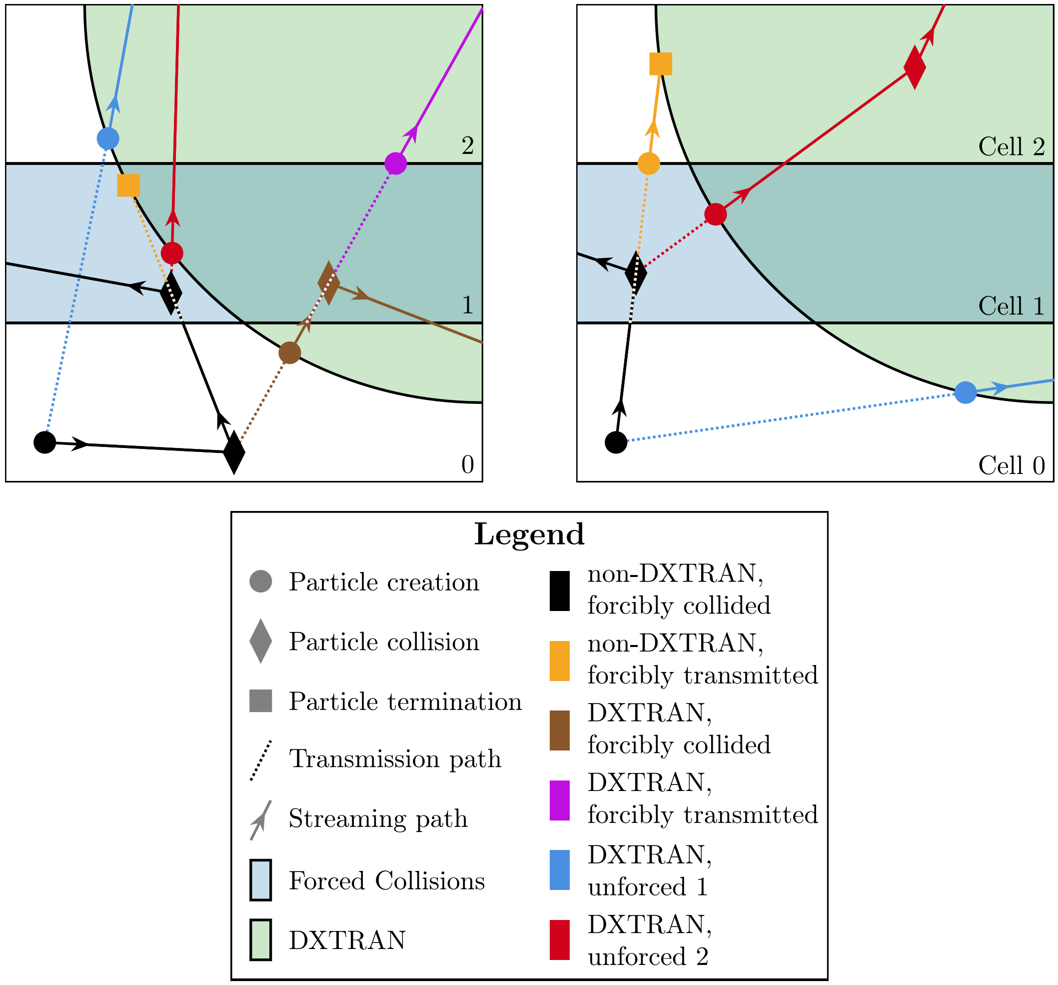

Figure 3: Representative portions of two histories in which the forced-collision and DXTRAN variance-reduction techniques are applied together. Different colors distinguish parts of the history following intervention from the variance-reduction techniques.

case of the cell with forced collisions specified being entirely outside of the DXTRAN region. If the particle is traveling towards the DXTRAN region, a collision is forced in the cell along the streaming path before the DXTRAN region is intersected and the transmitted particle is killed. In this case $\boldsymbol{x}_{DX}(\boldsymbol{x}, \hat{\boldsymbol{\Omega}})$ is used in Eq. 3 rather than $\boldsymbol{x}_S(\boldsymbol{x}, \hat{\boldsymbol{\Omega}})$. The behavior of DXTRAN particles created on the DXTRAN region within a cell with forced collisions specified must also be considered. Because forced collisions are assumed to be defined without further forced-collision influence after entering the cell, these particles do not undergo forced collisions, i.e., they are treated the same as particles that have already undergone a forced collision in the current cell. A representation of two particles that under go both the forced-collision and DXTRAN variance reduction techniques is given in Fig. 3. Note that this is likely not the only valid combination of techniques, but is analyzed here because it corresponds to the behavior of the MCNP code.

1.4 Definitions

This proof builds upon prior work on the History Score Moment Equations (HSMEs) for both the first and second score moments derived for simulations with either DXTRAN [5] or forced-collision [6] variance-reduction techniques employed. In prior work, both the HSMEs were derived to compute the variance;

however, only the first moment is needed to demonstrate a fair technique. Unfortunately, prior work employs conflicting notation. Here, the following notation[2] is used:

$\mathcal{T}(\boldsymbol{p},\boldsymbol{p}')$, the *free-flight transmission operator* governing the probability of free flight from phase space $\boldsymbol{p}$ to $\boldsymbol{p}'$;

$\mathcal{S}(\boldsymbol{p},\boldsymbol{p}')$, the *surface-crossing operator* governing the probability of crossing a surface at phase space $\boldsymbol{p}$ and emerging in $\boldsymbol{p}'$;

$\mathcal{K}_A(\boldsymbol{p},\boldsymbol{p}')$, the *absorptive collision operator* governing the probability of undergoing an absorptive collision at phase space $\boldsymbol{p}$ and emerging in $\boldsymbol{p}'$;

$\mathcal{K}_E(\boldsymbol{p},\boldsymbol{p}')$, the *emissive collision operator* governing the probability of undergoing an emissive collision at phase space $\boldsymbol{p}$ and emerging in $\boldsymbol{p}'$;

$\mathcal{B}_c(\boldsymbol{p},\boldsymbol{p}')$, the *flight-to-collision operator* governing the probability of forcing particle weight from phase space $\boldsymbol{p}$ to a collision at space space $\boldsymbol{p}'$;

$\mathcal{B}_t(\boldsymbol{p},\boldsymbol{p}')$, the *flight-to-transmission operator* governing the probability of forcing particle weight from phase space $\boldsymbol{p}$ to a surface crossing at space space $\boldsymbol{p}'$;

$\mathcal{B}_{DX}(\boldsymbol{p},\boldsymbol{p}')$, the *flight-to-DXTRAN operator* governing the probability of creating particle weight on the DXTRAN region at phase space $\boldsymbol{p}'$ from phase space $\boldsymbol{p}$;

$\mathcal{T}_{DX}(\boldsymbol{p},\boldsymbol{p}')$, the *DXTRAN free-flight transmission operator* governing the probability of free flight from phase space $\boldsymbol{p}$ to $\boldsymbol{p}'$ while disallowing flight into a DXTRAN region;

$f_e(\boldsymbol{p},s)$, the *scoring probability density function* governing the probability of contributing score s to the total score of the history due to operation e at phase space $\boldsymbol{p}$.

For formal definitions of the operators introduced above, see Appendix A. The presence of the scoring PDF implies the existence of an estimator for an event at a given phase space. To present the most complete proof of unbiased first-moment estimates, it is assumed that all possible estimators exist in the simulation. As a result the scoring PDF is included for all collision and surface-crossing events at all phase spaces.

2 Derivation of the History Score Probability Density Function

First, the analog HSPDF is derived in the same manor as Ref. [5] both to demonstrate the derivation procedure on a simple case and to present the analog HSPDF for later use. Then the HSPDFs with forced-collision, DXTRAN, and both variance-reduction techniques together are derived.

2.1 Analog Transport

The analog HSPDF is found as the sum of the partial HSPDFs governing each of the disjoint random-walk steps a computational particle may take. Intuitively, a particle undergoing analog simulation in non-multiplying media can either travel to a collision, collide, score an absorptive collision tally, and be absorbed as described by the partial HSPDF for absorptive collisions

$$\psi_0^A(\boldsymbol{p},s)=\mathcal{T}(\boldsymbol{p},\boldsymbol{p}_1)\mathcal{K}_A(\boldsymbol{p}_1,\boldsymbol{p}_2)\int f_A(\boldsymbol{p}_1,s_A)\delta(s-s_A)ds_A; \tag{7}$$

travel to a collision, collide, score an emissive collision tally, scatter, and continue on in the simulation as described by the partial HSPDF for emissive collisions

$$\psi_0^E(\boldsymbol{p},s)=\mathcal{T}(\boldsymbol{p},\boldsymbol{p}_1)\mathcal{K}_E(\boldsymbol{p}_1,\boldsymbol{p}_3)\int f_E(\boldsymbol{p}_1,s_E)\psi_0(\boldsymbol{p}_3,s-s_E)ds_E; \tag{8}$$

[2] Note that $\mathcal{B}$ is chosen to denote the biasing of particle transport from variance-reduction techniques.

or travel to the boundary of the current cell, cross the surface, score a surface-crossing tally, and continue on in the simulation as described by the partial HSPDF for surface crossings

$$\psi_0^S(\boldsymbol{p}, s) = \mathcal{T}(\boldsymbol{p}, \boldsymbol{p}_4)\mathcal{S}(\boldsymbol{p}_4, \boldsymbol{p}_5) \int f_S(\boldsymbol{p}_4, s_S)\psi_0(\boldsymbol{p}_5, s - s_S)ds_S. \tag{9}$$

A subscript of 0 is added to the partial HSPDFs to denote that no variance-reduction technique is applied. Note that in Eq. 7 the history is terminated by the absorption so the probability of the history contributing a total score of s depends on the absorption contributing that score, as enforced by the Dirac delta $\delta(s - s_A)$. In contrast, the history is not immediately terminated in both Eq. 8 and 9, so the probability of the total score of s depends on the particle continuing on and contributing the portion of s remaining following what is contributed by the emissive collision or surface crossing as given by the analog HSPDF evaluated at the resulting phase space and remaining score, $\psi_0(\boldsymbol{p}_3, s - s_E)$ and $\psi_0(\boldsymbol{p}_5, s - s_S)$ respectively. The analog HSPDF is then the sum of each partial HSPDFs,

$$\psi_0(\boldsymbol{p}, s)ds = \psi_0^A(\boldsymbol{p}, s)ds + \psi_0^E(\boldsymbol{p}, s)ds + \psi_0^S(\boldsymbol{p}, s)ds \tag{10}$$

or explicitly,

$$\begin{aligned}\psi_0(\boldsymbol{p}, s) = &\mathcal{T}(\boldsymbol{p}, \boldsymbol{p}_1)\mathcal{K}_A(\boldsymbol{p}_1, \boldsymbol{p}_2) \int f_A(\boldsymbol{p}_1, s_A)\delta(s - s_A)ds_A \\ &+ \mathcal{T}(\boldsymbol{p}, \boldsymbol{p}_1)\mathcal{K}_E(\boldsymbol{p}_1, \boldsymbol{p}_3) \int f_E(\boldsymbol{p}_1, s_E)\psi_0(\boldsymbol{p}_3, s - s_E)ds_E \\ &+ \mathcal{T}(\boldsymbol{p}, \boldsymbol{p}_4)\mathcal{S}(\boldsymbol{p}_4, \boldsymbol{p}_5) \int f_S(\boldsymbol{p}_4, s_S)\psi_0(\boldsymbol{p}_5, s - s_S)ds_S.\end{aligned} \tag{11}$$

Note that ds is divided out between Eqs. 10 and 11 for ease of notation. Multiplying by ds is necessary in Eq. 10 so that probabilities, not probability densities, are being equated. This step will not be commented on in the derivation of other HSPDFs to avoid redundancy.

2.2 Forced-Collision Variance-Reduction Technique

The HSPDF with the forced-collision technique in play is again formed from each of the disjoint random-walk steps a computational particle may take; however, when a forced collision is specified, there are only two possible steps. The computational particle is split in two, one of the resulting particles travels to a collision and collides, and the other travels to the next surface intersecting the streaming path, crosses the surface, scores a surface-crossing tally, and continues on in the simulation. In the first possible step, the forcibly collided particle collides, scores an absorptive collision tally, and is absorbed as described by the partial HSPDF for forced absorptive collisions

$$\begin{aligned}\psi_{FC}^A(\boldsymbol{p}, s) = &\mathcal{B}_c(\boldsymbol{p}, \boldsymbol{p}_1)\mathcal{K}_A(\boldsymbol{p}_1, \boldsymbol{p}_2) \int f_A(\boldsymbol{p}_1, s_A) \\ &\times \mathcal{B}_t(\boldsymbol{p}, \boldsymbol{p}_4)\mathcal{S}(\boldsymbol{p}_4, \boldsymbol{p}_5) \int f_S(\boldsymbol{p}_4, s_S)\psi_{FC}(\boldsymbol{p}_5, s - s_S - s_A)ds_S ds_A.\end{aligned} \tag{12}$$

In the other possible step, the forcibly collided particle collides, scores an emissive collision tally, scatters, and continues on in the simulation as described by the partial HSPDF for forced emissive collisions

$$\begin{aligned}\psi_{FC}^E(\boldsymbol{p}, s) = &\mathcal{B}_c(\boldsymbol{p}, \boldsymbol{p}_1)\mathcal{K}_E(\boldsymbol{p}_1, \boldsymbol{p}_3) \int f_E(\boldsymbol{p}_1, s_E) \int \psi_{FC}^0(\boldsymbol{p}_3, s_3) \\ &\times \mathcal{B}_t(\boldsymbol{p}, \boldsymbol{p}_4)\mathcal{S}(\boldsymbol{p}_4,\boldsymbol{p}_5) \int f_S(\boldsymbol{p}_4, s_S)\psi_{FC}(\boldsymbol{p}_5, s - s_S - s_3 - s_E)ds_S ds_3 ds_E,\end{aligned} \tag{13}$$

where ψ^0_{FC} is identical to Eq. 11 except that it is recursive with ψ_{FC} to account for the particle traveling to a forced flight region,

$$\begin{aligned}\psi^0_{FC}(\boldsymbol{p},s) &= \mathcal{T}(\boldsymbol{p},\boldsymbol{p}_1)\mathcal{K}_A(\boldsymbol{p}_1,\boldsymbol{p}_2)\int f_A(\boldsymbol{p}_1,s_A)\delta(s-s_A)ds_A \\ &+ \mathcal{T}(\boldsymbol{p},\boldsymbol{p}_1)\mathcal{K}_E(\boldsymbol{p}_1,\boldsymbol{p}_3)\int f_E(\boldsymbol{p}_1,s_E)\psi^0_{FC}(\boldsymbol{p}_3,s-s_E)ds_E \\ &+ \mathcal{T}(\boldsymbol{p},\boldsymbol{p}_4)\mathcal{S}(\boldsymbol{p}_4,\boldsymbol{p}_5)\int f_S(\boldsymbol{p}_4,s_S)\psi_{FC}(\boldsymbol{p}_5,s-s_S)ds_S.\end{aligned} \tag{14}$$

Note that in Eq. 13 and 14, ψ_{FC} is only used recursively following a surface crossing because forced collisions, as defined herein, are only specified upon entering a new cell. The variance-reduction HSPDF in a cell for which forced collisions are specified is then the sum of these partial HSPDFs and follows analog behavior otherwise,

$$\psi_{FC}(\boldsymbol{p},s)ds = \begin{cases}\psi^A_{FC}(\boldsymbol{p},s)ds + \psi^E_{FC}(\boldsymbol{p},s)ds, & \boldsymbol{p}\in\{\boldsymbol{p}_{FC}\}, \\ \psi^0_{FC}(\boldsymbol{p},s)ds, & \text{otherwise},\end{cases} \tag{15}$$

where $\{\boldsymbol{p}_{FC}\}$ is the set of all phase spaces with forced collisions specified. Writing out the case of $\boldsymbol{p}\in\{\boldsymbol{p}_{FC}\}$ explicitly,

$$\begin{aligned}\psi_{FC}(\boldsymbol{p},s) &= \mathcal{B}_c(\boldsymbol{p},\boldsymbol{p}_1)\mathcal{K}_A(\boldsymbol{p}_1,\boldsymbol{p}_2)\int f_A(\boldsymbol{p}_1,s_A)\mathcal{B}_t(\boldsymbol{p},\boldsymbol{p}_4)\mathcal{S}(\boldsymbol{p}_4,\boldsymbol{p}_5)\int f_S(\boldsymbol{p}_4,s_S)\psi_{FC}(\boldsymbol{p}_5,s-s_S-s_A)ds_S ds_A \\ &+ \mathcal{B}_c(\boldsymbol{p},\boldsymbol{p}_1)\mathcal{K}_E(\boldsymbol{p}_1,\boldsymbol{p}_3)\int f_E(\boldsymbol{p}_1,s_E)\int \psi^0_{FC}(\boldsymbol{p}_3,s_3) \\ &\times \mathcal{B}_t(\boldsymbol{p},\boldsymbol{p}_4)\mathcal{S}(\boldsymbol{p}_4,\boldsymbol{p}_5)\int f_S(\boldsymbol{p}_4,s_S)\psi_{FC}(\boldsymbol{p}_5,s-s_S-s_3-s_E)ds_S ds_3 ds_E,\ \boldsymbol{p}\in\{\boldsymbol{p}_{FC}\}.\end{aligned} \tag{16}$$

2.3 DXTRAN Variance-Reduction Technique

The HSPDF with DXTRAN variance reduction in play is similar to the analog HSPDF given in Eq. 10. With DXTRAN in play, absorptive collisions and surface crossings are handled identically to the analog case except that particles continuing after a surface crossing are killed if they attempt to enter the DXTRAN region. This is described using the DXTRAN free-flight transmission operator in the DXTRAN partial HSPDF for absorptive collisions

$$\psi^A_{DX}(\boldsymbol{p},s) = \mathcal{T}_{DX}(\boldsymbol{p},\boldsymbol{p}_1)\mathcal{K}_A(\boldsymbol{p}_1,\boldsymbol{p}_2)\int f_A(\boldsymbol{p}_1,s_A)\delta(s-s_A)ds_A \tag{17}$$

and in the DXTRAN partial HSPDF for surface crossings

$$\psi^S_{DX}(\boldsymbol{p},s) = \mathcal{T}_{DX}(\boldsymbol{p},\boldsymbol{p}_4)\mathcal{S}(\boldsymbol{p}_4,\boldsymbol{p}_5)\int f_S(\boldsymbol{p}_4,s_S)\psi_{DX}(\boldsymbol{p}_5,s-s_S)ds_S. \tag{18}$$

The emissive collision partial HSPDF differs significantly from analog transport when DXTRAN is in play. Following a collision, in addition to the non-DXTRAN particle continuing on without modification, a DXTRAN particle is created on the surface of the DXTRAN region as described by the flight-to-DXTRAN operator in the DXTRAN partial HSPDF for emissive collisions

$$\begin{aligned}\psi^E_{DX}(\boldsymbol{p},s) = \mathcal{T}_{DX}(\boldsymbol{p},\boldsymbol{p}_1)\mathcal{K}_E(\boldsymbol{p}_1,\boldsymbol{p}_3)\int f_E(\boldsymbol{p}_1,s_E)\int \psi_{DX}(\boldsymbol{p}_3,s_3) \\ \times \mathcal{B}_{DX}(\boldsymbol{p}_1,\boldsymbol{p}_6)\psi_{DX}(\boldsymbol{p}_6,s-s_3-s_E)ds_3 ds_E.\end{aligned} \tag{19}$$

Note that in Eq. 17, 18, and 19, it appears as if the DXTRAN technique is always played; however, inside of the DXTRAN region the partial HSPDFs reduce to the analog form by the definitions of the DXTRAN free-flight transmission and the flight-to-DXTRAN operators. The HSPDF with DXTRAN in play is defined as the sum of these partial HSPDFs,

$$\psi_{DX}(\boldsymbol{p}, s)ds = \psi^{A}_{DX}(\boldsymbol{p}, s)ds + \psi^{E}_{DX}(\boldsymbol{p}, s)ds + \psi^{E}_{DX}(\boldsymbol{p}, s)ds \tag{20}$$

or explicitly,

$$\begin{aligned} \psi_{DX}(\boldsymbol{p}, s) = \mathcal{T}_{DX}(\boldsymbol{p}, \boldsymbol{p}_1)\mathcal{K}_A(\boldsymbol{p}_1, \boldsymbol{p}_2) \int f_A(\boldsymbol{p}_1, s_A)\delta(s - s_A)ds_A \\ + \mathcal{T}_{DX}(\boldsymbol{p}, \boldsymbol{p}_1)\mathcal{K}_E(\boldsymbol{p}_1, \boldsymbol{p}_3) \int f_E(\boldsymbol{p}_1, s_E) \int \psi_{DX}(\boldsymbol{p}_3, s_3) \\ \times \mathcal{B}_{DX}(\boldsymbol{p}_1, \boldsymbol{p}_6)\psi_{DX}(\boldsymbol{p}_6, s - s_3 - s_E)ds_3 ds_E \\ + \mathcal{T}_{DX}(\boldsymbol{p}, \boldsymbol{p}_4)\mathcal{S}(\boldsymbol{p}_4, \boldsymbol{p}_5) \int f_S(\boldsymbol{p}_4, s_S)\psi_{DX}(\boldsymbol{p}_5, s - s_S)ds_S. \end{aligned} \tag{21}$$

2.4 Forced-Collision and DXTRAN Combined

With the HSPDFs for analog transport, transport with forced collisions in play, and transport with DXTRAN in play, the HSPDF with both variance-reduction techniques can now be defined. Recall from Eq. 15 that the forced-collision HSPDF reduces to analog behavior in phase spaces where forced collisions are not specified. In these phase spaces DXTRAN is the only technique in play, so the combined-technique HSPDF is nearly identical to the DXTRAN HSPDF.

Recall from the derivation of Eq. 16 that a particle may only take one of two disjoint random-walk steps where forced collisions are specified. The first is a forced absorptive collision coupled with a forced transmission and the second is a forced emissive collision coupled with a forced transmission. As described in Sec. 1.3, when the DXTRAN technique is in play a forced absorptive collision must occur before the DXTRAN region is encountered and a forced transmission particle is killed if it intersects the DXTRAN region. This is handled implicitly by the definition of the flight-to-collision and flight-to-transmission operators, so the combined-technique partial HSPDF for absorptive collisions is equivalent to Eq. 12,

$$\begin{aligned} \psi^{A}_{FC,DX}(\boldsymbol{p}, s) = \mathcal{B}_c(\boldsymbol{p}, \boldsymbol{p}_1)\mathcal{K}_A(\boldsymbol{p}_1, \boldsymbol{p}_2) \int f_A(\boldsymbol{p}_1, s_A) \\ \times \mathcal{B}_t(\boldsymbol{p}, \boldsymbol{p}_4)\mathcal{S}(\boldsymbol{p}_4, \boldsymbol{p}_5) \int f_S(\boldsymbol{p}_4, s_S)\psi_{FC,DX}(\boldsymbol{p}_5, s - s_S - s_A)ds_S ds_A. \end{aligned} \tag{22}$$

Similarly, the step to a forced emissive collision described by Eq. 13 is modified by DXTRAN to force the collision prior to entering the DXTRAN region, terminate forced transmission particles entering the DXTRAN region, terminate the collided particle if it enters the DXTRAN region following the collision, and to create a DXTRAN particle following the collision. These modifications are described by the combined-technique partial HSPDF for emissive collisions

$$\begin{aligned} \psi^{E}_{FC,DX}(\boldsymbol{p}, s) = \mathcal{B}_c(\boldsymbol{p}, \boldsymbol{p}_1)\mathcal{K}_E(\boldsymbol{p}_1, \boldsymbol{p}_3) \int f_E(\boldsymbol{p}_1, s_E) \int \psi^{DX}_{FC,DX}(\boldsymbol{p}_3, s_3)\mathcal{B}_{DX}(\boldsymbol{p}_1,\boldsymbol{p}_6) \int \psi^{DX}_{FC,DX}(\boldsymbol{p}_6, s_6) \\ \times \mathcal{B}_t(\boldsymbol{p}, \boldsymbol{p}_4)\mathcal{S}(\boldsymbol{p}_4, \boldsymbol{p}_5) \int f_S(\boldsymbol{p}_4, s_S)\psi_{FC,DX}(\boldsymbol{p}_5, s - s_S - s_6 - s_3 - s_E)ds_S ds_6 ds_3 ds_E. \end{aligned} \tag{23}$$

where $\psi^{DX}_{FC,DX}$ is identical to Eq. 21 expect that it is recursive with $\psi_{FC,DX}$ to account for the particle traveling to a region where forced collisions are specified,

$$\begin{aligned} \psi^{DX}_{FC,DX}(\boldsymbol{p}, s) = \mathcal{T}_{DX}(\boldsymbol{p}, \boldsymbol{p}_1)\mathcal{K}_A(\boldsymbol{p}_1, \boldsymbol{p}_2) \int f_A(\boldsymbol{p}_1, s_A)\delta(s - s_A)ds_A \\ + \mathcal{T}_{DX}(\boldsymbol{p}, \boldsymbol{p}_1)\mathcal{K}_E(\boldsymbol{p}_1, \boldsymbol{p}_3) \int f_E(\boldsymbol{p}_1, s_E) \int \psi^{DX}_{FC,DX}(\boldsymbol{p}_3, s_3) \\ \times \mathcal{B}_{DX}(\boldsymbol{p}_1, \boldsymbol{p}_6)\psi^{DX}_{FC,DX}(\boldsymbol{p}_4, s - s_3 - s_E)ds_3 ds_E \\ + \mathcal{T}_{DX}(\boldsymbol{p}, \boldsymbol{p}_4)\mathcal{S}(\boldsymbol{p}_4, \boldsymbol{p}_5) \int f_S(\boldsymbol{p}_4, s_S)\psi_{FC,DX}(\boldsymbol{p}_5, s - s_S)ds_S. \end{aligned} \tag{24}$$

Note that $\psi_{FC,DX}$ is only used following a surface crossing because another collision can only be forced following entering a new cell. This neglects the case of a DXTRAN region that is coincident with a cell because such a system is not handled herein for simplicity and because doing so does not change the conclusions of this work. In Eq. 23, the altered collision location and transmitted particle termination are handled by operator definitions implicitly; the termination of collided particles entering the DXTRAN region is handled by the DXTRAN free-flight transmission operator, and the creation of DXTRAN particles is handled by the flight-to-DXTRAN operator. The combined-technique HSPDF is defined as the sum of these partial HSPDFs where forced collisions are specified and follows DXTRAN behavior where they are not,

$$\psi_{FC,DX}(\boldsymbol{p},s)ds = \begin{cases} \psi^{A}_{FC,DX}(\boldsymbol{p},s)ds + \psi^{E}_{FC,DX}(\boldsymbol{p},s)ds, & \boldsymbol{p} \in \{\boldsymbol{p}_{FC}\}, \\ \psi^{DX}_{FC,DX}(\boldsymbol{p},s)ds, & \text{otherwise}. \end{cases} \tag{25}$$

Writing the case of $\boldsymbol{p} \in \{\boldsymbol{p}_{FC}\}$ explicitly,

$$\begin{aligned} \psi_{FC,DX}(\boldsymbol{p},s) = \mathcal{B}_c(\boldsymbol{p},\boldsymbol{p}_1)\mathcal{K}_A(\boldsymbol{p}_1,\boldsymbol{p}_2) &\int f_A(\boldsymbol{p}_1,s_A) \\ &\times \mathcal{B}_t(\boldsymbol{p},\boldsymbol{p}_4)\mathcal{S}(\boldsymbol{p}_4,\boldsymbol{p}_5)\int f_S(\boldsymbol{p}_4,s_S)\psi_{FC,DX}(\boldsymbol{p}_5,s-s_S-s_A)ds_S ds_A \\ &+ \mathcal{B}_c(\boldsymbol{p},\boldsymbol{p}_1)\mathcal{K}_E(\boldsymbol{p}_1,\boldsymbol{p}_3)\int f_E(\boldsymbol{p}_1,s_E)\int \psi^{DX}_{FC,DX}(\boldsymbol{p}_3,s_3)\mathcal{B}_{DX}(\boldsymbol{p}_1,\boldsymbol{p}_6)\int \psi^{DX}_{FC,DX}(\boldsymbol{p}_6,s_6) \\ &\times \mathcal{B}_t(\boldsymbol{p},\boldsymbol{p}_4)\mathcal{S}(\boldsymbol{p}_4,\boldsymbol{p}_5)\int f_S(\boldsymbol{p}_4,s_S)\psi_{FC,DX}(\boldsymbol{p}_5,s-s_S-s_6-s_3-s_E)ds_S ds_6 ds_3 ds_E, \\ &\boldsymbol{p} \in \{\boldsymbol{p}_{FC}\}. \end{aligned} \tag{26}$$

3 Derivation of the First History Score Moment Equation

The first HSME gives the expected total contribution of score to all estimates specified in the Monte Carlo simulation and is found as the first score moment of the HSPDF derived in Sec. 2. Here the analog first HSME is derived both to demonstrate the derivation procedure on a simple case and for comparison later to prove fairness. The first moments of Eqs. 15, 21, and 25 are also derived.

3.1 Analog Transport

The analog HSME is found by taking the first score moment of the analog HSPDF,

$$\Psi_0(\boldsymbol{p}) = \int s\psi_0(\boldsymbol{p},s)ds. \tag{27}$$

Using the form of the HSPDF given in Eq. 11,

$$\begin{aligned} \Psi_0(\boldsymbol{p}) = \int s\Big(&\mathcal{T}(\boldsymbol{p},\boldsymbol{p}_1)\mathcal{K}_A(\boldsymbol{p}_1,\boldsymbol{p}_2)\int f_A(\boldsymbol{p}_1,s_A)\delta(s-s_A)ds_A \\ &+ \mathcal{T}(\boldsymbol{p},\boldsymbol{p}_1)\mathcal{K}_E(\boldsymbol{p}_1,\boldsymbol{p}_3)\int f_E(\boldsymbol{p}_1,s_E)\psi_0(\boldsymbol{p}_3,s-s_E)ds_E \\ &+ \mathcal{T}(\boldsymbol{p},\boldsymbol{p}_4)\mathcal{S}(\boldsymbol{p}_4,\boldsymbol{p}_5)\int f_S(\boldsymbol{p}_4,s_S)\psi_0(\boldsymbol{p}_5,s-s_S)ds_S\Big)ds. \end{aligned} \tag{28}$$

Distributing the integration over s,

$$\begin{aligned} \Psi_0(\boldsymbol{p}) = \mathcal{T}(\boldsymbol{p},\boldsymbol{p}_1)\mathcal{K}_A(\boldsymbol{p}_1,\boldsymbol{p}_2)&\int f_A(\boldsymbol{p}_1,s_A)\int s\delta(s-s_A)ds ds_A \\ &+ \mathcal{T}(\boldsymbol{p},\boldsymbol{p}_1)\mathcal{K}_E(\boldsymbol{p}_1,\boldsymbol{p}_3)\int f_E(\boldsymbol{p}_1,s_E)\int s\psi_0(\boldsymbol{p}_3,s-s_E)ds ds_E \\ &+ \mathcal{T}(\boldsymbol{p},\boldsymbol{p}_4)\mathcal{S}(\boldsymbol{p}_4,\boldsymbol{p}_5)\int f_S(\boldsymbol{p}_4,s_S)\int s\psi_0(\boldsymbol{p}_5,s-s_S)ds ds_S. \end{aligned} \tag{29}$$

Setting $q = s - s_E$ and $r = s - s_S$,

$$\begin{aligned}\Psi_0(\boldsymbol{p}) &= \mathcal{T}(\boldsymbol{p},\boldsymbol{p}_1)\mathcal{K}_A(\boldsymbol{p}_1,\boldsymbol{p}_2)\int f_A(\boldsymbol{p}_1,s_A)\int s\delta(s-s_A)ds ds_A \\ &+ \mathcal{T}(\boldsymbol{p},\boldsymbol{p}_1)\mathcal{K}_E(\boldsymbol{p}_1,\boldsymbol{p}_3)\int f_E(\boldsymbol{p}_1,s_E)\int (q+s_E)\psi_0(\boldsymbol{p}_3,q)dq ds_E \\ &+ \mathcal{T}(\boldsymbol{p},\boldsymbol{p}_4)\mathcal{S}(\boldsymbol{p}_4,\boldsymbol{p}_5)\int f_S(\boldsymbol{p}_4,s_S)\int (r+s_S)\psi_0(\boldsymbol{p}_5,r)dr ds_S.\end{aligned} \tag{30}$$

Distributing $(q + s_E)$ and $(r + s_S)$,

$$\begin{aligned}\Psi_0(\boldsymbol{p}) &= \mathcal{T}(\boldsymbol{p},\boldsymbol{p}_1)\mathcal{K}_A(\boldsymbol{p}_1,\boldsymbol{p}_2)\int f_A(\boldsymbol{p}_1,s_A)\int s\delta(s-s_A)ds ds_A \\ &+ \mathcal{T}(\boldsymbol{p},\boldsymbol{p}_1)\mathcal{K}_E(\boldsymbol{p}_1,\boldsymbol{p}_3)\int f_E(\boldsymbol{p}_1,s_E)\int q\psi_0(\boldsymbol{p}_3,q)dq ds_E \\ &+ \mathcal{T}(\boldsymbol{p},\boldsymbol{p}_1)\mathcal{K}_E(\boldsymbol{p}_1,\boldsymbol{p}_3)\int f_E(\boldsymbol{p}_1,s_E)\int s_E\psi_0(\boldsymbol{p}_3,q)dq ds_E \\ &+ \mathcal{T}(\boldsymbol{p},\boldsymbol{p}_4)\mathcal{S}(\boldsymbol{p}_4,\boldsymbol{p}_5)\int f_S(\boldsymbol{p}_4,s_S)\int r\psi_0(\boldsymbol{p}_5,r)dr ds_S \\ &+ \mathcal{T}(\boldsymbol{p},\boldsymbol{p}_4)\mathcal{S}(\boldsymbol{p}_4,\boldsymbol{p}_5)\int f_S(\boldsymbol{p}_4,s_S)\int s_S\psi_0(\boldsymbol{p}_5,r)dr ds_S.\end{aligned} \tag{31}$$

Evaluating the integral over the Dirac delta, using Eq. 27, and rearranging terms,

$$\begin{aligned}\Psi_0(\boldsymbol{p}) &= \mathcal{T}(\boldsymbol{p},\boldsymbol{p}_1)\mathcal{K}_A(\boldsymbol{p}_1,\boldsymbol{p}_2)\int s_A f_A(\boldsymbol{p}_1,s_A)ds_A \\ &+ \mathcal{T}(\boldsymbol{p},\boldsymbol{p}_1)\mathcal{K}_E(\boldsymbol{p}_1,\boldsymbol{p}_3)\Psi_0(\boldsymbol{p}_3)\int f_E(\boldsymbol{p}_1,s_E)ds_E \\ &+ \mathcal{T}(\boldsymbol{p},\boldsymbol{p}_1)\mathcal{K}_E(\boldsymbol{p}_1,\boldsymbol{p}_3)\int s_E f_E(\boldsymbol{p}_1,s_E)ds_E\int \psi_0(\boldsymbol{p}_3,q)dq \\ &+ \mathcal{T}(\boldsymbol{p},\boldsymbol{p}_4)\mathcal{S}(\boldsymbol{p}_4,\boldsymbol{p}_5)\Psi_0(\boldsymbol{p}_5)\int f_S(\boldsymbol{p}_4,s_S)ds_S \\ &+ \mathcal{T}(\boldsymbol{p},\boldsymbol{p}_4)\mathcal{S}(\boldsymbol{p}_4,\boldsymbol{p}_5)\int s_S f_S(\boldsymbol{p}_4,s_S)ds_S\int \psi_0(\boldsymbol{p}_5,r)dr.\end{aligned} \tag{32}$$

Defining $\bar{s}(\boldsymbol{p}) = \int s f_e(\boldsymbol{p},s)ds$ and using the fact that the integration of PDFs over their entire domain results in unity,

$$\begin{aligned}\Psi_0(\boldsymbol{p}) &= \mathcal{T}(\boldsymbol{p},\boldsymbol{p}_1)\mathcal{K}_A(\boldsymbol{p}_1,\boldsymbol{p}_2)\bar{s}_A(\boldsymbol{p}_1) \\ &+ \mathcal{T}(\boldsymbol{p},\boldsymbol{p}_1)\mathcal{K}_E(\boldsymbol{p}_1,\boldsymbol{p}_3)\Psi_0(\boldsymbol{p}_3) \\ &+ \mathcal{T}(\boldsymbol{p},\boldsymbol{p}_1)\mathcal{K}_E(\boldsymbol{p}_1,\boldsymbol{p}_3)\bar{s}_A(\boldsymbol{p}_1) \\ &+ \mathcal{T}(\boldsymbol{p},\boldsymbol{p}_4)\mathcal{S}(\boldsymbol{p}_4,\boldsymbol{p}_5)\Psi_0(\boldsymbol{p}_5) \\ &+ \mathcal{T}(\boldsymbol{p},\boldsymbol{p}_4)\mathcal{S}(\boldsymbol{p}_4,\boldsymbol{p}_5)\bar{s}_S(\boldsymbol{p}_4).\end{aligned} \tag{33}$$

Collecting terms yields the final result,

$$\begin{aligned}\Psi_0(\boldsymbol{p}) &= \mathcal{T}(\boldsymbol{p},\boldsymbol{p}_1)\mathcal{K}_A(\boldsymbol{p}_1,\boldsymbol{p}_2)\bar{s}_A(\boldsymbol{p}_1) \\ &+ \mathcal{T}(\boldsymbol{p},\boldsymbol{p}_1)\mathcal{K}_E(\boldsymbol{p}_1,\boldsymbol{p}_3)(\bar{s}_E(\boldsymbol{p}_1) + \Psi_0(\boldsymbol{p}_3)) \\ &+ \mathcal{T}(\boldsymbol{p},\boldsymbol{p}_4)\mathcal{S}(\boldsymbol{p}_4,\boldsymbol{p}_5)(\bar{s}_S(\boldsymbol{p}_4) + \Psi_0(\boldsymbol{p}_5)).\end{aligned} \tag{34}$$

Eq. 34 may be interpreted as accounting for the expected score following an absorption weighted by the probability of undergoing an absorption, continuing on in the simulation following a scatter weighted by the probability of undergoing a scatter, and continuing on in the simulation following a surface crossing weighted by the probability of crossing a surface.

3.2 Forced-Collision Variance-Reduction Technique

The forced-collision HSME is found by taking the first score moment of the forced-collision HSPDF given in Eq. 15,

$$\Psi_{FC}(\boldsymbol{p}) = \int s\psi_{FC}(\boldsymbol{p}, s)ds. \tag{35}$$

Recall from Eq. 15 that the forced-collision HSPDF is defined for the cases of whether or not forced collisions are specified in a given phase space. If forced collisions are not specified then the forced-collision HSPDF is given by Eq. 14. This equation is of the same form as Eq. 11, so by taking steps identical to those in Sec. 3.1 the first score moment is found to be

$$\begin{aligned}\Psi^0_{FC}(\boldsymbol{p}) = &\mathcal{T}(\boldsymbol{p},\boldsymbol{p}_1)\mathcal{K}_A(\boldsymbol{p}_1,\boldsymbol{p}_2)\bar{s}_A(\boldsymbol{p}_1)\\ &+ \mathcal{T}(\boldsymbol{p},\boldsymbol{p}_1)\mathcal{K}_E(\boldsymbol{p}_1,\boldsymbol{p}_3)\big(\bar{s}_E(\boldsymbol{p}_1) + \Psi^0_{FC}(\boldsymbol{p}_3)\big)\\ &+ \mathcal{T}(\boldsymbol{p},\boldsymbol{p}_4)\mathcal{S}(\boldsymbol{p}_4,\boldsymbol{p}_5)(\bar{s}_S(\boldsymbol{p}_4) + \Psi_{FC}(\boldsymbol{p}_5)).\end{aligned} \tag{36}$$

The steps to derive Eq. 36 are omitted to avoid redundancy. For the opposite case, the forced-collision HSPDF is given by Eq. 16. Expanding Eq. 35 for this case,

$$\begin{aligned}\Psi_{FC}(\boldsymbol{p}) = \int s\Bigg(&\mathcal{B}_c(\boldsymbol{p},\boldsymbol{p}_1)\mathcal{K}_A(\boldsymbol{p}_1,\boldsymbol{p}_2)\int f_A(\boldsymbol{p}_1,s_A)\\ &\times\mathcal{B}_t(\boldsymbol{p},\boldsymbol{p}_4)\mathcal{S}(\boldsymbol{p}_4,\boldsymbol{p}_5)\int f_S(\boldsymbol{p}_4,s_S)\psi_{FC}(\boldsymbol{p}_5,s-s_S-s_A)ds_Sds_A\\ &+\mathcal{B}_c(\boldsymbol{p},\boldsymbol{p}_1)\mathcal{K}_E(\boldsymbol{p}_1,\boldsymbol{p}_3)\int f_E(\boldsymbol{p}_1,s_E)\int\psi^0_{FC}(\boldsymbol{p}_3,s_3)\\ &\times\mathcal{B}_t(\boldsymbol{p},\boldsymbol{p}_4)\mathcal{S}(\boldsymbol{p}_4,\boldsymbol{p}_5)\int f_S(\boldsymbol{p}_4,s_S)\psi_{FC}(\boldsymbol{p}_5,s-s_S-s_3-s_E)ds_Sds_3ds_E\Bigg)ds,\ \boldsymbol{p}\in\{\boldsymbol{p}_{FC}\}.\end{aligned} \tag{37}$$

Temporarily dropping the notation of $\boldsymbol{p}\in\{\boldsymbol{p}_{FC}\}$ for ease of notation and distributing the integration over s,

$$\begin{aligned}\Psi_{FC}(\boldsymbol{p}) = &\mathcal{B}_c(\boldsymbol{p},\boldsymbol{p}_1)\mathcal{K}_A(\boldsymbol{p}_1,\boldsymbol{p}_2)\int f_A(\boldsymbol{p}_1,s_A)\\ &\times\mathcal{B}_t(\boldsymbol{p},\boldsymbol{p}_4)\mathcal{S}(\boldsymbol{p}_4,\boldsymbol{p}_5)\int f_S(\boldsymbol{p}_4,s_S)\int s\psi_{FC}(\boldsymbol{p}_5,s-s_S-s_A)dsds_Sds_A\\ &+\mathcal{B}_c(\boldsymbol{p},\boldsymbol{p}_1)\mathcal{K}_E(\boldsymbol{p}_1,\boldsymbol{p}_3)\int f_E(\boldsymbol{p}_1,s_E)\int\psi^0_{FC}(\boldsymbol{p}_3,s_3)\\ &\times\mathcal{B}_t(\boldsymbol{p},\boldsymbol{p}_4)\mathcal{S}(\boldsymbol{p}_4,\boldsymbol{p}_5)\int f_S(\boldsymbol{p}_4,s_S)\int s\psi_{FC}(\boldsymbol{p}_5,s-s_S-s_3-s_E)dsds_Sds_3ds_E.\end{aligned} \tag{38}$$

Setting $q = s - s_S - s_A$ and $r = s - s_S - s_3 - s_E$,

$$\begin{aligned}\Psi_{FC}(\boldsymbol{p}) = &\mathcal{B}_c(\boldsymbol{p},\boldsymbol{p}_1)\mathcal{K}_A(\boldsymbol{p}_1,\boldsymbol{p}_2)\int f_A(\boldsymbol{p}_1,s_A)\\ &\times\mathcal{B}_t(\boldsymbol{p},\boldsymbol{p}_4)\mathcal{S}(\boldsymbol{p}_4,\boldsymbol{p}_5)\int f_S(\boldsymbol{p}_4,s_S)\int(q+s_S+s_A)\psi_{FC}(\boldsymbol{p}_5,q)dqds_Sds_A\\ &+\mathcal{B}_c(\boldsymbol{p},\boldsymbol{p}_1)\mathcal{K}_E(\boldsymbol{p}_1,\boldsymbol{p}_3)\int f_E(\boldsymbol{p}_1,s_E)\int\psi^0_{FC}(\boldsymbol{p}_3,s_3)\\ &\times\mathcal{B}_t(\boldsymbol{p},\boldsymbol{p}_4)\mathcal{S}(\boldsymbol{p}_4,\boldsymbol{p}_5)\int f_S(\boldsymbol{p}_4,s_S)\int(r+s_S+s_3+s_E)\psi_{FC}(\boldsymbol{p}_5,r)drds_Sds_3ds_E.\end{aligned} \tag{39}$$

Distributing $(q + s_S + s_A)$ and $(r + s_S + s_3 + s_E)$,

$$\begin{aligned}
\Psi_{FC}(\boldsymbol{p}) = &\mathcal{B}_c(\boldsymbol{p}, \boldsymbol{p}_1)\mathcal{K}_A(\boldsymbol{p}_1, \boldsymbol{p}_2) \\
&\times \Bigg(\int f_A(\boldsymbol{p}_1, s_A)ds_A \mathcal{B}_t(\boldsymbol{p}, \boldsymbol{p}_4)\mathcal{S}(\boldsymbol{p}_4, \boldsymbol{p}_5) \int f_S(\boldsymbol{p}_4, s_S)ds_S \int q\psi_{FC}(\boldsymbol{p}_5, q)dq \\
&+ \int f_A(\boldsymbol{p}_1, s_A)ds_A \mathcal{B}_t(\boldsymbol{p}, \boldsymbol{p}_4)\mathcal{S}(\boldsymbol{p}_4, \boldsymbol{p}_5) \int s_S f_S(\boldsymbol{p}_4, s_S)ds_S \int \psi_{FC}(\boldsymbol{p}_5, q)dq \\
&+ \int s_A f_A(\boldsymbol{p}_1, s_A)ds_A \mathcal{B}_t(\boldsymbol{p}, \boldsymbol{p}_4)\mathcal{S}(\boldsymbol{p}_4, \boldsymbol{p}_5) \int f_S(\boldsymbol{p}_4, s_S)ds_S \int \psi_{FC}(\boldsymbol{p}_5, q)dq\Bigg) \\
&+ \mathcal{B}_c(\boldsymbol{p}, \boldsymbol{p}_1)\mathcal{K}_E(\boldsymbol{p}_1, \boldsymbol{p}_3) \\
&\times \Bigg(\int f_E(\boldsymbol{p}_1, s_E)ds_E \int \psi^0_{FC}(\boldsymbol{p}_3, s_3)ds_3 \mathcal{B}_t(\boldsymbol{p}, \boldsymbol{p}_4)\mathcal{S}(\boldsymbol{p}_{4,}\boldsymbol{p}_5) \int f_S(\boldsymbol{p}_4, s_S)ds_S \int r\psi_{FC}(\boldsymbol{p}_5, r)dr \\
&+ \int f_E(\boldsymbol{p}_1, s_E)ds_E \int \psi^0_{FC}(\boldsymbol{p}_3, s_3)ds_3 \mathcal{B}_t(\boldsymbol{p}, \boldsymbol{p}_4)\mathcal{S}(\boldsymbol{p}_{4,}\boldsymbol{p}_5) \int s_S f_S(\boldsymbol{p}_4, s_S)ds_S \int \psi_{FC}(\boldsymbol{p}_5, r)dr \\
&+ \int f_E(\boldsymbol{p}_1, s_E)ds_E \int s_3\psi^0_{FC}(\boldsymbol{p}_3, s_3)ds_3 \mathcal{B}_t(\boldsymbol{p}, \boldsymbol{p}_4)\mathcal{S}(\boldsymbol{p}_{4,}\boldsymbol{p}_5) \int f_S(\boldsymbol{p}_4, s_S)ds_S \int \psi_{FC}(\boldsymbol{p}_5, r)dr \\
&+ \int s_E f_E(\boldsymbol{p}_1, s_E)ds_E \int \psi^0_{FC}(\boldsymbol{p}_3, s_3)ds_3 \mathcal{B}_t(\boldsymbol{p}, \boldsymbol{p}_4)\mathcal{S}(\boldsymbol{p}_{4,}\boldsymbol{p}_5) \int f_S(\boldsymbol{p}_4, s_S)ds_S \int \psi_{FC}(\boldsymbol{p}_5, r)dr\Bigg).
\end{aligned} \tag{40}$$

Defining $\bar{s}(\boldsymbol{p}) = \int sf_e(\boldsymbol{p}, s)ds$, using the fact that the integration over of the full domain of PDFs results in unity, and using Eq. 35,

$$\begin{aligned}
\Psi_{FC}(\boldsymbol{p}) = &\mathcal{B}_c(\boldsymbol{p}, \boldsymbol{p}_1)\mathcal{K}_A(\boldsymbol{p}_1, \boldsymbol{p}_2) \\
&\times (\mathcal{B}_t(\boldsymbol{p}, \boldsymbol{p}_4)\mathcal{S}(\boldsymbol{p}_4, \boldsymbol{p}_5)\Psi_{FC}(\boldsymbol{p}_5) \\
&+ \mathcal{B}_t(\boldsymbol{p}, \boldsymbol{p}_4)\mathcal{S}(\boldsymbol{p}_4, \boldsymbol{p}_5)\bar{s}_S(\boldsymbol{p}_4) \\
&+ \bar{s}_A(\boldsymbol{p}_1)\mathcal{B}_t(\boldsymbol{p}, \boldsymbol{p}_4)\mathcal{S}(\boldsymbol{p}_4, \boldsymbol{p}_5)) \\
&+ \mathcal{B}_c(\boldsymbol{p}, \boldsymbol{p}_1)\mathcal{K}_E(\boldsymbol{p}_1, \boldsymbol{p}_3) \\
&\times (\mathcal{B}_t(\boldsymbol{p}, \boldsymbol{p}_4)\mathcal{S}(\boldsymbol{p}_{4,}\boldsymbol{p}_5)\Psi_{FC}(\boldsymbol{p}_5) \\
&+ \mathcal{B}_t(\boldsymbol{p}, \boldsymbol{p}_4)\mathcal{S}(\boldsymbol{p}_{4,}\boldsymbol{p}_5)\bar{s}_S(\boldsymbol{p}_4) \\
&+ \Psi^0_{FC}(\boldsymbol{p}_3)\mathcal{B}_t(\boldsymbol{p}, \boldsymbol{p}_4)\mathcal{S}(\boldsymbol{p}_{4,}\boldsymbol{p}_5) \\
&+ \bar{s}_E(\boldsymbol{p}_1)\mathcal{B}_t(\boldsymbol{p}, \boldsymbol{p}_4)\mathcal{S}(\boldsymbol{p}_{4,}\boldsymbol{p}_5)).
\end{aligned} \tag{41}$$

Using the property of the surface-crossing and flight-to-transmission operators evident from Eqs. 188 and 192, respectively, that they reduce to unity when acting on nothing yields the final result,

$$\begin{aligned}
\Psi_{FC}(\boldsymbol{p}) = &\mathcal{B}_c(\boldsymbol{p}, \boldsymbol{p}_1)\mathcal{K}_A(\boldsymbol{p}_1, \boldsymbol{p}_2)(\bar{s}_A(\boldsymbol{p}_1) + \mathcal{B}_t(\boldsymbol{p}, \boldsymbol{p}_4)\mathcal{S}(\boldsymbol{p}_4, \boldsymbol{p}_5)(\bar{s}_S(\boldsymbol{p}_4) + \Psi_{FC}(\boldsymbol{p}_5))) \\
&+ \mathcal{B}_c(\boldsymbol{p}, \boldsymbol{p}_1)\mathcal{K}_E(\boldsymbol{p}_1, \boldsymbol{p}_3) \\
&\times \big(\bar{s}_E(\boldsymbol{p}_1) + \Psi^0_{FC}(\boldsymbol{p}_3) + \mathcal{B}_t(\boldsymbol{p}, \boldsymbol{p}_4)\mathcal{S}(\boldsymbol{p}_{4,}\boldsymbol{p}_5)(\bar{s}_S(\boldsymbol{p}_4) + \Psi_{FC}(\boldsymbol{p}_5))\big),\ \boldsymbol{p} \in \{\boldsymbol{p}_{FC}\}.
\end{aligned} \tag{42}$$

Compared with Eq. 34, Eq. 42 has only two terms which both have score contributions due to a collision and surface crossing.

3.3 DXTRAN Variance-Reduction Technique

The HSME with only DXTRAN variance reduction in play is found by taking the first score moment of Eq. 21,

$$\Psi_{DX}(\boldsymbol{p}) = \int s\psi_{DX}(\boldsymbol{p}, s)ds. \tag{43}$$

Expanding ψ_{DX} using Eq. 21,

$$\begin{aligned}\Psi_{DX}(\boldsymbol{p}) = \int s\Bigg(&\mathcal{T}_{DX}(\boldsymbol{p},\boldsymbol{p}_1)\mathcal{K}_A(\boldsymbol{p}_1,\boldsymbol{p}_2)\int f_A(\boldsymbol{p}_1,s_A)\delta(s-s_A)ds_A \\ &+\mathcal{T}_{DX}(\boldsymbol{p},\boldsymbol{p}_1)\mathcal{K}_E(\boldsymbol{p}_1,\boldsymbol{p}_3)\int f_E(\boldsymbol{p}_1,s_E)\int \psi_{DX}(\boldsymbol{p}_3,s_3) \\ &\times \mathcal{B}_{DX}(\boldsymbol{p}_1,\boldsymbol{p}_6)\psi_{DX}(\boldsymbol{p}_6,s-s_3-s_E)ds_3ds_E \\ &+\mathcal{T}_{DX}(\boldsymbol{p},\boldsymbol{p}_4)\mathcal{S}(\boldsymbol{p}_4,\boldsymbol{p}_5)\int f_S(\boldsymbol{p}_4,s_S)\psi_{DX}(\boldsymbol{p}_5,s-s_S)ds_S\Bigg)ds.\end{aligned} \tag{44}$$

Distributing the integration over s,

$$\begin{aligned}\Psi_{DX}(\boldsymbol{p}) = &\mathcal{T}_{DX}(\boldsymbol{p},\boldsymbol{p}_1)\mathcal{K}_A(\boldsymbol{p}_1,\boldsymbol{p}_2)\int f_A(\boldsymbol{p}_1,s_A)\int s\delta(s-s_A)dsds_A \\ &+\mathcal{T}_{DX}(\boldsymbol{p},\boldsymbol{p}_1)\mathcal{K}_E(\boldsymbol{p}_1,\boldsymbol{p}_3)\int f_E(\boldsymbol{p}_1,s_E)\int \psi_{DX}(\boldsymbol{p}_3,s_3) \\ &\times \mathcal{B}_{DX}(\boldsymbol{p}_1,\boldsymbol{p}_6)\int s\psi_{DX}(\boldsymbol{p}_6,s-s_3-s_E)dsds_3ds_E \\ &+\mathcal{T}_{DX}(\boldsymbol{p},\boldsymbol{p}_4)\mathcal{S}(\boldsymbol{p}_4,\boldsymbol{p}_5)\int f_S(\boldsymbol{p}_4,s_S)\int s\psi_{DX}(\boldsymbol{p}_5,s-s_S)dsds_S.\end{aligned} \tag{45}$$

Setting $q = s - s_3 - s_E$ and $r = s - s_S$,

$$\begin{aligned}\Psi_{DX}(\boldsymbol{p}) = &\mathcal{T}_{DX}(\boldsymbol{p},\boldsymbol{p}_1)\mathcal{K}_A(\boldsymbol{p}_1,\boldsymbol{p}_2)\int f_A(\boldsymbol{p}_1,s_A)\int s\delta(s-s_A)dsds_A \\ &+\mathcal{T}_{DX}(\boldsymbol{p},\boldsymbol{p}_1)\mathcal{K}_E(\boldsymbol{p}_1,\boldsymbol{p}_3)\int f_E(\boldsymbol{p}_1,s_E)\int \psi_{DX}(\boldsymbol{p}_3,s_3) \\ &\times \mathcal{B}_{DX}(\boldsymbol{p}_1,\boldsymbol{p}_6)\int (q+s_3+s_E)\psi_{DX}(\boldsymbol{p}_6,q)dqds_3ds_E \\ &+\mathcal{T}_{DX}(\boldsymbol{p},\boldsymbol{p}_4)\mathcal{S}(\boldsymbol{p}_4,\boldsymbol{p}_5)\int f_S(\boldsymbol{p}_4,s_S)\int (r+s_S)\psi_{DX}(\boldsymbol{p}_5,r)drds_S.\end{aligned} \tag{46}$$

Distributing $(q + s_3 + s_E)$ and $(r + s_S)$,

$$\begin{aligned}\Psi_{DX}(\boldsymbol{p}) = &\mathcal{T}_{DX}(\boldsymbol{p},\boldsymbol{p}_1)\mathcal{K}_A(\boldsymbol{p}_1,\boldsymbol{p}_2)\int f_A(\boldsymbol{p}_1,s_A)\int s\delta(s-s_A)dsds_A \\ &+\mathcal{T}_{DX}(\boldsymbol{p},\boldsymbol{p}_1)\mathcal{K}_E(\boldsymbol{p}_1,\boldsymbol{p}_3)\int f_E(\boldsymbol{p}_1,s_E)\int \psi_{DX}(\boldsymbol{p}_3,s_3) \\ &\times\Bigg(\mathcal{B}_{DX}(\boldsymbol{p}_1,\boldsymbol{p}_6)\int q\psi_{DX}(\boldsymbol{p}_6,q)dq \\ &\quad+\mathcal{B}_{DX}(\boldsymbol{p}_1,\boldsymbol{p}_6)\int s_3\psi_{DX}(\boldsymbol{p}_6,q)dq \\ &\quad+\mathcal{B}_{DX}(\boldsymbol{p}_1,\boldsymbol{p}_6)\int s_E\psi_{DX}(\boldsymbol{p}_6,q)dq\Bigg)ds_3ds_E \\ &+\mathcal{T}_{DX}(\boldsymbol{p},\boldsymbol{p}_4)\mathcal{S}(\boldsymbol{p}_4,\boldsymbol{p}_5)\int f_S(\boldsymbol{p}_4,s_S)\int r\psi_{DX}(\boldsymbol{p}_5,r)drds_S \\ &+\mathcal{T}_{DX}(\boldsymbol{p},\boldsymbol{p}_4)\mathcal{S}(\boldsymbol{p}_4,\boldsymbol{p}_5)\int f_S(\boldsymbol{p}_4,s_S)\int s_S\psi_{DX}(\boldsymbol{p}_5,r)drds_S.\end{aligned} \tag{47}$$

Evaluating the integral over the Dirac delta, using Eq. 43, and rearranging terms,

$$\begin{aligned}
\Psi_{DX}(\boldsymbol{p}) = \mathcal{T}_{DX}(\boldsymbol{p},\boldsymbol{p}_1)\mathcal{K}_A(\boldsymbol{p}_1,\boldsymbol{p}_2)\int s_A f_A(\boldsymbol{p}_1,s_A)ds_A \\
&+ \mathcal{T}_{DX}(\boldsymbol{p},\boldsymbol{p}_1)\mathcal{K}_E(\boldsymbol{p}_1,\boldsymbol{p}_3)\int f_E(\boldsymbol{p}_1,s_E)\int \psi_{DX}(\boldsymbol{p}_3,s_3) \\
&\times\Bigg(\mathcal{B}_{DX}(\boldsymbol{p}_1,\boldsymbol{p}_6)\psi_{DX}(\boldsymbol{p}_6) \\
&+ s_3\mathcal{B}_{DX}(\boldsymbol{p}_1,\boldsymbol{p}_6)\int\psi_{DX}(\boldsymbol{p}_6,q)dq \\
&+ s_E\mathcal{B}_{DX}(\boldsymbol{p}_1,\boldsymbol{p}_6)\int\psi_{DX}(\boldsymbol{p}_6,q)dq\Bigg)ds_3ds_E \\
&+ \mathcal{T}_{DX}(\boldsymbol{p},\boldsymbol{p}_4)\mathcal{S}(\boldsymbol{p}_4,\boldsymbol{p}_5)\psi_{DX}(\boldsymbol{p}_5)\int f_S(\boldsymbol{p}_4,s_S)ds_S \\
&+ \mathcal{T}_{DX}(\boldsymbol{p},\boldsymbol{p}_4)\mathcal{S}(\boldsymbol{p}_4,\boldsymbol{p}_5)\int s_S f_S(\boldsymbol{p}_4,s_S)ds_S\int\psi_{DX}(\boldsymbol{p}_5,r)dr.
\end{aligned} \tag{48}$$

Defining $\bar{s}(\boldsymbol{p}) = \int sf_e(\boldsymbol{p},s)ds$ and using the fact that the integration over the full domain of PDFs results in unity,

$$\begin{aligned}
\Psi_{DX}(\boldsymbol{p}) = \mathcal{T}_{DX}(\boldsymbol{p},\boldsymbol{p}_1)\mathcal{K}_A(\boldsymbol{p}_1,\boldsymbol{p}_2)\bar{s}_A(\boldsymbol{p}_1) \\
&+ \mathcal{T}_{DX}(\boldsymbol{p},\boldsymbol{p}_1)\mathcal{K}_E(\boldsymbol{p}_1,\boldsymbol{p}_3)\int f_E(\boldsymbol{p}_1,s_E)\int \psi_{DX}(\boldsymbol{p}_3,s_3) \\
&\times\Bigg(\mathcal{B}_{DX}(\boldsymbol{p}_1,\boldsymbol{p}_6)\psi_{DX}(\boldsymbol{p}_6) \\
&+ s_3\mathcal{B}_{DX}(\boldsymbol{p}_1,\boldsymbol{p}_6) \\
&+ s_E\mathcal{B}_{DX}(\boldsymbol{p}_1,\boldsymbol{p}_6)\Bigg)ds_3ds_E \\
&+ \mathcal{T}_{DX}(\boldsymbol{p},\boldsymbol{p}_4)\mathcal{S}(\boldsymbol{p}_4,\boldsymbol{p}_5)\psi_{DX}(\boldsymbol{p}_5) \\
&+ \mathcal{T}_{DX}(\boldsymbol{p},\boldsymbol{p}_4)\mathcal{S}(\boldsymbol{p}_4,\boldsymbol{p}_5)\bar{s}_S(\boldsymbol{p}_4).
\end{aligned} \tag{49}$$

Using the property of the $\mathcal{B}_{DX}(\boldsymbol{p},\boldsymbol{p}')$ evident in Eq. 193 that if the operator is acting on nothing it reduces to unity and rearranging terms,

$$\begin{aligned}
\Psi_{DX}(\boldsymbol{p}) = \mathcal{T}_{DX}(\boldsymbol{p},\boldsymbol{p}_1)\mathcal{K}_A(\boldsymbol{p}_1,\boldsymbol{p}_2)\bar{s}_A(\boldsymbol{p}_1) \\
&+ \mathcal{T}_{DX}(\boldsymbol{p},\boldsymbol{p}_1)\mathcal{K}_E(\boldsymbol{p}_1,\boldsymbol{p}_3)\int f_E(\boldsymbol{p}_1,s_E)ds_E\int \psi_{DX}(\boldsymbol{p}_3,s_3)ds_3\mathcal{B}_{DX}(\boldsymbol{p}_1,\boldsymbol{p}_6)\psi_{DX}(\boldsymbol{p}_6) \\
&+ \mathcal{T}_{DX}(\boldsymbol{p},\boldsymbol{p}_1)\mathcal{K}_E(\boldsymbol{p}_1,\boldsymbol{p}_3)\int f_E(\boldsymbol{p}_1,s_E)ds_E\int s_3\psi_{DX}(\boldsymbol{p}_3,s_3)ds_3 \\
&+ \mathcal{T}_{DX}(\boldsymbol{p},\boldsymbol{p}_1)\mathcal{K}_E(\boldsymbol{p}_1,\boldsymbol{p}_3)\int s_E f_E(\boldsymbol{p}_1,s_E)ds_E\int \psi_{DX}(\boldsymbol{p}_3,s_3)ds_3 \\
&+ \mathcal{T}_{DX}(\boldsymbol{p},\boldsymbol{p}_4)\mathcal{S}(\boldsymbol{p}_4,\boldsymbol{p}_5)\psi_{DX}(\boldsymbol{p}_5) \\
&+ \mathcal{T}_{DX}(\boldsymbol{p},\boldsymbol{p}_4)\mathcal{S}(\boldsymbol{p}_4,\boldsymbol{p}_5)\bar{s}_S(\boldsymbol{p}_4).
\end{aligned} \tag{50}$$

Again using $\bar{s} = \int sf_e(\boldsymbol{p},s)ds$, Eq. 43, and the integration of PDFs to unity,

$$\begin{aligned}
\Psi_{DX}(\boldsymbol{p}) = \mathcal{T}_{DX}(\boldsymbol{p},\boldsymbol{p}_1)\mathcal{K}_A(\boldsymbol{p}_1,\boldsymbol{p}_2)\bar{s}_A(\boldsymbol{p}_1) \\
&+ \mathcal{T}_{DX}(\boldsymbol{p},\boldsymbol{p}_1)\mathcal{K}_E(\boldsymbol{p}_1,\boldsymbol{p}_3)\mathcal{B}_{DX}(\boldsymbol{p}_1,\boldsymbol{p}_6)\Psi_{DX}(\boldsymbol{p}_6) \\
&+ \mathcal{T}_{DX}(\boldsymbol{p},\boldsymbol{p}_1)\mathcal{K}_E(\boldsymbol{p}_1,\boldsymbol{p}_3)\Psi_{DX}(\boldsymbol{p}_3) \\
&+ \mathcal{T}_{DX}(\boldsymbol{p},\boldsymbol{p}_1)\mathcal{K}_E(\boldsymbol{p}_1,\boldsymbol{p}_3)\bar{s}_E(\boldsymbol{p}_1) \\
&+ \mathcal{T}_{DX}(\boldsymbol{p},\boldsymbol{p}_4)\mathcal{S}(\boldsymbol{p}_4,\boldsymbol{p}_5)\Psi_{DX}(\boldsymbol{p}_5) \\
&+ \mathcal{T}_{DX}(\boldsymbol{p},\boldsymbol{p}_4)\mathcal{S}(\boldsymbol{p}_4,\boldsymbol{p}_5)\bar{s}_S(\boldsymbol{p}_4).
\end{aligned} \tag{51}$$

Collecting terms yields the final result,

$$\begin{aligned}\Psi_{DX}(\boldsymbol{p}) = &\mathcal{T}_{DX}(\boldsymbol{p},\boldsymbol{p}_1)\mathcal{K}_A(\boldsymbol{p}_1,\boldsymbol{p}_2)\bar{s}_A(\boldsymbol{p}_1)\\ &+\mathcal{T}_{DX}(\boldsymbol{p},\boldsymbol{p}_1)\mathcal{K}_E(\boldsymbol{p}_1,\boldsymbol{p}_3)\big(\bar{s}_E(\boldsymbol{p}_1)+\Psi_{DX}(\boldsymbol{p}_3)\big)\\ &+\mathcal{T}_{DX}(\boldsymbol{p},\boldsymbol{p}_4)\mathcal{S}(\boldsymbol{p}_4,\boldsymbol{p}_5)(\bar{s}_S(\boldsymbol{p}_4)+\Psi_{DX}(\boldsymbol{p}_5))\\ &+\mathcal{T}_{DX}(\boldsymbol{p},\boldsymbol{p}_1)\mathcal{K}_E(\boldsymbol{p}_1,\boldsymbol{p}_3)\mathcal{B}_{DX}(\boldsymbol{p}_1,\boldsymbol{p}_6)\Psi_{DX}(\boldsymbol{p}_6).\end{aligned} \tag{52}$$

Comparing Eq. 52 with Eq. 34, the only difference is the substitution of the DXTRAN free-flight transmission operator for the free-flight transmission operator and the addition of the branch containing the flight-to-DXTRAN operator.

3.4 Forced-Collision and DXTRAN Variance-Reduction Techniques

The combined forced-collision and DXTRAN HSME is found by taking the first score moment of the combined-technique HSPDF given in Eq. 25,

$$\Psi_{FC,DX}(\boldsymbol{p}) = \int s\psi_{FC,DX}(\boldsymbol{p},s)ds. \tag{53}$$

Recall from Eq. 25 that the combined-technique HSPDF is defined for the cases of whether or not forced collisions are specified in a given phase space, similar to the forced-collision HSPDF. If forced collisions are not specified then the combined-technique HSPDF is given by Eq. 24. This equation is of the same form as Eq. 21, so by taking steps identical to those in Sec. 3.3 the first score moment is found to be

$$\begin{aligned}\Psi^{DX}_{FC,DX}(\boldsymbol{p}) = &\mathcal{T}_{DX}(\boldsymbol{p},\boldsymbol{p}_1)\mathcal{K}_A(\boldsymbol{p}_1,\boldsymbol{p}_2)\bar{s}_A(\boldsymbol{p}_1)\\ &+\mathcal{T}_{DX}(\boldsymbol{p},\boldsymbol{p}_1)\mathcal{K}_E(\boldsymbol{p}_1,\boldsymbol{p}_3)\big(\bar{s}_E(\boldsymbol{p}_1)+\Psi^{DX}_{FC,DX}(\boldsymbol{p}_3)\big)\\ &+\mathcal{T}_{DX}(\boldsymbol{p},\boldsymbol{p}_4)\mathcal{S}(\boldsymbol{p}_4,\boldsymbol{p}_5)(\bar{s}_S(\boldsymbol{p}_4)+\Psi_{FC,DX}(\boldsymbol{p}_5))\\ &+\mathcal{T}_{DX}(\boldsymbol{p},\boldsymbol{p}_1)\mathcal{K}_E(\boldsymbol{p}_1,\boldsymbol{p}_3)\mathcal{B}_{DX}(\boldsymbol{p}_1,\boldsymbol{p}_6)\Psi^{DX}_{FC,DX}(\boldsymbol{p}_6).\end{aligned} \tag{54}$$

The steps to derive Eq. 54 are omitted to avoid redundancy. For the opposite case, the combined-technique HSPDF is given by Eq. 26. Expanding Eq. 53 for this case,

$$\begin{aligned}\Psi_{FC,DX}(\boldsymbol{p}) = &\int s\Bigg(\mathcal{B}_c(\boldsymbol{p},\boldsymbol{p}_1)\mathcal{K}_A(\boldsymbol{p}_1,\boldsymbol{p}_2)\int f_A(\boldsymbol{p}_1,s_A)\\ &\times\mathcal{B}_t(\boldsymbol{p},\boldsymbol{p}_4)\mathcal{S}(\boldsymbol{p}_4,\boldsymbol{p}_5)\int f_S(\boldsymbol{p}_4,s_S)\psi_{FC,DX}(\boldsymbol{p}_5,s-s_S-s_A)ds_S ds_A\\ &+\mathcal{B}_c(\boldsymbol{p},\boldsymbol{p}_1)\mathcal{K}_E(\boldsymbol{p}_1,\boldsymbol{p}_3)\int f_E(\boldsymbol{p}_1,s_E)\int\psi^{DX}_{FC,DX}(\boldsymbol{p}_3,s_3)\mathcal{B}_{DX}(\boldsymbol{p}_1,\boldsymbol{p}_6)\int\psi^{DX}_{FC,DX}(\boldsymbol{p}_6,s_6)\\ &\times\mathcal{B}_t(\boldsymbol{p},\boldsymbol{p}_4)\mathcal{S}(\boldsymbol{p}_4,\boldsymbol{p}_5)\int f_S(\boldsymbol{p}_4,s_S)\psi_{FC,DX}(\boldsymbol{p}_5,s-s_S-s_6-s_3-s_E)ds_S ds_6 ds_3 ds_E\Bigg)ds,\\ &\boldsymbol{p}\in\{\boldsymbol{p}_{FC}\}.\end{aligned} \tag{55}$$

Temporarily dropping the $\boldsymbol{p}\in\{\boldsymbol{p}_{FC}\}$ notation and distributing the integration over s,

$$\begin{aligned}\Psi_{FC,DX}(\boldsymbol{p}) = &\mathcal{B}_c(\boldsymbol{p},\boldsymbol{p}_1)\mathcal{K}_A(\boldsymbol{p}_1,\boldsymbol{p}_2)\int f_A(\boldsymbol{p}_1,s_A)\\ &\times\mathcal{B}_t(\boldsymbol{p},\boldsymbol{p}_4)\mathcal{S}(\boldsymbol{p}_4,\boldsymbol{p}_5)\int f_S(\boldsymbol{p}_4,s_S)\int s\psi_{FC,DX}(\boldsymbol{p}_5,s-s_S-s_A)ds ds_S ds_A\\ &+\mathcal{B}_c(\boldsymbol{p},\boldsymbol{p}_1)\mathcal{K}_E(\boldsymbol{p}_1,\boldsymbol{p}_3)\int f_E(\boldsymbol{p}_1,s_E)\int\psi^{DX}_{FC,DX}(\boldsymbol{p}_3,s_3)\mathcal{B}_{DX}(\boldsymbol{p}_1,\boldsymbol{p}_6)\int\psi^{DX}_{FC,DX}(\boldsymbol{p}_6,s_6)\\ &\times\mathcal{B}_t(\boldsymbol{p},\boldsymbol{p}_4)\mathcal{S}(\boldsymbol{p}_4,\boldsymbol{p}_5)\int f_S(\boldsymbol{p}_4,s_S)\\ &\times\int s\psi_{FC,DX}(\boldsymbol{p}_5,s-s_S-s_6-s_3-s_E)ds ds_S ds_6 ds_3 ds_E.\end{aligned} \tag{56}$$

Setting $q = s - s_S - s_A$ and $r = s - s_S - s_6 - s_3 - s_E$,

$$\begin{aligned}\Psi_{FC,DX}(\boldsymbol{p}) = {} & \mathcal{B}_c(\boldsymbol{p},\boldsymbol{p}_1)\mathcal{K}_A(\boldsymbol{p}_1,\boldsymbol{p}_2)\int f_A(\boldsymbol{p}_1,s_A) \\ & \times \mathcal{B}_t(\boldsymbol{p},\boldsymbol{p}_4)\mathcal{S}(\boldsymbol{p}_4,\boldsymbol{p}_5)\int f_S(\boldsymbol{p}_4,s_S)\int (q+s_S+s_A)\psi_{FC,DX}(\boldsymbol{p}_5,q)dq ds_S ds_A \\ & + \mathcal{B}_c(\boldsymbol{p},\boldsymbol{p}_1)\mathcal{K}_E(\boldsymbol{p}_1,\boldsymbol{p}_3)\int f_E(\boldsymbol{p}_1,s_E)\int \psi^{DX}_{FC,DX}(\boldsymbol{p}_3,s_3)\mathcal{B}_{DX}(\boldsymbol{p}_1,\boldsymbol{p}_6)\int \psi^{DX}_{FC,DX}(\boldsymbol{p}_6,s_6) \\ & \times \mathcal{B}_t(\boldsymbol{p},\boldsymbol{p}_4)\mathcal{S}(\boldsymbol{p}_4,\boldsymbol{p}_5)\int f_S(\boldsymbol{p}_4,s_S) \\ & \times \int (r+s_S+s_6+s_3+s_E)\psi_{FC,DX}(\boldsymbol{p}_5,r)dr ds_S ds_6 ds_3 ds_E.\end{aligned} \tag{57}$$

Distributing $(q + s_S + s_A)$ and $(r + s_S + s_6 + s_3 + s_E)$,

$$\begin{aligned}\Psi_{FC,DX}(\boldsymbol{p}) = {} & \mathcal{B}_c(\boldsymbol{p},\boldsymbol{p}_1)\mathcal{K}_A(\boldsymbol{p}_1,\boldsymbol{p}_2) \\ & \times \Bigg(\int f_A(\boldsymbol{p}_1,s_A)ds_A\mathcal{B}_t(\boldsymbol{p},\boldsymbol{p}_4)\mathcal{S}(\boldsymbol{p}_4,\boldsymbol{p}_5)\int f_S(\boldsymbol{p}_4,s_S)ds_S\int q\psi_{FC,DX}(\boldsymbol{p}_5,q)dq \\ & + \int f_A(\boldsymbol{p}_1,s_A)ds_A\mathcal{B}_t(\boldsymbol{p},\boldsymbol{p}_4)\mathcal{S}(\boldsymbol{p}_4,\boldsymbol{p}_5)\int s_S f_S(\boldsymbol{p}_4,s_S)ds_S\int \psi_{FC,DX}(\boldsymbol{p}_5,q)dq \\ & + \int s_A f_A(\boldsymbol{p}_1,s_A)ds_A\mathcal{B}_t(\boldsymbol{p},\boldsymbol{p}_4)\mathcal{S}(\boldsymbol{p}_4,\boldsymbol{p}_5)\int f_S(\boldsymbol{p}_4,s_S)ds_S\int \psi_{FC,DX}(\boldsymbol{p}_5,q)dq\Bigg) \\ & + \mathcal{B}_c(\boldsymbol{p},\boldsymbol{p}_1)\mathcal{K}_E(\boldsymbol{p}_1,\boldsymbol{p}_3) \\ & \times \Bigg(\int f_E(\boldsymbol{p}_1,s_E)ds_E\int \psi^{DX}_{FC,DX}(\boldsymbol{p}_3,s_3)ds_3\mathcal{B}_{DX}(\boldsymbol{p}_1,\boldsymbol{p}_6)\int \psi^{DX}_{FC,DX}(\boldsymbol{p}_6,s_6)ds_6 \\ & \times \mathcal{B}_t(\boldsymbol{p},\boldsymbol{p}_4)\mathcal{S}(\boldsymbol{p}_4,\boldsymbol{p}_5)\int f_S(\boldsymbol{p}_4,s_S)ds_S\int r\psi_{FC,DX}(\boldsymbol{p}_5,r)dr \\ & + \int f_E(\boldsymbol{p}_1,s_E)ds_E\int \psi^{DX}_{FC,DX}(\boldsymbol{p}_3,s_3)ds_3\mathcal{B}_{DX}(\boldsymbol{p}_1,\boldsymbol{p}_6)\int \psi^{DX}_{FC,DX}(\boldsymbol{p}_6,s_6)ds_6 \\ & \times \mathcal{B}_t(\boldsymbol{p},\boldsymbol{p}_4)\mathcal{S}(\boldsymbol{p}_4,\boldsymbol{p}_5)\int s_S f_S(\boldsymbol{p}_4,s_S)ds_S\int \psi_{FC,DX}(\boldsymbol{p}_5,r)dr \\ & + \int f_E(\boldsymbol{p}_1,s_E)ds_E\int \psi^{DX}_{FC,DX}(\boldsymbol{p}_3,s_3)ds_3\mathcal{B}_{DX}(\boldsymbol{p}_1,\boldsymbol{p}_6)\int s_6\psi^{DX}_{FC,DX}(\boldsymbol{p}_6,s_6)ds_6 \\ & \times \mathcal{B}_t(\boldsymbol{p},\boldsymbol{p}_4)\mathcal{S}(\boldsymbol{p}_4,\boldsymbol{p}_5)\int f_S(\boldsymbol{p}_4,s_S)ds_S\int \psi_{FC,DX}(\boldsymbol{p}_5,r)dr \\ & + \int f_E(\boldsymbol{p}_1,s_E)ds_E\int s_3\psi^{DX}_{FC,DX}(\boldsymbol{p}_3,s_3)ds_3\mathcal{B}_{DX}(\boldsymbol{p}_1,\boldsymbol{p}_6)\int \psi^{DX}_{FC,DX}(\boldsymbol{p}_6,s_6)ds_6 \\ & \times \mathcal{B}_t(\boldsymbol{p},\boldsymbol{p}_4)\mathcal{S}(\boldsymbol{p}_4,\boldsymbol{p}_5)\int f_S(\boldsymbol{p}_4,s_S)ds_S\int \psi_{FC,DX}(\boldsymbol{p}_5,r)dr \\ & + \int s_E f_E(\boldsymbol{p}_1,s_E)ds_E\int \psi^{DX}_{FC,DX}(\boldsymbol{p}_3,s_3)ds_3\mathcal{B}_{DX}(\boldsymbol{p}_1,\boldsymbol{p}_6)\int \psi^{DX}_{FC,DX}(\boldsymbol{p}_6,s_6)ds_6 \\ & \times \mathcal{B}_t(\boldsymbol{p},\boldsymbol{p}_4)\mathcal{S}(\boldsymbol{p}_4,\boldsymbol{p}_5)\int f_S(\boldsymbol{p}_4,s_S)ds_S\int \psi_{FC,DX}(\boldsymbol{p}_5,r)dr\Bigg).\end{aligned} \tag{58}$$

Defining $\bar{s}(\boldsymbol{p}) = \int s f_e(\boldsymbol{p}, s) ds$, using the fact that the integration of PDFs over their full domain results in unity, and using Eq. 53,

$$\begin{aligned}
\Psi_{FC,DX}(\boldsymbol{p}) = {} & \mathcal{B}_c(\boldsymbol{p},\boldsymbol{p}_1)\mathcal{K}_A(\boldsymbol{p}_1,\boldsymbol{p}_2) \\
& \times (\mathcal{B}_t(\boldsymbol{p},\boldsymbol{p}_4)\mathcal{S}(\boldsymbol{p}_4,\boldsymbol{p}_5)\Psi_{FC,DX}(\boldsymbol{p}_5) \\
& + \mathcal{B}_t(\boldsymbol{p},\boldsymbol{p}_4)\mathcal{S}(\boldsymbol{p}_4,\boldsymbol{p}_5)\bar{s}_S(\boldsymbol{p}_4) \\
& + \bar{s}_A(\boldsymbol{p}_1)\mathcal{B}_t(\boldsymbol{p},\boldsymbol{p}_4)\mathcal{S}(\boldsymbol{p}_4,\boldsymbol{p}_5)) \\
& + \mathcal{B}_c(\boldsymbol{p},\boldsymbol{p}_1)\mathcal{K}_E(\boldsymbol{p}_1,\boldsymbol{p}_3) \\
& \times (\mathcal{B}_{DX}(\boldsymbol{p}_1,\boldsymbol{p}_6)\mathcal{B}_t(\boldsymbol{p},\boldsymbol{p}_4)\mathcal{S}(\boldsymbol{p}_4,\boldsymbol{p}_5)\Psi_{FC,DX}(\boldsymbol{p}_5) \\
& + \mathcal{B}_{DX}(\boldsymbol{p}_1,\boldsymbol{p}_6)\mathcal{B}_t(\boldsymbol{p},\boldsymbol{p}_4)\mathcal{S}(\boldsymbol{p}_4,\boldsymbol{p}_5)\bar{s}_S(\boldsymbol{p}_4) \\
& + \mathcal{B}_{DX}(\boldsymbol{p}_1,\boldsymbol{p}_6)\Psi^{DX}_{FC,DX}(\boldsymbol{p}_6)\mathcal{B}_t(\boldsymbol{p},\boldsymbol{p}_4)\mathcal{S}(\boldsymbol{p}_4,\boldsymbol{p}_5) \\
& + \Psi^{DX}_{FC,DX}(\boldsymbol{p}_3)\mathcal{B}_{DX}(\boldsymbol{p}_1,\boldsymbol{p}_6)\mathcal{B}_t(\boldsymbol{p},\boldsymbol{p}_4)\mathcal{S}(\boldsymbol{p}_4,\boldsymbol{p}_5) \\
& + \bar{s}_E(\boldsymbol{p}_1)\mathcal{B}_{DX}(\boldsymbol{p}_1,\boldsymbol{p}_6)\mathcal{B}_t(\boldsymbol{p},\boldsymbol{p}_4)\mathcal{S}(\boldsymbol{p}_4,\boldsymbol{p}_5)).
\end{aligned} \tag{59}$$

Using the property of the surface-crossing, flight-to-transmission, and flight-to-DXTRAN operators evident from Eqs. 188, 192, and 193 respectively, that they reduce to unity when acting on nothing yields the final result,

$$\begin{aligned}
\Psi_{FC,DX}(\boldsymbol{p}) = {} & \mathcal{B}_c(\boldsymbol{p},\boldsymbol{p}_1)\mathcal{K}_A(\boldsymbol{p}_1,\boldsymbol{p}_2) \\
& \times (\bar{s}_A(\boldsymbol{p}_1) + \mathcal{B}_t(\boldsymbol{p},\boldsymbol{p}_4)\mathcal{S}(\boldsymbol{p}_4,\boldsymbol{p}_5)(\bar{s}_S(\boldsymbol{p}_4) + \Psi_{FC,DX}(\boldsymbol{p}_5))) \\
& + \mathcal{B}_c(\boldsymbol{p},\boldsymbol{p}_1)\mathcal{K}_E(\boldsymbol{p}_1,\boldsymbol{p}_3) \\
& \times \big(\bar{s}_E(\boldsymbol{p}_1) + \Psi^{DX}_{FC,DX}(\boldsymbol{p}_3) + \mathcal{B}_{DX}(\boldsymbol{p}_1,\boldsymbol{p}_6)\Psi^{DX}_{FC,DX}(\boldsymbol{p}_6) \\
& + \mathcal{B}_t(\boldsymbol{p},\boldsymbol{p}_4)\mathcal{S}(\boldsymbol{p}_4,\boldsymbol{p}_5)(\bar{s}_S(\boldsymbol{p}_4) + \Psi_{FC,DX}(\boldsymbol{p}_5))\big), \ \boldsymbol{p} \in \{\boldsymbol{p}_{FC}\}.
\end{aligned} \tag{60}$$

Comparing Eq. 60 with Eq. 42, the only difference is the addition of the branch containing the flight-to-DXTRAN operator and the recursion $\Psi^{DX}_{FC,DX}$ rather than an analog form.

4 Proof that the Forced-Collision Technique is Unbiased

The forced-collision variance-reduction technique is shown to be fair by reducing the HSME derived for transport with the technique in play to the analog HSME. This is done by using the definitions of several transport operators given in Appendix A to cast both the analog and forced-collision HSME into characteristic coordinates in which the two may be directly compared. In this technique, particle weight is adjusted before making contributions to the total history score in a single random-walk step, so the weight of the particle must be explicitly considered when reducing the forced-collision HSME to the analog HSME.

4.1 Forced Collisions Not Specified

Recall that the forced-collision HSME takes two forms depending on whether forced collisions are specified in a given phase space. In the case that forced collisions are not specified, the forced-collision HSME is given by Eq. 36. Note that Eq. 36 is identical to the analog HSME given by Eq. 34 except that it is recursive with itself and Ψ_{FC}. The recursion with Ψ_{FC} is used to account for the particle leaving the current cell and entering one with forced collisions specified. Temporarily assuming that $\Psi_{FC}(\boldsymbol{p}) = \Psi_0(\boldsymbol{p}),\ \boldsymbol{p} \in \{\boldsymbol{p}_{FC}\}$, Eq. 36 becomes

$$\begin{aligned}
\Psi^0_{FC}(\boldsymbol{p}) = {} & \mathcal{T}(\boldsymbol{p},\boldsymbol{p}_1)\mathcal{K}_A(\boldsymbol{p}_1,\boldsymbol{p}_2)\bar{s}_A(\boldsymbol{p}_1) \\
& + \mathcal{T}(\boldsymbol{p},\boldsymbol{p}_1)\mathcal{K}_E(\boldsymbol{p}_1,\boldsymbol{p}_3)\big(\bar{s}_E(\boldsymbol{p}_1) + \Psi^0_{FC}(\boldsymbol{p}_3)\big) \\
& + \mathcal{T}(\boldsymbol{p},\boldsymbol{p}_4)\mathcal{S}(\boldsymbol{p}_4,\boldsymbol{p}_5)(\bar{s}_S(\boldsymbol{p}_4) + \Psi_0(\boldsymbol{p}_5)), \ \boldsymbol{p} \notin \{\boldsymbol{p}_{FC}\},
\end{aligned} \tag{61}$$

which is equivalent to Eq. 34. In other words, if the technique is shown to be fair where forced collisions are specified, then the technique is also known to be fair in the phase spaces of a simulation with the technique in play where forced collisions are not specified by Eq. 61. Because the forced-collision HSME is defined for two recursively interdependent cases, this temporary assumption must be made for one before the other can be shown to be fair. Here, the assumption is made for the simpler of the two cases. The unbiased first moment of the technique where forced collision are specified is shown in Sec. 4.2, proving the validity of Eq. 61.

4.2 Forced Collisions Specified

Unlike the trivial evidence of equivalence between the forced-collision HSME and the analog HSME given in Sec. 4.1, work must be done to reduce the forced-collision HSME in phase spaces where forced collisions are specified to the analog HSME. The analog HSME is cast into characteristic coordinates followed by the forced-collision HSME and they are shown to be equivalent in this form. When the forced-collision technique is played, weight adjustment is performed in a single random-walk step prior to particle-score contributions. This means that average score contribution terms, $\bar{s}_A$, $\bar{s}_E$, and $\bar{s}_S$, must be decomposed into a form that allows consideration of the weight of the particle when scoring to compare the forced-collision HSME to the analog HSME. For many applications, the average score contributed at a given event is the product of the weight of the particle and some event-specific multiplicative factor,

$$\bar{s}_e(\boldsymbol{p}) = w \cdot m_e(\boldsymbol{x}, \hat{\boldsymbol{\Omega}}, E) \equiv w \cdot m_e(\boldsymbol{r}). \tag{62}$$

This multiplicative factor may often be one but is included here for generality. A possible alternative value of the multiplicative constant is the cross section of a reaction, in which case the expected score of the tally is the expected reaction rate. Here, the general form is assumed for all score contributions.

4.2.1 Analog HSME in Characteristic Coordinates

To convert to characteristic coordinates, Eq. 34 is first written with the free-flight transmission operator expanded using Eq. 187 and the score contributions expanded with Eq. 62,

$$\begin{aligned}
\Psi_0(\boldsymbol{p}) = &\int_{\boldsymbol{x}\in\{\boldsymbol{x}_\Gamma\}} \int_{4\pi} \int_0^\infty \int_{-\infty}^\infty \exp(-\ell(\boldsymbol{x}, \boldsymbol{x}_1))\delta(\hat{\boldsymbol{\Omega}}_1 - \hat{\boldsymbol{\Omega}})\delta(E_1 - E)\delta(w_1 - w) \\
&\times \mathcal{K}_A(\boldsymbol{p}_1, \boldsymbol{p}_2) w_1 m_A(\boldsymbol{r}_1) dw_1 dE_1 d\Omega_1 dx_1 \\
&+ \int_{\boldsymbol{x}\in\{\boldsymbol{x}_\Gamma\}} \int_{4\pi} \int_0^\infty \int_{-\infty}^\infty \exp(-\ell(\boldsymbol{x}, \boldsymbol{x}_1))\delta(\hat{\boldsymbol{\Omega}}_1 - \hat{\boldsymbol{\Omega}})\delta(E_1 - E)\delta(w_1 - w) \\
&\times \mathcal{K}_E(\boldsymbol{p}_1, \boldsymbol{p}_3)(w_1 m_E(\boldsymbol{r}_1) + \Psi_0(\boldsymbol{p}_3)) dw_1 dE_1 d\Omega_1 dx_1 \\
&+ \int_{\boldsymbol{x}\in\{\boldsymbol{x}_\Gamma\}} \int_{4\pi} \int_0^\infty \int_{-\infty}^\infty \exp(-\ell(\boldsymbol{x}, \boldsymbol{x}_4))\delta(\hat{\boldsymbol{\Omega}}_4 - \hat{\boldsymbol{\Omega}})\delta(E_4 - E)\delta(w_4 - w) \\
&\times \mathcal{S}(\boldsymbol{p}_4, \boldsymbol{p}_5)(w_4 m_S(\boldsymbol{r}_4) + \Psi_0(\boldsymbol{p}_5)) dw_4 dE_4 d\Omega_4 dx_4.
\end{aligned} \tag{63}$$

Evaluating integrals over dimensions with Dirac delta functions specified,

$$\begin{aligned}
\Psi_0(\boldsymbol{p}) = &\int_{\boldsymbol{x}\in\{\boldsymbol{x}_\Gamma\}} \exp(-\ell(\boldsymbol{x}, \boldsymbol{x}_1))\mathcal{K}_A(\boldsymbol{x}_1, \hat{\boldsymbol{\Omega}}, E, w, \boldsymbol{p}_2) w m_A(\boldsymbol{x}_1, \hat{\boldsymbol{\Omega}}, E) dx_1 \\
&+ \int_{\boldsymbol{x}\in\{\boldsymbol{x}_\Gamma\}} \exp(-\ell(\boldsymbol{x}, \boldsymbol{x}_1))\mathcal{K}_E(\boldsymbol{x}_1, \hat{\boldsymbol{\Omega}}, E, w, \boldsymbol{p}_3)\Big(w m_E(\boldsymbol{x}_1, \hat{\boldsymbol{\Omega}}, E) + \Psi_0(\boldsymbol{p}_3)\Big) dx_1 \\
&+ \int_{\boldsymbol{x}\in\{\boldsymbol{x}_\Gamma\}} \exp(-\ell(\boldsymbol{x}, \boldsymbol{x}_4))\mathcal{S}(\boldsymbol{x}_4, \hat{\boldsymbol{\Omega}}, E, w, \boldsymbol{p}_5)\Big(w m_S(\boldsymbol{x}_4, \hat{\boldsymbol{\Omega}}, E) + \Psi_0(\boldsymbol{p}_5)\Big) dx_4.
\end{aligned} \tag{64}$$

Inserting the definitions of all remaining operators, given in Appendix A,

$$\begin{aligned}\Psi_0(\boldsymbol{p}) = &\int_{\boldsymbol{x}\in\{\boldsymbol{x}_\Gamma\}} \exp(-\ell(\boldsymbol{x},\boldsymbol{x}_1))\\ &\times \int \Sigma_a(\boldsymbol{x}_1,E)\delta(\boldsymbol{x}_2-\boldsymbol{x}_1)\delta(\hat{\boldsymbol{\Omega}}_2-\hat{\boldsymbol{\Omega}})\delta(E_2-E)\delta(w_2-0)wm_A(\boldsymbol{x}_1,\hat{\boldsymbol{\Omega}},E)d\boldsymbol{p}_2dx_1\\ &+\int_{\boldsymbol{x}\in\{\boldsymbol{x}_\Gamma\}} \exp(-\ell(\boldsymbol{x},\boldsymbol{x}_1))\\ &\times \int \Sigma_s(\boldsymbol{x}_1,\hat{\boldsymbol{\Omega}}\to\hat{\boldsymbol{\Omega}}_3,E\to E_3)\delta(\boldsymbol{x}_3-\boldsymbol{x}_1)\delta(w_3-w)\Big(wm_E(\boldsymbol{x}_1,\hat{\boldsymbol{\Omega}},E)+\Psi_0(\boldsymbol{p}_3)\Big)d\boldsymbol{p}_3dx_1\\ &+\exp(-\ell(\boldsymbol{x},\boldsymbol{x}_S(\boldsymbol{x},\hat{\boldsymbol{\Omega}})))\\ &\times\int \delta(\boldsymbol{x}_5-\boldsymbol{x}_S(\boldsymbol{x},\hat{\boldsymbol{\Omega}}))\delta(\hat{\boldsymbol{\Omega}}_5-\hat{\boldsymbol{\Omega}})\delta(E_5-E)\delta(w_5-w)\Big(wm_S(\boldsymbol{x}_S(\boldsymbol{x},\hat{\boldsymbol{\Omega}}),\hat{\boldsymbol{\Omega}},E)+\Psi_0(\boldsymbol{p}_5)\Big)d\boldsymbol{p}_5.\end{aligned} \tag{65}$$

Note that Eq. 65 assumes that the next surface is not a system boundary for ease of notation; the opposite case is considered when analyzing the third term in isolation for brevity, see Eq. 96. Evaluating the integration over the dimensions of $\boldsymbol{p}_2$, $\boldsymbol{p}_3$, and $\boldsymbol{p}_5$ that have Dirac delta functions,

$$\begin{aligned}\Psi_0(\boldsymbol{p}) = &\int_{\boldsymbol{x}\in\{\boldsymbol{x}_\Gamma\}} \exp(-\ell(\boldsymbol{x},\boldsymbol{x}_1))\Sigma_a(\boldsymbol{x}_1,E)wm_A(\boldsymbol{x}_1,\hat{\boldsymbol{\Omega}},E)dx_1\\ &+\int_{\boldsymbol{x}\in\{\boldsymbol{x}_\Gamma\}} \exp(-\ell(\boldsymbol{x},\boldsymbol{x}_1))\iint \Sigma_s(\boldsymbol{x}_1,\hat{\boldsymbol{\Omega}}\to\hat{\boldsymbol{\Omega}}_3,E\to E_3)\\ &\times\Big(wm_E(\boldsymbol{x}_1,\hat{\boldsymbol{\Omega}},E)+\Psi_0(\boldsymbol{x}_1,\hat{\boldsymbol{\Omega}}_3,E_3,w)\Big)d\Omega_3dE_3dx_1\\ &+\exp(-\ell(\boldsymbol{x},\boldsymbol{x}_S(\boldsymbol{x},\hat{\boldsymbol{\Omega}})))\Big(wm_S(\boldsymbol{x}_S(\boldsymbol{x},\hat{\boldsymbol{\Omega}}),\hat{\boldsymbol{\Omega}},E)+\Psi_0(\boldsymbol{x}_S(\boldsymbol{x},\hat{\boldsymbol{\Omega}}),\hat{\boldsymbol{\Omega}},E,w)\Big).\end{aligned} \tag{66}$$

Using $\boldsymbol{x}_1=\boldsymbol{x}+a\hat{\boldsymbol{\Omega}}$ yields Ψ_0 in characteristic form,

$$\begin{aligned}\Psi_0(\boldsymbol{p}) = &\int_0^{a_S(\boldsymbol{x},\hat{\boldsymbol{\Omega}})} \exp(-\ell(\boldsymbol{x},\boldsymbol{x}+a\hat{\boldsymbol{\Omega}}))\Sigma_a(\boldsymbol{x}+a\hat{\boldsymbol{\Omega}},E)wm_A(\boldsymbol{x}+a\hat{\boldsymbol{\Omega}},\hat{\boldsymbol{\Omega}},E)da\\ &+\int_0^{a_S(\boldsymbol{x},\hat{\boldsymbol{\Omega}})} \exp(-\ell(\boldsymbol{x},\boldsymbol{x}+a\hat{\boldsymbol{\Omega}}))\iint \Sigma_s(\boldsymbol{x}+a\hat{\boldsymbol{\Omega}},\hat{\boldsymbol{\Omega}}\to\hat{\boldsymbol{\Omega}}_3,E\to E_3)\\ &\times\Big(wm_E(\boldsymbol{x}+a\hat{\boldsymbol{\Omega}},\hat{\boldsymbol{\Omega}},E)+\Psi_0(\boldsymbol{x}+a\hat{\boldsymbol{\Omega}},\hat{\boldsymbol{\Omega}}_3,E_3,w)\Big)d\Omega_3dE_3da\\ &+\exp(-\ell(\boldsymbol{x},\boldsymbol{x}+a_S(\boldsymbol{x},\hat{\boldsymbol{\Omega}})\hat{\boldsymbol{\Omega}}))\Big(wm_S(\boldsymbol{x}+a_S(\boldsymbol{x},\hat{\boldsymbol{\Omega}})\hat{\boldsymbol{\Omega}},\hat{\boldsymbol{\Omega}},E)+\Psi_0(\boldsymbol{x}+a_S(\boldsymbol{x},\hat{\boldsymbol{\Omega}})\hat{\boldsymbol{\Omega}},\hat{\boldsymbol{\Omega}},E,w)\Big),\end{aligned} \tag{67}$$

where a_S is the distance from $\boldsymbol{x}$ along $\hat{\boldsymbol{\Omega}}$ to the first intersection with a surface.

4.2.2 Forced-Collision HSME in Characteristic Coordinates

In phase spaces in which forced collisions are specified, the forced-collision HSME takes the form of Eq. 42. Rearranging terms of Eq. 42 and applying Eq. 62,

$$\begin{aligned}\Psi_{FC}(\boldsymbol{p}) = &\,\mathcal{B}_c(\boldsymbol{p},\boldsymbol{p}_1)\mathcal{K}_A(\boldsymbol{p}_1,\boldsymbol{p}_2)w_1m_A(\boldsymbol{r}_1)\\ &+\mathcal{B}_c(\boldsymbol{p},\boldsymbol{p}_1)\mathcal{K}_E(\boldsymbol{p}_1,\boldsymbol{p}_3)\big(w_1m_E(\boldsymbol{r}_1)+\Psi^0_{FC}(\boldsymbol{p}_3)\big)\\ &+(\mathcal{B}_c(\boldsymbol{p},\boldsymbol{p}_1)\mathcal{K}_A(\boldsymbol{p}_1,\boldsymbol{p}_2)+\mathcal{B}_c(\boldsymbol{p},\boldsymbol{p}_1)\mathcal{K}_E(\boldsymbol{p}_1,\boldsymbol{p}_3))\\ &\times\mathcal{B}_t(\boldsymbol{p},\boldsymbol{p}_4)\mathcal{S}(\boldsymbol{p}_4,\boldsymbol{p}_5)(w_4m_S(\boldsymbol{r}_4)+\Psi_{FC}(\boldsymbol{p}_5)),\ \boldsymbol{p}\in\{\boldsymbol{p}_{FC}\}.\end{aligned} \tag{68}$$

Each term of Eq. 68 is now cast into characteristic coordinates and shown to be identical to the corresponding terms of Eq. 67. For ease of notation, $\boldsymbol{p}\in\{\boldsymbol{p}_{FC}\}$ is temporarily dropped.

First, considering only the first term of Eq. 68 and applying the definition of the flight-to-collision operator given in Eq. 191,

$$\begin{aligned}\text{Term}_1 = &\int_{\boldsymbol{x}\in\{\boldsymbol{x}_\Gamma\}}\int_{4\pi}\int_0^\infty\int_{-\infty}^\infty \frac{\exp(-\ell(\boldsymbol{x},\boldsymbol{x}_1))}{1-\exp(-\ell(\boldsymbol{x},\boldsymbol{x}_S(\boldsymbol{x},\hat{\boldsymbol{\Omega}})))}\delta(\hat{\boldsymbol{\Omega}}_1-\hat{\boldsymbol{\Omega}})\delta(E_1-E)\delta(w_1-w_c)\\ &\times \mathcal{K}_A(\boldsymbol{p}_1,\boldsymbol{p}_2)w_1 m_A(\boldsymbol{r}_1)dw_1dE_1d\Omega_1dx_1.\end{aligned} \tag{69}$$

Evaluating integrals over dimensions with Dirac delta functions,

$$\text{Term}_1 = \int_{\boldsymbol{x}\in\{\boldsymbol{x}_\Gamma\}}\frac{\exp(-\ell(\boldsymbol{x},\boldsymbol{x}_1))}{1-\exp(-\ell(\boldsymbol{x},\boldsymbol{x}_S(\boldsymbol{x},\hat{\boldsymbol{\Omega}})))}\mathcal{K}_A(\boldsymbol{x}_1,\hat{\boldsymbol{\Omega}},E,w_c,\boldsymbol{p}_2)w_c m_A(\boldsymbol{x}_1,\hat{\boldsymbol{\Omega}},E)dx_1. \tag{70}$$

Using the definition of the absorptive collision operator given by Eq. 189,

$$\begin{aligned}\text{Term}_1 = &\int_{\boldsymbol{x}\in\{\boldsymbol{x}_\Gamma\}}\frac{\exp(-\ell(\boldsymbol{x},\boldsymbol{x}_1))}{1-\exp(-\ell(\boldsymbol{x},\boldsymbol{x}_S(\boldsymbol{x},\hat{\boldsymbol{\Omega}})))}\\ &\times\int \Sigma_a(\boldsymbol{x}_1,E)\delta(\boldsymbol{x}_2-\boldsymbol{x}_1)\delta(\hat{\boldsymbol{\Omega}}_2-\hat{\boldsymbol{\Omega}})\delta(E_2-E)\delta(w_2-0)w_c m_A(\boldsymbol{x}_1,\hat{\boldsymbol{\Omega}},E)d\boldsymbol{p}_2dx_1.\end{aligned} \tag{71}$$

Evaluating the integration over $\boldsymbol{p}_2$,

$$\text{Term}_1 = \int_{\boldsymbol{x}\in\{\boldsymbol{x}_\Gamma\}}\frac{\exp(-\ell(\boldsymbol{x},\boldsymbol{x}_1))}{1-\exp(-\ell(\boldsymbol{x},\boldsymbol{x}_S(\boldsymbol{x},\hat{\boldsymbol{\Omega}})))}\Sigma_a(\boldsymbol{x}_1,E)w_c m_A(\boldsymbol{x}_1,\hat{\boldsymbol{\Omega}},E)dx_1. \tag{72}$$

Note that combining Eqs. 3 and 5 yields

$$w_c = w_0(1-\exp(-\ell(\boldsymbol{x},\boldsymbol{x}_S(\boldsymbol{x},\hat{\boldsymbol{\Omega}})). \tag{73}$$

Inserting Eq. 73 into Eq. 72,

$$\text{Term}_1 = \int_{\boldsymbol{x}\in\{\boldsymbol{x}_\Gamma\}}\frac{\exp(-\ell(\boldsymbol{x},\boldsymbol{x}_1))}{1-\exp(-\ell(\boldsymbol{x},\boldsymbol{x}_S(\boldsymbol{x},\hat{\boldsymbol{\Omega}})))}\Sigma_a(\boldsymbol{x}_1,E)w(1-\exp(-\ell(\boldsymbol{x},\boldsymbol{x}_S(\boldsymbol{x},\hat{\boldsymbol{\Omega}}))m_A(\boldsymbol{x}_1,\hat{\boldsymbol{\Omega}},E)dx_1. \tag{74}$$

Simplifying and using $\boldsymbol{x}_1=\boldsymbol{x}+a\hat{\boldsymbol{\Omega}}$ to convert to characteristic coordinates gives an identical expression as the first term of Eq. 67,

$$\text{Term}_1 = \int_0^{a_S(\boldsymbol{x},\hat{\boldsymbol{\Omega}})}\exp(-\ell(\boldsymbol{x},\boldsymbol{x}+a\hat{\boldsymbol{\Omega}}))\Sigma_a(\boldsymbol{x}+a\hat{\boldsymbol{\Omega}},E)w m_A(\boldsymbol{x}+a\hat{\boldsymbol{\Omega}},\hat{\boldsymbol{\Omega}},E)da. \tag{75}$$

Second, considering only the second term of Eq. 68 and again expanding the flight-to-collision operator,

$$\begin{aligned}\text{Term}_2 = &\int_{\boldsymbol{x}\in\{\boldsymbol{x}_\Gamma\}}\int_{4\pi}\int_0^\infty\int_{-\infty}^\infty \frac{\exp(-\ell(\boldsymbol{x},\boldsymbol{x}_1))}{1-\exp(-\ell(\boldsymbol{x},\boldsymbol{x}_S(\boldsymbol{x},\hat{\boldsymbol{\Omega}})))}\delta(\hat{\boldsymbol{\Omega}}_1-\hat{\boldsymbol{\Omega}})\delta(E_1-E)\delta(w_1-w_c)\\ &\times \mathcal{K}_E(\boldsymbol{p}_1,\boldsymbol{p}_3)\big(w_1 m_E(\boldsymbol{r}_1)+\Psi^0_{FC}(\boldsymbol{p}_3)\big)dw_1dE_1d\Omega_1dx_1.\end{aligned} \tag{76}$$

Evaluating the integrals over dimensions with Dirac delta functions specified,

$$\text{Term}_2 = \int_{\boldsymbol{x}\in\{\boldsymbol{x}_\Gamma\}}\frac{\exp(-\ell(\boldsymbol{x},\boldsymbol{x}_1))}{1-\exp(-\ell(\boldsymbol{x},\boldsymbol{x}_S(\boldsymbol{x},\hat{\boldsymbol{\Omega}})))}\mathcal{K}_E(\boldsymbol{x}_1,\hat{\boldsymbol{\Omega}},E,w_c,\boldsymbol{p}_3)\Big(w_c m_E(\boldsymbol{x}_1,\hat{\boldsymbol{\Omega}},E)+\Psi^0_{FC}(\boldsymbol{p}_3)\Big)dx_1. \tag{77}$$

Inserting the definition of the emissive collision operator,

$$\begin{aligned}\text{Term}_2 = &\int_{\boldsymbol{x}\in\{\boldsymbol{x}_\Gamma\}}\frac{\exp(-\ell(\boldsymbol{x},\boldsymbol{x}_1))}{1-\exp(-\ell(\boldsymbol{x},\boldsymbol{x}_S(\boldsymbol{x},\hat{\boldsymbol{\Omega}})))}\\ &\times\int \Sigma_s(\boldsymbol{x}_1,\hat{\boldsymbol{\Omega}}\to\hat{\boldsymbol{\Omega}}_3,E\to E_3)\delta(\boldsymbol{x}_3-\boldsymbol{x}_1)\delta(w_3-w_c)\Big(w_c m_E(\boldsymbol{x}_1,\hat{\boldsymbol{\Omega}},E)+\Psi^0_{FC}(\boldsymbol{p}_3)\Big)d\boldsymbol{p}_3dx_1.\end{aligned} \tag{78}$$

Again evaluating the integrals over dimensions with Dirac delta functions specified,

$$\begin{aligned}\text{Term}_2 = &\int_{\boldsymbol{x}\in\{\boldsymbol{x}_\Gamma\}} \frac{\exp(-\ell(\boldsymbol{x},\boldsymbol{x}_1))}{1-\exp(-\ell(\boldsymbol{x},\boldsymbol{x}_S(\boldsymbol{x},\hat{\boldsymbol{\Omega}})))} \\ &\times \iint \Sigma_s(\boldsymbol{x}_1,\hat{\boldsymbol{\Omega}}\to\hat{\boldsymbol{\Omega}}_3,E\to E_3)\Big(w_c m_E(\boldsymbol{x}_1,\hat{\boldsymbol{\Omega}},E) + \Psi^0_{FC}(\boldsymbol{x}_1,\hat{\boldsymbol{\Omega}}_3,E_3,w_c)\Big)d\Omega_3 dE_3 dx_1.\end{aligned} \tag{79}$$

Using Eq. 73,

$$\begin{aligned}\text{Term}_2 = &\int_{\boldsymbol{x}\in\{\boldsymbol{x}_\Gamma\}} \frac{\exp(-\ell(\boldsymbol{x},\boldsymbol{x}_1))}{1-\exp(-\ell(\boldsymbol{x},\boldsymbol{x}_S(\boldsymbol{x},\hat{\boldsymbol{\Omega}})))} \iint \Sigma_s(\boldsymbol{x}_1,\hat{\boldsymbol{\Omega}}\to\hat{\boldsymbol{\Omega}}_3,E\to E_3) \\ &\times \Big(w(1-\exp(-\ell(\boldsymbol{x},\boldsymbol{x}_S(\boldsymbol{x},\hat{\boldsymbol{\Omega}}))))m_E(\boldsymbol{x}_1,\hat{\boldsymbol{\Omega}},E) \\ &+ \Psi^0_{FC}(\boldsymbol{x}_1,\hat{\boldsymbol{\Omega}}_3,E_3,w(1-\exp(-\ell(\boldsymbol{x},\boldsymbol{x}_S(\boldsymbol{x},\hat{\boldsymbol{\Omega}})))))\Big)d\Omega_3 dE_3 dx_1.\end{aligned} \tag{80}$$

Using the separability of weight and score moment in weight-independent techniques $\Psi(\boldsymbol{r},cw) = c\Psi(\boldsymbol{r},w)$ [7],

$$\begin{aligned}\text{Term}_2 = &\int_{\boldsymbol{x}\in\{\boldsymbol{x}_\Gamma\}} \frac{\exp(-\ell(\boldsymbol{x},\boldsymbol{x}_1))}{1-\exp(-\ell(\boldsymbol{x},\boldsymbol{x}_S(\boldsymbol{x},\hat{\boldsymbol{\Omega}})))} \iint \Sigma_s(\boldsymbol{x}_1,\hat{\boldsymbol{\Omega}}\to\hat{\boldsymbol{\Omega}}_3,E\to E_3) \\ &\times (1-\exp(-\ell(\boldsymbol{x},\boldsymbol{x}_S(\boldsymbol{x},\hat{\boldsymbol{\Omega}}))))\Big(w m_E(\boldsymbol{x}_1,\hat{\boldsymbol{\Omega}},E) + \Psi^0_{FC}(\boldsymbol{x}_1,\hat{\boldsymbol{\Omega}}_3,E_3,w)\Big)d\Omega_3 dE_3 dx_1.\end{aligned} \tag{81}$$

Simplifying and using $\boldsymbol{x}_1 = \boldsymbol{x} + a\hat{\boldsymbol{\Omega}}$ to convert to characteristic coordinates gives an expression similar to the second term of Eq. 67,

$$\begin{aligned}\text{Term}_2 = &\int_0^{a_S(\boldsymbol{x},\hat{\boldsymbol{\Omega}})} \exp(-\ell(\boldsymbol{x},\boldsymbol{x}+a\hat{\boldsymbol{\Omega}})) \iint \Sigma_s(\boldsymbol{x}+a\hat{\boldsymbol{\Omega}},\hat{\boldsymbol{\Omega}}\to\hat{\boldsymbol{\Omega}}_3,E\to E_3) \\ &\times \Big(w m_E(\boldsymbol{x}+a\hat{\boldsymbol{\Omega}},\hat{\boldsymbol{\Omega}},E) + \Psi^0_{FC}(\boldsymbol{x}+a\hat{\boldsymbol{\Omega}},\hat{\boldsymbol{\Omega}}_3,E_3,w)\Big)d\Omega_3 dE_3 da.\end{aligned} \tag{82}$$

Third, considering only the third term of Eq. 68 and expanding the flight-to-collision operator,

$$\begin{aligned}\text{Term}_3 = &\Bigg(\int_{\boldsymbol{x}\in\{\boldsymbol{x}_\Gamma\}}\int_{4\pi}\int_0^\infty\int_{-\infty}^\infty \frac{\exp(-\ell(\boldsymbol{x},\boldsymbol{x}_1))}{1-\exp(-\ell(\boldsymbol{x},\boldsymbol{x}_S(\boldsymbol{x},\hat{\boldsymbol{\Omega}})))}\delta(\hat{\boldsymbol{\Omega}}_1-\hat{\boldsymbol{\Omega}})\delta(E_1-E)\delta(w_1-w_c)\mathcal{K}_A(\boldsymbol{p}_1,\boldsymbol{p}_2)d\boldsymbol{p}_1 \\ &+ \int_{\boldsymbol{x}\in\{\boldsymbol{x}_\Gamma\}}\int_{4\pi}\int_0^\infty\int_{-\infty}^\infty \frac{\exp(-\ell(\boldsymbol{x},\boldsymbol{x}_1))}{1-\exp(-\ell(\boldsymbol{x},\boldsymbol{x}_S(\boldsymbol{x},\hat{\boldsymbol{\Omega}})))}\delta(\hat{\boldsymbol{\Omega}}_1-\hat{\boldsymbol{\Omega}})\delta(E_1-E)\delta(w_1-w_c)\mathcal{K}_E(\boldsymbol{p}_1,\boldsymbol{p}_3)d\boldsymbol{p}_1\Bigg) \\ &\times \mathcal{B}_t(\boldsymbol{p},\boldsymbol{p}_4)\mathcal{S}(\boldsymbol{p}_4,\boldsymbol{p}_5)(w_4 m_S(\boldsymbol{r}_4) + \Psi_{FC}(\boldsymbol{p}_5)).\end{aligned} \tag{83}$$

Evaluating the integration over dimensions with Dirac delta functions and combining the absorptive and emissive terms,

$$\begin{aligned}\text{Term}_3 = &\int_{\boldsymbol{x}\in\{\boldsymbol{x}_\Gamma\}} \frac{\exp(-\ell(\boldsymbol{x},\boldsymbol{x}_1))}{1-\exp(-\ell(\boldsymbol{x},\boldsymbol{x}_S(\boldsymbol{x},\hat{\boldsymbol{\Omega}})))}\Big(\mathcal{K}_A(\boldsymbol{x}_1,\hat{\boldsymbol{\Omega}},E,w_c,\boldsymbol{p}_2) + \mathcal{K}_E(\boldsymbol{x}_1,\hat{\boldsymbol{\Omega}},E,w_c,\boldsymbol{p}_3)\Big)dx_1 \\ &\times \mathcal{B}_t(\boldsymbol{p},\boldsymbol{p}_4)\mathcal{S}(\boldsymbol{p}_4,\boldsymbol{p}_5)(w_4 m_S(\boldsymbol{r}_4) + \Psi_{FC}(\boldsymbol{p}_5)).\end{aligned} \tag{84}$$

Expanding the absorptive collision and emissive collision operators,

$$\begin{aligned}\text{Term}_3 = &\int_{\boldsymbol{x}\in\{\boldsymbol{x}_\Gamma\}} \frac{\exp(-\ell(\boldsymbol{x},\boldsymbol{x}_1))}{1-\exp(-\ell(\boldsymbol{x},\boldsymbol{x}_S(\boldsymbol{x},\hat{\boldsymbol{\Omega}})))} \\ &\times \Big(\int \Sigma_a(\boldsymbol{x}_1,E)\delta(\boldsymbol{x}_2-\boldsymbol{x}_1)\delta(\hat{\boldsymbol{\Omega}}_2-\hat{\boldsymbol{\Omega}})\delta(E_2-E)\delta(w_2-0)d\boldsymbol{p}_2 \\ &+ \int \Sigma_s(\boldsymbol{x}_1,\hat{\boldsymbol{\Omega}}\to\hat{\boldsymbol{\Omega}}_3,E\to E_3)\delta(\boldsymbol{x}_3-\boldsymbol{x}_1)\delta(w_3-w_c)d\boldsymbol{p}_3\Big)dx_1 \\ &\times \mathcal{B}_t(\boldsymbol{p},\boldsymbol{p}_4)\mathcal{S}(\boldsymbol{p}_4,\boldsymbol{p}_5)(w_4 m_S(\boldsymbol{r}_4) + \Psi_{FC}(\boldsymbol{p}_5)).\end{aligned} \tag{85}$$

Evaluating the integrals over the dimensions of $\boldsymbol{p}_2$ and $\boldsymbol{p}_3$ that have Dirac delta functions,

$$\begin{aligned}\text{Term}_3 = &\int_{\boldsymbol{x}\in\{\boldsymbol{x}_\Gamma\}} \frac{\exp(-\ell(\boldsymbol{x},\boldsymbol{x}_1))}{1-\exp(-\ell(\boldsymbol{x},\boldsymbol{x}_S(\boldsymbol{x},\hat{\boldsymbol{\Omega}})))} \\ &\times\left(\Sigma_a(\boldsymbol{x}_1,E)+\iint \Sigma_s(\boldsymbol{x}_1,\hat{\boldsymbol{\Omega}}\to\hat{\boldsymbol{\Omega}}_3,E\to E_3)d\Omega_3 dE_3\right)dx_1 \\ &\times \mathcal{B}_t(\boldsymbol{p},\boldsymbol{p}_4)\mathcal{S}(\boldsymbol{p}_4,\boldsymbol{p}_5)(w_4 m_S(\boldsymbol{r}_4)+\Psi_{FC}(\boldsymbol{p}_5)).\end{aligned} \tag{86}$$

Using the fact that the integration of the double-differential scattering cross section over all angles and energy results in the macroscopic scattering cross section,

$$\begin{aligned}\text{Term}_3 = &\int_{\boldsymbol{x}\in\{\boldsymbol{x}_\Gamma\}} \frac{\exp(-\ell(\boldsymbol{x},\boldsymbol{x}_1))}{1-\exp(-\ell(\boldsymbol{x},\boldsymbol{x}_S(\boldsymbol{x},\hat{\boldsymbol{\Omega}})))} \\ &\times(\Sigma_a(\boldsymbol{x}_1,E)+\Sigma_s(\boldsymbol{x}_1,E))dx_1 \\ &\times \mathcal{B}_t(\boldsymbol{p},\boldsymbol{p}_4)\mathcal{S}(\boldsymbol{p}_4,\boldsymbol{p}_5)(w_4 m_S(\boldsymbol{r}_4)+\Psi_{FC}(\boldsymbol{p}_5)).\end{aligned} \tag{87}$$

Using the definition of the total macroscopic cross section and expanding the optical thickness term using Eq. 4,

$$\begin{aligned}\text{Term}_3 = &\int_{\boldsymbol{x}\in\{\boldsymbol{x}_\Gamma\}} \frac{\Sigma_t(\boldsymbol{x}_1,E)\exp\left(-\int_0^{\|\boldsymbol{x}_1-\boldsymbol{x}\|}\Sigma_t\left(\boldsymbol{x}+a\frac{\boldsymbol{x}_1-\boldsymbol{x}}{\|\boldsymbol{x}_1-\boldsymbol{x}\|}\right)da\right)}{1-\exp\left(-\int_0^{\|\boldsymbol{x}_S-\boldsymbol{x}\|}\Sigma_t\left(\boldsymbol{x}+a\frac{\boldsymbol{x}_S-\boldsymbol{x}}{\|\boldsymbol{x}_S-\boldsymbol{x}\|}\right)da\right)}dx_1 \\ &\times \mathcal{B}_t(\boldsymbol{p},\boldsymbol{p}_4)\mathcal{S}(\boldsymbol{p}_4,\boldsymbol{p}_5)(w_4 m_S(\boldsymbol{r}_4)+\Psi_{FC}(\boldsymbol{p}_5)).\end{aligned} \tag{88}$$

Assuming a constant cross section inside the current cell and using the integral identity $\int_0^X \frac{a\cdot\exp(-a\cdot x)}{1-\exp(-a\cdot X)}dx=1$ proven in Appendix B.1,

$$\begin{aligned}\text{Term}_3 = &\cancelto{1}{\int_{\boldsymbol{x}\in\{\boldsymbol{x}_\Gamma\}} \frac{\Sigma_t\exp(-\Sigma_t\|\boldsymbol{x}_1-\boldsymbol{x}\|)}{1-\exp(-\Sigma_t\|\boldsymbol{x}_S-\boldsymbol{x}\|)}dx_1} \\ &\times \mathcal{B}_t(\boldsymbol{p},\boldsymbol{p}_4)\mathcal{S}(\boldsymbol{p}_4,\boldsymbol{p}_5)(w_4 m_S(\boldsymbol{r}_4)+\Psi_{FC}(\boldsymbol{p}_5)).\end{aligned} \tag{89}$$

Expanding the flight-to-transmission operator given by Eq. 192,

$$\text{Term}_3 = \int \delta(\boldsymbol{x}_4-\boldsymbol{x}_S(\boldsymbol{x},\hat{\boldsymbol{\Omega}}))\delta(\hat{\boldsymbol{\Omega}}_4-\hat{\boldsymbol{\Omega}})\delta(E_4-E)\delta(w_4-w_t)\mathcal{S}(\boldsymbol{p}_4,\boldsymbol{p}_5)(w_4 m_S(\boldsymbol{r}_4)+\Psi_{FC}(\boldsymbol{p}_5))d\boldsymbol{p}_4. \tag{90}$$

Evaluating the integration over $\boldsymbol{p}_4$,

$$\text{Term}_3 = \mathcal{S}(\boldsymbol{x}_S(\boldsymbol{x},\hat{\boldsymbol{\Omega}}),\hat{\boldsymbol{\Omega}},E,w_t,\boldsymbol{p}_5)\Big(w_t m_S(\boldsymbol{x}_S(\boldsymbol{x},\hat{\boldsymbol{\Omega}}),\hat{\boldsymbol{\Omega}},E)+\Psi_{FC}(\boldsymbol{p}_5)\Big). \tag{91}$$

Expanding the surface-crossing operator,

$$\begin{aligned}\text{Term}_3 = &\int \delta(\boldsymbol{x}_5-\boldsymbol{x}_S(\boldsymbol{x},\hat{\boldsymbol{\Omega}}))\delta(\hat{\boldsymbol{\Omega}}_5-\hat{\boldsymbol{\Omega}})\delta(E_5-E)\delta(w_5-w_t) \\ &\times\Big(w_t m_S(\boldsymbol{x}_S(\boldsymbol{x},\hat{\boldsymbol{\Omega}}),\hat{\boldsymbol{\Omega}},E)+\Psi_{FC}(\boldsymbol{p}_5)\Big)d\boldsymbol{p}_5.\end{aligned} \tag{92}$$

Evaluating the integration over $\boldsymbol{p}_5$,

$$\text{Term}_3 = w_t m_S(\boldsymbol{x}_S(\boldsymbol{x},\hat{\boldsymbol{\Omega}}),\hat{\boldsymbol{\Omega}},E)+\Psi_{FC}(\boldsymbol{x}_S(\boldsymbol{x},\hat{\boldsymbol{\Omega}}),\hat{\boldsymbol{\Omega}},E,w_t). \tag{93}$$

Inserting Eq. 3,

$$\begin{aligned}\text{Term}_3 = &\,w\exp(-\ell(\boldsymbol{x},\boldsymbol{x}_S(\boldsymbol{x},\hat{\boldsymbol{\Omega}})))m_S(\boldsymbol{x}_S(\boldsymbol{x},\hat{\boldsymbol{\Omega}}),\hat{\boldsymbol{\Omega}},E) \\ &+\Psi_{FC}(\boldsymbol{x}_S(\boldsymbol{x},\hat{\boldsymbol{\Omega}}),\hat{\boldsymbol{\Omega}},E,w\exp(-\ell(\boldsymbol{x},\boldsymbol{x}_S(\boldsymbol{x},\hat{\boldsymbol{\Omega}})))).\end{aligned} \tag{94}$$

Again using the separability of weight and score moment in weight-independent techniques and using $\boldsymbol{x}_S(\boldsymbol{x}, \hat{\boldsymbol{\Omega}}) = \boldsymbol{x} + a_S(\boldsymbol{x}, \hat{\boldsymbol{\Omega}})\hat{\boldsymbol{\Omega}}$ to convert to characteristic coordinates yields an expression identical to the third term of Eq. 67,

$$\begin{aligned}\text{Term}_3 = &\exp(-\ell(\boldsymbol{x}, \boldsymbol{x} + a_S(\boldsymbol{x}, \hat{\boldsymbol{\Omega}})\hat{\boldsymbol{\Omega}})) \\ &\times \Big(w m_S(\boldsymbol{x} + a_S(\boldsymbol{x}, \hat{\boldsymbol{\Omega}})\hat{\boldsymbol{\Omega}}, \hat{\boldsymbol{\Omega}}, E) + \Psi_{FC}(\boldsymbol{x} + a_S(\boldsymbol{x}, \hat{\boldsymbol{\Omega}})\hat{\boldsymbol{\Omega}}, \hat{\boldsymbol{\Omega}}, E, w) \Big).\end{aligned} \tag{95}$$

Note that Eqs. 65 and 92 assume that the surface being crossed is not a system boundary. If the opposite is assumed, the integration over statistical weight is instead $\int (\cdot) \delta(w_5 - 0) dw_5$. Evaluating this integration over weight results in a HSME that is evaluated at a weight of zero, $\Psi_{0 \text{ or } FC}(\boldsymbol{x}_S(\boldsymbol{x}, \hat{\boldsymbol{\Omega}}), \hat{\boldsymbol{\Omega}}, E, 0)$. The separability of weight and score moment then reduces this term to zero. In this case, Eq. 95 and the third term of Eq. 67 are both equivalent to

$$\text{Term}_3 = \exp(-\ell(\boldsymbol{x}, \boldsymbol{x} + a_S(\boldsymbol{x}, \hat{\boldsymbol{\Omega}})\hat{\boldsymbol{\Omega}})) w m_S(\boldsymbol{x} + a_S(\boldsymbol{x}, \hat{\boldsymbol{\Omega}})\hat{\boldsymbol{\Omega}}, \hat{\boldsymbol{\Omega}}, E). \tag{96}$$

Finally, combining Eqs. 75, 82, and 95 results in the characteristic form of the forced-collision HSME,

$$\begin{aligned}\Psi_{FC}(\boldsymbol{p}) = &\int_0^{a_S(\boldsymbol{x}, \hat{\boldsymbol{\Omega}})} \exp(-\ell(\boldsymbol{x}, \boldsymbol{x} + a\hat{\boldsymbol{\Omega}})) \Sigma_a(\boldsymbol{x} + a\hat{\boldsymbol{\Omega}}, E) w m_A da. \\ &+ \int_0^{a_S(\boldsymbol{x}, \hat{\boldsymbol{\Omega}})} \exp(-\ell(\boldsymbol{x}, \boldsymbol{x} + a\hat{\boldsymbol{\Omega}})) \iint \Sigma_s(\boldsymbol{x} + a\hat{\boldsymbol{\Omega}}, \hat{\boldsymbol{\Omega}} \to \hat{\boldsymbol{\Omega}}_3, E \to E_3) \\ &\times \Big(w m_E + \Psi^0_{FC}(\boldsymbol{x} + a\hat{\boldsymbol{\Omega}}, \hat{\boldsymbol{\Omega}}_3, E_3, w) \Big) d\Omega_3 dE_3 da. \\ &+ \exp(-\ell(\boldsymbol{x}, \boldsymbol{x} + a_S(\boldsymbol{x}, \hat{\boldsymbol{\Omega}})\hat{\boldsymbol{\Omega}})) \Big(w m_S + \Psi_{FC}(\boldsymbol{x} + a_S(\boldsymbol{x}, \hat{\boldsymbol{\Omega}})\hat{\boldsymbol{\Omega}}, \hat{\boldsymbol{\Omega}}, E, w) \Big), \ \boldsymbol{p} \in \{\boldsymbol{p}_{FC}\}.\end{aligned} \tag{97}$$

Compared with the characteristic form of the analog HSME given in Eq. 67, Eq. 97 is identical except that it is recursive with Ψ_{FC} and Ψ^0_{FC}. Recall from Eq. 61 that the forced-collision HSME is equivalent to the analog HSME where forced collisions are not specified. Eq. 97 shows that the forced-collision HSME is equivalent to the analog HSME except where forced collisions aren't specified. Considered together, Eqs. 61 and 97 prove that the forced-collision HSME is equivalent to the analog HSME for all phase spaces, so the technique played in isolation is shown to be unbiased,

$$\Psi_{FC}(\boldsymbol{p}) = \Psi_0(\boldsymbol{p}). \tag{98}$$

5 Proof that the DXTRAN Technique is Unbiased

The DXTRAN variance-reduction technique is shown to be fair by reducing the corresponding HSME down to the analog HSME. This is done by first separating the HSMEs into two equations, the α/β form, and then casting them into characteristic coordinates using the formal definition of transport operators given in Appendix A. In characteristic coordinates, the DXTRAN HSME is shown to reduce to the analog HSME, demonstrating that the technique does not alter first-moment results, making it unbiased. Note that, unlike the forced-collision technique, weight adjustment is not performed directly prior to score contributions. This allows weight adjustment to be accounted for solely through the separation of weight and score moment used in Eq. 122. As a result, the average score contribution terms, $\bar{s}_A$, $\bar{s}_E$, and $\bar{s}_S$, are not decomposed into any particular form such as that in Eq. 62.

5.1 History Score Moment Equations in α/β Form

Eq. 52 gives the expected score of a particle history continuing on from any point in phase space; however, the DXTRAN variance-reduction technique is not a fair technique when considering an arbitrary portion of the particle history. The DXTRAN technique disallows particles from entering the DXTRAN region through normal transport, so the conservation of statistical weight is dependent on DXTRAN particles spawned following the construction of the particle from the source or collisions prior to entering a region. To show fairness, Eq. 52 is analyzed at DXTRAN particle creation by breaking the equation into two different forms, with each governing a different set of points in particle transport. The first form, termed the α form, governs a particle immediately following construction from the source or emission from a collision. The second form, termed the β form, governs a particle at all other points in the history. For direct comparison, the α/β forms of both the analog and DXTRAN HSMEs are derived.

To find the DXTRAN HSME at these points, Eq. 52 is first written with the terms following the emissive collision operator combined,

$$\begin{aligned}\Psi_{DX}(\boldsymbol{p}) = {} & \mathcal{T}_{DX}(\boldsymbol{p},\boldsymbol{p}_1)\mathcal{K}_A(\boldsymbol{p}_1,\boldsymbol{p}_2)\bar{s}_A(\boldsymbol{p}_1) \\ & + \mathcal{T}_{DX}(\boldsymbol{p},\boldsymbol{p}_1)\mathcal{K}_E(\boldsymbol{p}_1,\boldsymbol{p}_3) \\ & \quad \times (\bar{s}_E(\boldsymbol{p}_1) + \Psi_{DX}(\boldsymbol{p}_3) + \mathcal{B}_{DX}(\boldsymbol{p}_1,\boldsymbol{p}_6)\Psi_{DX}(\boldsymbol{p}_6)) \\ & + \mathcal{T}_{DX}(\boldsymbol{p},\boldsymbol{p}_4)\mathcal{S}(\boldsymbol{p}_4,\boldsymbol{p}_5)(\bar{s}_S(\boldsymbol{p}_4) + \Psi_{DX}(\boldsymbol{p}_5)).\end{aligned} \tag{99}$$

Expanding the emissive collision operator defined in Eq. 190,

$$\begin{aligned}\Psi_{DX}(\boldsymbol{p}) = {} & \mathcal{T}_{DX}(\boldsymbol{p},\boldsymbol{p}_1)\mathcal{K}_A(\boldsymbol{p}_1,\boldsymbol{p}_2)\bar{s}_A(\boldsymbol{p}_1) \\ & + \mathcal{T}_{DX}(\boldsymbol{p},\boldsymbol{p}_1)\int \Sigma_s(\boldsymbol{x}_1,\hat{\boldsymbol{\Omega}}_1 \to \hat{\boldsymbol{\Omega}}_3, E_1 \to E_3)\delta(\boldsymbol{x}_3 - \boldsymbol{x}_1)\delta(w_3 - w_1) \\ & \quad \times (\bar{s}_E(\boldsymbol{p}_1) + \Psi_{DX}(\boldsymbol{p}_3) + \mathcal{B}_{DX}(\boldsymbol{p}_1,\boldsymbol{p}_6)\Psi_{DX}(\boldsymbol{p}_6))d\boldsymbol{p}_3 \\ & + \mathcal{T}_{DX}(\boldsymbol{p},\boldsymbol{p}_4)\mathcal{S}(\boldsymbol{p}_4,\boldsymbol{p}_5)(\bar{s}_S(\boldsymbol{p}_4) + \Psi_{DX}(\boldsymbol{p}_5)).\end{aligned} \tag{100}$$

Separating the double-differential macroscopic scattering cross into the scattering cross section and the PDF governing the outgoing angle and energy,

$$\begin{aligned}\Psi_{DX}(\boldsymbol{p}) = {} & \mathcal{T}_{DX}(\boldsymbol{p},\boldsymbol{p}_1)\mathcal{K}_A(\boldsymbol{p}_1,\boldsymbol{p}_2)\bar{s}_A(\boldsymbol{p}_1) \\ & + \mathcal{T}_{DX}(\boldsymbol{p},\boldsymbol{p}_1)\int \Sigma_s(\boldsymbol{x}_1,E_1)f(\boldsymbol{x}_1,\hat{\boldsymbol{\Omega}}_1 \to \hat{\boldsymbol{\Omega}}_3, E_1 \to E_3)\delta(\boldsymbol{x}_3 - \boldsymbol{x}_1)\delta(w_3 - w_1) \\ & \quad \times (\bar{s}_E(\boldsymbol{p}_1) + \Psi_{DX}(\boldsymbol{p}_3) + \mathcal{B}_{DX}(\boldsymbol{p}_1,\boldsymbol{p}_6)\Psi_{DX}(\boldsymbol{p}_6))d\boldsymbol{p}_3 \\ & + \mathcal{T}_{DX}(\boldsymbol{p},\boldsymbol{p}_4)\mathcal{S}(\boldsymbol{p}_4,\boldsymbol{p}_5)(\bar{s}_S(\boldsymbol{p}_4) + \Psi_{DX}(\boldsymbol{p}_5)).\end{aligned} \tag{101}$$

Utilizing the property that integrating over the entire domain of a PDF results in unity,

$$\begin{aligned}\Psi_{DX}(\boldsymbol{p}) = {} & \mathcal{T}_{DX}(\boldsymbol{p},\boldsymbol{p}_1)\mathcal{K}_A(\boldsymbol{p}_1,\boldsymbol{p}_2)\bar{s}_A(\boldsymbol{p}_1) \\ & + \mathcal{T}_{DX}(\boldsymbol{p},\boldsymbol{p}_1)\Sigma_s(\boldsymbol{x}_1,E_1) \\ & \times \Bigg(\bar{s}_E(\boldsymbol{p}_1) + \int f(\boldsymbol{x}_1,\hat{\boldsymbol{\Omega}}_1 \to \hat{\boldsymbol{\Omega}}_3, E_1 \to E_3)\Psi_{DX}(\boldsymbol{p}_3)\delta(\boldsymbol{x}_3 - \boldsymbol{x}_1)\delta(w_3 - w_1)d\boldsymbol{p}_3 \\ & \quad + \mathcal{B}_{DX}(\boldsymbol{p}_1,\boldsymbol{p}_6)\Psi_{DX}(\boldsymbol{p}_6)\Bigg) \\ & + \mathcal{T}_{DX}(\boldsymbol{p},\boldsymbol{p}_4)\mathcal{S}(\boldsymbol{p}_4,\boldsymbol{p}_5)(\bar{s}_S(\boldsymbol{p}_4) + \Psi_{DX}(\boldsymbol{p}_5)).\end{aligned} \tag{102}$$

Defining an augmented emissive collision operator to separate terms concerning the initiation of an emissive collision and the emergence from that collision,

$$\mathcal{K}'_E(\boldsymbol{p},\boldsymbol{p}') \equiv \int \Sigma_s(\boldsymbol{x},E)\delta(\boldsymbol{x}' - \boldsymbol{x})\delta(\hat{\boldsymbol{\Omega}}' - \hat{\boldsymbol{\Omega}})\delta(E' - E)\delta(w' - w)d\boldsymbol{p}', \tag{103}$$

and inserting it into Eq. 102,

$$
\begin{aligned}
\Psi_{DX}(\boldsymbol{p}) &= \mathcal{T}_{DX}(\boldsymbol{p},\boldsymbol{p}_1)\mathcal{K}_A(\boldsymbol{p}_1,\boldsymbol{p}_2)\bar{s}_A(\boldsymbol{p}_1) \\
&\quad + \mathcal{T}_{DX}(\boldsymbol{p},\boldsymbol{p}_1)\mathcal{K}'_E(\boldsymbol{p}_1,\boldsymbol{p}_3) \\
&\quad \times \Bigg(\bar{s}_E(\boldsymbol{p}_1) + \int f(\boldsymbol{x}_3,\hat{\boldsymbol{\Omega}}_3 \to \hat{\boldsymbol{\Omega}}_7, E_3 \to E_7)\Psi_{DX}(\boldsymbol{p}_7)\delta(\boldsymbol{x}_7-\boldsymbol{x}_3)\delta(w_7-w_3)d\boldsymbol{p}_7 \\
&\quad + \mathcal{B}_{DX}(\boldsymbol{p}_1,\boldsymbol{p}_6)\Psi_{DX}(\boldsymbol{p}_6)\Bigg) \\
&\quad + \mathcal{T}_{DX}(\boldsymbol{p},\boldsymbol{p}_4)\mathcal{S}(\boldsymbol{p}_4,\boldsymbol{p}_5)(\bar{s}_S(\boldsymbol{p}_4)+\Psi_{DX}(\boldsymbol{p}_5)).
\end{aligned} \tag{104}
$$

Eq. 104 is split into two different HSMEs by first defining the HSME for a particle following an emissive collision or particle construction,

$$
\begin{aligned}
\Psi^{\alpha}_{DX}(\boldsymbol{p}) &= \int f(\boldsymbol{x},\hat{\boldsymbol{\Omega}} \to \hat{\boldsymbol{\Omega}}_1, E \to E_1)\Psi^{\beta}_{DX}(\boldsymbol{p}_1)\delta(\boldsymbol{x}_1-\boldsymbol{x})\delta(w_1-w)d\boldsymbol{p}_1 \\
&\quad + \mathcal{B}_{DX}(\boldsymbol{p},\boldsymbol{p}_2)\Psi^{\beta}_{DX}(\boldsymbol{p}_2),
\end{aligned} \tag{105}
$$

where Ψ^{β}_{DX} is defined by inserting Eq. 105 into Eq. 104. The HSME for a particle not directly following an emissive collision or particle construction is then

$$
\begin{aligned}
\Psi^{\beta}_{DX}(\boldsymbol{p}) &= \mathcal{T}_{DX}(\boldsymbol{p},\boldsymbol{p}_1)\mathcal{K}_A(\boldsymbol{p}_1,\boldsymbol{p}_2)\bar{s}_A(\boldsymbol{p}_1) \\
&\quad + \mathcal{T}_{DX}(\boldsymbol{p},\boldsymbol{p}_1)\mathcal{K}'_E(\boldsymbol{p}_1,\boldsymbol{p}_3)(\bar{s}_E(\boldsymbol{p}_1)+\Psi^{\alpha}_{DX}(\boldsymbol{p}_3)) \\
&\quad + \mathcal{T}_{DX}(\boldsymbol{p},\boldsymbol{p}_4)\mathcal{S}(\boldsymbol{p}_4,\boldsymbol{p}_5)\Big(\bar{s}_S(\boldsymbol{p}_4)+\Psi^{\beta}_{DX}(\boldsymbol{p}_5)\Big).
\end{aligned} \tag{106}
$$

Because Eq. 106 is derived without approximation from Eq. 52, it is an exact representation of the first history score moment, but the moment directly following a scattering collision or source event Ψ^{α}_{DX}, where DXTRAN particle creation takes place, is now available for analysis. For reference the same form of the analog HSME is derived in much the same way as follows. First, the emissive scattering operator in Eq. 34 is expanded using Eq. 190,

$$
\begin{aligned}
\Psi_0(\boldsymbol{p}) &= \mathcal{T}(\boldsymbol{p},\boldsymbol{p}_1)\mathcal{K}_A(\boldsymbol{p}_1,\boldsymbol{p}_2)\bar{s}_A(\boldsymbol{p}_1) \\
&\quad + \mathcal{T}(\boldsymbol{p},\boldsymbol{p}_1)\int \Sigma_s(\boldsymbol{x}_1,\hat{\boldsymbol{\Omega}}_1 \to \hat{\boldsymbol{\Omega}}_3, E_1 \to E_3)\delta(\boldsymbol{x}_3-\boldsymbol{x}_1)\delta(w_3-w_1) \\
&\quad \times (\bar{s}_E(\boldsymbol{p}_1)+\Psi_0(\boldsymbol{p}_3))d\boldsymbol{p}_3 \\
&\quad + \mathcal{T}(\boldsymbol{p},\boldsymbol{p}_4)\mathcal{S}(\boldsymbol{p}_4,\boldsymbol{p}_5)(\bar{s}_S(\boldsymbol{p}_4)+\Psi_0(\boldsymbol{p}_5)).
\end{aligned} \tag{107}
$$

Separating the double-differential macroscopic cross section into the scattering cross section and the PDF governing the outgoing angle and energy,

$$
\begin{aligned}
\Psi_0(\boldsymbol{p}) &= \mathcal{T}(\boldsymbol{p},\boldsymbol{p}_1)\mathcal{K}_A(\boldsymbol{p}_1,\boldsymbol{p}_2)\bar{s}_A(\boldsymbol{p}_1) \\
&\quad + \mathcal{T}(\boldsymbol{p},\boldsymbol{p}_1)\int \Sigma_s(\boldsymbol{x}_1,E_1)f(\boldsymbol{x}_1,\hat{\boldsymbol{\Omega}}_1 \to \hat{\boldsymbol{\Omega}}_3, E_1 \to E_3)\delta(\boldsymbol{x}_3-\boldsymbol{x}_1)\delta(w_3-w_1) \\
&\quad \times (\bar{s}_E(\boldsymbol{p}_1)+\Psi_0(\boldsymbol{p}_3))d\boldsymbol{p}_3 \\
&\quad + \mathcal{T}(\boldsymbol{p},\boldsymbol{p}_4)\mathcal{S}(\boldsymbol{p}_4,\boldsymbol{p}_5)(\bar{s}_S(\boldsymbol{p}_4)+\Psi_0(\boldsymbol{p}_5)).
\end{aligned} \tag{108}
$$

Applying the fact that the integration over the full domain of PDFs results in unity,

$$
\begin{aligned}
\Psi_0(\boldsymbol{p}) &= \mathcal{T}(\boldsymbol{p},\boldsymbol{p}_1)\mathcal{K}_A(\boldsymbol{p}_1,\boldsymbol{p}_2)\bar{s}_A(\boldsymbol{p}_1) \\
&\quad + \mathcal{T}(\boldsymbol{p},\boldsymbol{p}_1)\Sigma_s(\boldsymbol{x}_1,E_1) \\
&\quad \times \left(\bar{s}_E(\boldsymbol{p}_1) + \int f(\boldsymbol{x}_1,\hat{\boldsymbol{\Omega}}_1 \to \hat{\boldsymbol{\Omega}}_3, E_1 \to E_3)\Psi_0(\boldsymbol{p}_3)\delta(\boldsymbol{x}_3-\boldsymbol{x}_1)\delta(w_3-w_1)d\boldsymbol{p}_3\right) \\
&\quad + \mathcal{T}(\boldsymbol{p},\boldsymbol{p}_4)\mathcal{S}(\boldsymbol{p}_4,\boldsymbol{p}_5)(\bar{s}_S(\boldsymbol{p}_4)+\Psi_0(\boldsymbol{p}_5)).
\end{aligned} \tag{109}
$$

Inserting the augmented emissive collision operator defined in Eq. 103,

$$\begin{aligned}\Psi_0(\boldsymbol{p}) &= \mathcal{T}(\boldsymbol{p},\boldsymbol{p}_1)\mathcal{K}_A(\boldsymbol{p}_1,\boldsymbol{p}_2)\bar{s}_A(\boldsymbol{p}_1)\\ &\quad + \mathcal{T}(\boldsymbol{p},\boldsymbol{p}_1)\mathcal{K}'_E(\boldsymbol{p}_1,\boldsymbol{p}_3)\\ &\quad \times \left(\bar{s}_E(\boldsymbol{p}_1) + \int f(\boldsymbol{x}_3, \hat{\boldsymbol{\Omega}}_3 \to \hat{\boldsymbol{\Omega}}_7, E_3 \to E_7)\Psi_0(\boldsymbol{p}_7)\delta(\boldsymbol{x}_7 - \boldsymbol{x}_3)\delta(w_7 - w_3)d\boldsymbol{p}_7\right)\\ &\quad + \mathcal{T}(\boldsymbol{p},\boldsymbol{p}_4)\mathcal{S}(\boldsymbol{p}_4,\boldsymbol{p}_5)(\bar{s}_S(\boldsymbol{p}_4) + \Psi_0(\boldsymbol{p}_5)).\end{aligned} \tag{110}$$

As with the DXTRAN HSME, the analog HSME is split into two forms, each governing a different set of points in particle transport by defining

$$\Psi_0^\alpha(\boldsymbol{p}) = \int f(\boldsymbol{x}, \hat{\boldsymbol{\Omega}} \to \hat{\boldsymbol{\Omega}}_1, E \to E_1)\Psi_0^\beta(\boldsymbol{p}_1)\delta(\boldsymbol{x}_1 - \boldsymbol{x})\delta(w_1 - w)d\boldsymbol{p}_1 \tag{111}$$

governing a particle following a scattering collision or particle construction. Inserting Eq. 111 into Eq. 110,

$$\begin{aligned}\Psi_0^\beta(\boldsymbol{p}) &= \mathcal{T}(\boldsymbol{p},\boldsymbol{p}_1)\mathcal{K}_A(\boldsymbol{p}_1,\boldsymbol{p}_2)\bar{s}_A(\boldsymbol{p}_1)\\ &\quad + \mathcal{T}(\boldsymbol{p},\boldsymbol{p}_1)\mathcal{K}'_E(\boldsymbol{p}_1,\boldsymbol{p}_3)(\bar{s}_E(\boldsymbol{p}_1) + \Psi_0^\alpha(\boldsymbol{p}_3))\\ &\quad + \mathcal{T}(\boldsymbol{p},\boldsymbol{p}_4)\mathcal{S}(\boldsymbol{p}_4,\boldsymbol{p}_5)\Big(\bar{s}_S(\boldsymbol{p}_4) + \Psi_0^\beta(\boldsymbol{p}_5)\Big).\end{aligned} \tag{112}$$

Note that the two modifications to analog transport from DXTRAN variance reduction, the DXTRAN free-flight transmission operator and the flight-to-DXTRAN operator, are now accounted for separately by the β and α forms, respectively. Additionally, note that phase space subscripts have been altered in the α/β forms relative to the DXTRAN HSME given in Eq. 52.

5.2 Characteristic Form of α/β History Score Moment Equations

After casting the analog and DXTRAN HSMEs into α/β form, some operator notation is expanded to cast the equations into a partially characteristic form. It is possible to cast both equations into a purely characteristic form by expanding all operators, but this is not necessary to show fairness. In the case of transport not following particle creation or emission and outside of a DXTRAN region, the HSME given by Eq. 106 can be expanded using Eq. 194 to

$$\begin{aligned}\Psi_{DX}^\beta(\boldsymbol{p}) &= \int_{\boldsymbol{x}\in\{\boldsymbol{x}_\Gamma\cap\neg\boldsymbol{x}_{DX}\}}\int_{4\pi}\int_0^\infty\int_{-\infty}^\infty \exp(-\ell(\boldsymbol{x},\boldsymbol{x}_1))\delta(\hat{\boldsymbol{\Omega}}_1 - \hat{\boldsymbol{\Omega}})\delta(E_1 - E)\delta(w_1 - w)\\ &\quad \times (\mathcal{K}_A(\boldsymbol{p}_1,\boldsymbol{p}_2)\bar{s}_A(\boldsymbol{p}_1) + \mathcal{K}'_E(\boldsymbol{p}_1,\boldsymbol{p}_3)(\bar{s}_E(\boldsymbol{p}_1) + \Psi_{DX}^\alpha(\boldsymbol{p}_3)))dw_1dE_1d\Omega_1dx_1\\ &\quad + \int_{\boldsymbol{x}\in\{\boldsymbol{x}_\Gamma\cap\neg\boldsymbol{x}_{DX}\}}\int_{4\pi}\int_0^\infty\int_{-\infty}^\infty \exp(-\ell(\boldsymbol{x},\boldsymbol{x}_4))\delta(\hat{\boldsymbol{\Omega}}_4 - \hat{\boldsymbol{\Omega}})\delta(E_4 - E)\delta(w_4 - w)\\ &\quad \times \mathcal{S}(\boldsymbol{p}_4,\boldsymbol{p}_5)\Big(\bar{s}_S(\boldsymbol{p}_4) + \Psi_{DX}^\beta(\boldsymbol{p}_5)\Big)dw_4dE_4d\Omega_4dx_4,\end{aligned} \tag{113}$$

where $\{\boldsymbol{x}_\Gamma \cap \neg\boldsymbol{x}_{DX}\}$ is the set of all points on the ray from $\boldsymbol{x}$ along $\hat{\boldsymbol{\Omega}}_1$ in the current cell and not in the DXTRAN region. Evaluating the integrals over statistical weight, energy, and direction,

$$\begin{aligned}\Psi_{DX}^\beta(\boldsymbol{p}) &= \int_{\boldsymbol{x}\in\{\boldsymbol{x}_\Gamma\cap\neg\boldsymbol{x}_{DX}\}} \exp(-\ell(\boldsymbol{x},\boldsymbol{x}_1))\\ &\qquad \times \Big(\mathcal{K}_A(\boldsymbol{x}_1,\hat{\boldsymbol{\Omega}},E,w,\boldsymbol{p}_2)\bar{s}_A(\boldsymbol{x}_1,\hat{\boldsymbol{\Omega}},E,w)\\ &\qquad + \mathcal{K}'_E(\boldsymbol{x}_1,\hat{\boldsymbol{\Omega}},E,w,\boldsymbol{p}_3)\Big(\bar{s}_E(\boldsymbol{x}_1,\hat{\boldsymbol{\Omega}},E,w) + \Psi_{DX}^\alpha(\boldsymbol{p}_3)\Big)\Big)dx_1\\ &\quad + \int_{\{\boldsymbol{x}_\Gamma\cap\neg\boldsymbol{x}_{DX}\}} \exp(-\ell(\boldsymbol{x},\boldsymbol{x}_4))\\ &\qquad \times \mathcal{S}(\boldsymbol{x}_4,\hat{\boldsymbol{\Omega}},E,w,\boldsymbol{p}_5)\Big(\bar{s}_S(\boldsymbol{x}_4,\hat{\boldsymbol{\Omega}},E,w) + \Psi_{DX}^\beta(\boldsymbol{p}_5)\Big)dx_4.\end{aligned} \tag{114}$$

Combining the integrations over position and setting $\boldsymbol{x}_1 = \boldsymbol{x} + a\hat{\boldsymbol{\Omega}}$ yields $\Psi^{\beta}_{DX}(\boldsymbol{p})$ in characteristic coordinates,

$$\begin{aligned}\Psi^{\beta}_{DX}(\boldsymbol{p}) = \lim_{\epsilon\to 0}\int_0^{\min\left\{a_S(\boldsymbol{x},\hat{\boldsymbol{\Omega}}),a_{DX}(\boldsymbol{x},\hat{\boldsymbol{\Omega}})-\epsilon\right\}} &\exp\Big(-\ell(\boldsymbol{x},\boldsymbol{x}+a\hat{\boldsymbol{\Omega}})\Big)\\ \times\Big[&\mathcal{K}_A(\boldsymbol{x}+a\hat{\boldsymbol{\Omega}},\hat{\boldsymbol{\Omega}},E,w,\boldsymbol{p}_2)\bar{s}_A(\boldsymbol{x}+a\hat{\boldsymbol{\Omega}},\hat{\boldsymbol{\Omega}},E,w)\\ &+\mathcal{K}'_E(\boldsymbol{x}+a\hat{\boldsymbol{\Omega}},\hat{\boldsymbol{\Omega}},E,w,\boldsymbol{p}_3)\Big(\bar{s}_E(\boldsymbol{x}+a\hat{\boldsymbol{\Omega}},\hat{\boldsymbol{\Omega}},E,w)+\Psi^{\alpha}_{DX}(\boldsymbol{p}_3)\Big)\\ &+\mathcal{S}(\boldsymbol{x}+a\hat{\boldsymbol{\Omega}},\hat{\boldsymbol{\Omega}},E,w,\boldsymbol{p}_5)\Big(\bar{s}_S(\boldsymbol{x}+a\hat{\boldsymbol{\Omega}},\hat{\boldsymbol{\Omega}},E,w)+\Psi^{\beta}_{DX}(\boldsymbol{p}_5)\Big)\Big]da,\end{aligned} \tag{115}$$

where $a_S(\boldsymbol{x},\hat{\boldsymbol{\Omega}})$ is the distance to the first surface intersected by $\hat{\boldsymbol{\Omega}}$ from $\boldsymbol{x}$, $a_{DX}(\boldsymbol{x},\hat{\boldsymbol{\Omega}})$ is the distance to the point of intersection with the DXTRAN region from from $\boldsymbol{x}$ along $\hat{\boldsymbol{\Omega}}$, and ϵ is used to denote that the upper bound of the integration over a does not include $a_{DX}(\boldsymbol{x},\hat{\boldsymbol{\Omega}})$. For ease of notation, ϵ will be treated as arbitrarily small and the limit of ϵ to zero will not be explicitly denoted in later equations. The characteristic form in the case of analog transport not following a collision or particle construction is similarly found by expanding Eq. 112 using Eq. 187,

$$\begin{aligned}\Psi^{\beta}_0(\boldsymbol{p}) = &\int_{\boldsymbol{x}\in\{\boldsymbol{x}_\Gamma\}}\int_{4\pi}\int_0^{\infty}\int_{-\infty}^{\infty}\exp(-\ell(\boldsymbol{x},\boldsymbol{x}_1))\delta(\hat{\boldsymbol{\Omega}}_1-\hat{\boldsymbol{\Omega}})\delta(E_1-E)\delta(w_1-w)\\ &\times(\mathcal{K}_A(\boldsymbol{p}_1,\boldsymbol{p}_2)\bar{s}_A(\boldsymbol{p}_1)+\mathcal{K}'_E(\boldsymbol{p}_1,\boldsymbol{p}_3)(\bar{s}_E(\boldsymbol{p}_1)+\Psi^{\alpha}_0(\boldsymbol{p}_3)))dw_1dE_1d\Omega_1dx_1\\ +&\int_{\boldsymbol{x}\in\{\boldsymbol{x}_\Gamma\}}\int_{4\pi}\int_0^{\infty}\int_{-\infty}^{\infty}\exp(-\ell(\boldsymbol{x},\boldsymbol{x}_4))\delta(\hat{\boldsymbol{\Omega}}_4-\hat{\boldsymbol{\Omega}})\delta(E_4-E)\delta(w_4-w)\\ &\times\mathcal{S}(\boldsymbol{p}_4,\boldsymbol{p}_5)\Big(\bar{s}_S(\boldsymbol{p}_4)+\Psi^{\beta}_0(\boldsymbol{p}_5)\Big)dw_4dE_4d\Omega_4dx_4.\end{aligned} \tag{116}$$

Evaluating the integrals over statistical weight, energy, and direction,

$$\begin{aligned}\Psi^{\beta}_0(\boldsymbol{p}) = &\int_{\boldsymbol{x}\in\{\boldsymbol{x}_\Gamma\}}\exp(-\ell(\boldsymbol{x},\boldsymbol{x}_1))\Big(\mathcal{K}_A(\boldsymbol{x}_1,\hat{\boldsymbol{\Omega}},E,w,\boldsymbol{p}_2)\bar{s}_A(\boldsymbol{x}_1,\hat{\boldsymbol{\Omega}},E,w)\\ &+\mathcal{K}'_E(\boldsymbol{x}_1,\hat{\boldsymbol{\Omega}},E,w,\boldsymbol{p}_3)\Big(\bar{s}_E(\boldsymbol{x}_1,\hat{\boldsymbol{\Omega}},E,w)+\Psi^{\alpha}_0(\boldsymbol{p}_3)\Big)\Big)dx_1\\ &+\int_{\boldsymbol{x}\in\{\boldsymbol{x}_\Gamma\}}\exp(-\ell(\boldsymbol{x},\boldsymbol{x}_4))\\ &\times\mathcal{S}(\boldsymbol{x}_5,\hat{\boldsymbol{\Omega}},E,w,\boldsymbol{p}_5)\Big(\bar{s}_S(\boldsymbol{x}_4,\hat{\boldsymbol{\Omega}},E,w)+\Psi^{\beta}_0(\boldsymbol{p}_5)\Big)dx_4.\end{aligned} \tag{117}$$

Again, combining the integrations over position and setting $\boldsymbol{x}_1 = \boldsymbol{x} + a\hat{\boldsymbol{\Omega}}$ yields $\Psi^{\beta}_0(\boldsymbol{p})$ in characteristic coordinates,

$$\begin{aligned}\Psi^{\beta}_0(\boldsymbol{p}) = \int_0^{a_S(\boldsymbol{x},\hat{\boldsymbol{\Omega}})}&\exp\Big(-\ell(\boldsymbol{x},\boldsymbol{x}+a\hat{\boldsymbol{\Omega}})\Big)\Big[\mathcal{K}_A(\boldsymbol{x}+a\hat{\boldsymbol{\Omega}},\hat{\boldsymbol{\Omega}},E,w,\boldsymbol{p}_2)\bar{s}_A(\boldsymbol{x}+a\hat{\boldsymbol{\Omega}},\hat{\boldsymbol{\Omega}},E,w)\\ &+\mathcal{K}'_E(\boldsymbol{x}+a\hat{\boldsymbol{\Omega}},\hat{\boldsymbol{\Omega}},E,w,\boldsymbol{p}_3)\Big(\bar{s}_E(\boldsymbol{x}+a\hat{\boldsymbol{\Omega}},\hat{\boldsymbol{\Omega}},E,w)+\Psi^{\alpha}_0(\boldsymbol{p}_3)\Big)\\ &+\mathcal{S}(\boldsymbol{x}+a\hat{\boldsymbol{\Omega}},\hat{\boldsymbol{\Omega}},E,w,\boldsymbol{p}_5)\Big(\bar{s}_S(\boldsymbol{x}+a\hat{\boldsymbol{\Omega}},\hat{\boldsymbol{\Omega}},E,w)+\Psi^{\beta}_0(\boldsymbol{p}_5)\Big)\Big]da,\end{aligned} \tag{118}$$

It is clear from comparing Eq. 115 and Eq. 118 that score contributions from phase spaces inside and beyond the DXTRAN region, $a \geq a_{DX}(\boldsymbol{x},\hat{\boldsymbol{\Omega}})$, may not be accounted for depending on the minimum function in Eq. 115. This corresponds to the case of a particle starting a history at some point in phase space without the creation of a DXTRAN particle and being killed upon arrival to a DXTRAN region. The score contributed by these phase spaces is accounted for by the DXTRAN particles created previously in transport at phase spaces outside of the DXTRAN region according to Eq. 105. For the case of transport immediately following particle creation or emission and outside of a DXTRAN region, Eq. 105 is cast into characteristic form as follows. Expanding the second term of Eq. 105 using Eq. 193,

$$
\begin{aligned}
\Psi_{DX}^{\alpha}(\boldsymbol{p}) = &\int f(\boldsymbol{x}, \hat{\boldsymbol{\Omega}} \to \hat{\boldsymbol{\Omega}}_1, E \to E_1)\Psi_{DX}^{\beta}(\boldsymbol{p}_1)\delta(\boldsymbol{x}_1 - \boldsymbol{x})\delta(w_1 - w)dE_1 d\Omega_1 \\
&+ \int_V \int_{\hat{\boldsymbol{\Omega}}_2 \in \{\hat{\boldsymbol{\Omega}}_{DX}\}} \int_0^{\infty} \int_{-\infty}^{\infty} \mathbb{1}(\boldsymbol{x} \notin \{\boldsymbol{x}_{DX}\})\delta\Big(\boldsymbol{x}_2 - \boldsymbol{x}_{DX}(\boldsymbol{x}, \hat{\boldsymbol{\Omega}}_2)\Big) \\
&\times f_{DX}(\boldsymbol{x}, \hat{\boldsymbol{\Omega}} \to \hat{\boldsymbol{\Omega}}_2, E \to E_2)\delta(w_2 - w_{DX})\Psi_{DX}^{\beta}(\boldsymbol{p}_2)dw_2 dE_2 d\Omega_2 dx_2,
\end{aligned}
\tag{119}
$$

where $\{\hat{\boldsymbol{\Omega}}_{DX}\}$ is the set of vectors directed towards the DXTRAN region from $\boldsymbol{x}$ and V is the volume of the entire system. Using that positions outside of the DXTRAN region are considered in this case, $\boldsymbol{x} \notin \{\boldsymbol{x}_{DX}\}$, and integrating over $\boldsymbol{x}_1$, w_1, and $\boldsymbol{x}_2$,

$$
\begin{aligned}
\Psi_{DX}^{\alpha}(\boldsymbol{p}) = &\int_{4\pi} \int_0^{\infty} f(\boldsymbol{x}, \hat{\boldsymbol{\Omega}} \to \hat{\boldsymbol{\Omega}}_1, E \to E_1)\Psi_{DX}^{\beta}(\boldsymbol{x}, \hat{\boldsymbol{\Omega}}_1, E_1, w)dE_1 d\Omega_1 \\
&+ \int_{\hat{\boldsymbol{\Omega}}_2 \in \{\hat{\boldsymbol{\Omega}}_{DX}\}} \int_0^{\infty} \int_{-\infty}^{\infty} f_{DX}(\boldsymbol{x}, \hat{\boldsymbol{\Omega}} \to \hat{\boldsymbol{\Omega}}_2, E \to E_2)\delta(w_2 - w_{DX}) \\
&\times \Psi_{DX}^{\beta}(\boldsymbol{x}_{DX}(\boldsymbol{x}, \hat{\boldsymbol{\Omega}}_2), \hat{\boldsymbol{\Omega}}_2, E_2, w_2)dw_2 dE_2 d\Omega_2.
\end{aligned}
\tag{120}
$$

Inserting Eq. 6 and integrating over statistical weight w_2,

$$
\begin{aligned}
\Psi_{DX}^{\alpha}(\boldsymbol{p}) = &\int_{4\pi} \int_0^{\infty} f(\boldsymbol{x}, \hat{\boldsymbol{\Omega}} \to \hat{\boldsymbol{\Omega}}_1, E \to E_1)\Psi_{DX}^{\beta}(\boldsymbol{x}, \hat{\boldsymbol{\Omega}}_1, E_1, w)dE_1 d\Omega_1 \\
&+ \int_{\hat{\boldsymbol{\Omega}}_2 \in \{\hat{\boldsymbol{\Omega}}_{DX}\}} \int_0^{\infty} f_{DX}(\boldsymbol{x}, \hat{\boldsymbol{\Omega}} \to \hat{\boldsymbol{\Omega}}_2, E \to E_2) \\
&\times \Psi_{DX}^{\beta}\left(\boldsymbol{x}_{DX}(\boldsymbol{x}, \hat{\boldsymbol{\Omega}}_2), \hat{\boldsymbol{\Omega}}_2, E_2, w\frac{f(\boldsymbol{x}, \hat{\boldsymbol{\Omega}} \to \hat{\boldsymbol{\Omega}}_2, E \to E_2)}{f_{DX}(\boldsymbol{x}, \hat{\boldsymbol{\Omega}} \to \hat{\boldsymbol{\Omega}}_2, E \to E_2)}\exp\Big(-\ell(\boldsymbol{x}, \boldsymbol{x}_{DX}(\boldsymbol{x}, \hat{\boldsymbol{\Omega}}_2))\Big)\right)dE_2 d\Omega_2.
\end{aligned}
\tag{121}
$$

Using the separability of weight and score moment in weight-independent techniques $\Psi(\boldsymbol{r}, cw) = c\Psi(\boldsymbol{r}, w)$ [7], Eq. 121 yields the characteristic form of the α DXTRAN HSME,

$$
\begin{aligned}
\Psi_{DX}^{\alpha}(\boldsymbol{p}) = &\int_{4\pi} \int_0^{\infty} f(\boldsymbol{x}, \hat{\boldsymbol{\Omega}} \to \hat{\boldsymbol{\Omega}}_1, E \to E_1)\Psi_{DX}^{\beta}(\boldsymbol{x}, \hat{\boldsymbol{\Omega}}_1, E_1, w)dE_1 d\Omega_1 \\
&+ \int_{\hat{\boldsymbol{\Omega}}_2 \in \{\hat{\boldsymbol{\Omega}}_{DX}\}} \int_0^{\infty} f(\boldsymbol{x}, \hat{\boldsymbol{\Omega}} \to \hat{\boldsymbol{\Omega}}_2, E \to E_2)\exp\Big(-\ell(\boldsymbol{x}, \boldsymbol{x}_{DX}(\boldsymbol{x}, \hat{\boldsymbol{\Omega}}_2))\Big) \\
&\times \Psi_{DX}^{\beta}(\boldsymbol{x}_{DX}(\boldsymbol{x}, \hat{\boldsymbol{\Omega}}_2), \hat{\boldsymbol{\Omega}}_2, E_2, w)dE_2 d\Omega_2.
\end{aligned}
\tag{122}
$$

Eq. 111 is cast into characteristic coordinates by evaluating the integration over dimensions with Dirac delta functions, x_1 and w_1,

$$
\Psi_0^{\alpha}(\boldsymbol{p}) = \int_{4\pi} \int_0^{\infty} f(\boldsymbol{x}, \hat{\boldsymbol{\Omega}} \to \hat{\boldsymbol{\Omega}}_1, E \to E_1)\Psi_0^{\beta}(\boldsymbol{x}, \hat{\boldsymbol{\Omega}}_1, E_1, w)dE_1 d\Omega_1. \tag{123}
$$

The characteristic forms of the α/β DXTRAN and analog HSMEs are now derived and are shown to be equivalent in Sec. 5.3.

5.3 Reduction of DXTRAN HSME to Analog HSME

With the characteristic forms of the α/β DXTRAN and analog HSMEs, the DXTRAN form of the HSME is now shown to reduce to the analog HSME. This is shown first for the case of a particle following creation or emerging from a collision outside of the DXTRAN region and then inside the DXTRAN region. Beginning outside of the DXTRAN region, $\boldsymbol{x} \notin \{\boldsymbol{x}_{DX}\}$, the DXTRAN HSME is reduced to the analog HSME by analyzing the moment for sets of directions of flight as follows. All following equations are restricted to positions $\boldsymbol{x}$ outside of the DXTRAN region until stated otherwise. Expanding Eq. 122 with Eq. 115,

$$
\begin{aligned}
\Psi^{\alpha}_{DX}(\boldsymbol{p}) = &\int_{4\pi}\int_{0}^{\infty} f(\boldsymbol{x},\hat{\boldsymbol{\Omega}}\to\hat{\boldsymbol{\Omega}}_1,E\to E_1)\int_{0}^{\min\left\{a_S(\boldsymbol{x},\hat{\boldsymbol{\Omega}}_1),a_{DX}(\boldsymbol{x},\hat{\boldsymbol{\Omega}}_1)-\epsilon\right\}}\exp\Big(-\ell(\boldsymbol{x},\boldsymbol{x}+a\hat{\boldsymbol{\Omega}}_1)\Big)\\
&\times\Big[\mathcal{K}_A(\boldsymbol{x}+a\hat{\boldsymbol{\Omega}}_1,\hat{\boldsymbol{\Omega}}_1,E_1,w,\boldsymbol{p}_2)\bar{s}_A(\boldsymbol{x}+a\hat{\boldsymbol{\Omega}}_1,\hat{\boldsymbol{\Omega}}_1,E_1,w)\\
&+\mathcal{K}'_E(\boldsymbol{x}+a\hat{\boldsymbol{\Omega}}_1,\hat{\boldsymbol{\Omega}}_1,E_1,w,\boldsymbol{p}_3)\Big(\bar{s}_E(\boldsymbol{x}+a\hat{\boldsymbol{\Omega}}_1,\hat{\boldsymbol{\Omega}}_1,E_1,w)+\Psi^{\alpha}_{DX}(\boldsymbol{p}_3)\Big)\\
&+\mathcal{S}(\boldsymbol{x}+a\hat{\boldsymbol{\Omega}}_1,\hat{\boldsymbol{\Omega}}_1,E_1,w,\boldsymbol{p}_4)\Big(\bar{s}_S(\boldsymbol{x}+a\hat{\boldsymbol{\Omega}}_1,\hat{\boldsymbol{\Omega}}_1,E_1,w)+\Psi^{\beta}_{DX}(\boldsymbol{p}_4)\Big)\Big]\,da\,dE_1\,d\Omega_1,\\
&+\int_{\hat{\boldsymbol{\Omega}}_2\in\left\{\hat{\boldsymbol{\Omega}}_{DX}\right\}}\int_{0}^{\infty} f(\boldsymbol{x},\hat{\boldsymbol{\Omega}}\to\hat{\boldsymbol{\Omega}}_2,E\to E_2)\exp\Big(-\ell(\boldsymbol{x},\boldsymbol{x}_{DX}(\boldsymbol{x},\hat{\boldsymbol{\Omega}}_2))\Big)\\
&\times\int_{0}^{\min\left\{a_S(\boldsymbol{x}_{DX}(\boldsymbol{x},\hat{\boldsymbol{\Omega}}_2),\hat{\boldsymbol{\Omega}}_2),a_{DX}(\boldsymbol{x}_{DX}(\boldsymbol{x},\hat{\boldsymbol{\Omega}}_2),\hat{\boldsymbol{\Omega}}_2)-\epsilon\right\}}\exp\Big(-\ell(\boldsymbol{x}_{DX}(\boldsymbol{x},\hat{\boldsymbol{\Omega}}_2),\boldsymbol{x}_{DX}(\boldsymbol{x},\hat{\boldsymbol{\Omega}}_2)+a\hat{\boldsymbol{\Omega}}_2)\Big)\\
&\times\Big[\mathcal{K}_A(\boldsymbol{x}_{DX}(\boldsymbol{x},\hat{\boldsymbol{\Omega}}_2)+a\hat{\boldsymbol{\Omega}}_2,\hat{\boldsymbol{\Omega}}_2,E_2,w,\boldsymbol{p}_3)\bar{s}_A(\boldsymbol{x}_{DX}(\boldsymbol{x},\hat{\boldsymbol{\Omega}}_2)+a\hat{\boldsymbol{\Omega}}_2,\hat{\boldsymbol{\Omega}}_2,E_2,w)\\
&+\mathcal{K}'_E(\boldsymbol{x}_{DX}(\boldsymbol{x},\hat{\boldsymbol{\Omega}}_2)+a\hat{\boldsymbol{\Omega}}_2,\hat{\boldsymbol{\Omega}}_2,E_2,w,\boldsymbol{p}_4)\Big(\bar{s}_E(\boldsymbol{x}_{DX}(\boldsymbol{x},\hat{\boldsymbol{\Omega}}_2)+a\hat{\boldsymbol{\Omega}}_2,\hat{\boldsymbol{\Omega}}_2,E_2,w)+\Psi^{\alpha}_{DX}(\boldsymbol{p}_4)\Big)\\
&+\mathcal{S}(\boldsymbol{x}_{DX}(\boldsymbol{x},\hat{\boldsymbol{\Omega}}_2)+a\hat{\boldsymbol{\Omega}}_2,\hat{\boldsymbol{\Omega}}_2,E_2,w,\boldsymbol{p}_5)\\
&\times\Big(\bar{s}_S(\boldsymbol{x}_{DX}(\boldsymbol{x},\hat{\boldsymbol{\Omega}}_2)+a\hat{\boldsymbol{\Omega}}_2,\hat{\boldsymbol{\Omega}}_2,E_2,w)+\Psi^{\beta}_{DX}(\boldsymbol{p}_5)\Big)\Big]\,da\,dE_2\,d\Omega_2.
\end{aligned}
\tag{124}
$$

Changing the bounds of the second integration over a while keeping the range of integration identical and using the fact that $a_S(\boldsymbol{x}_{DX}(\boldsymbol{x},\hat{\boldsymbol{\Omega}}_2),\hat{\boldsymbol{\Omega}}_2) < a_{DX}(\boldsymbol{x}_{DX}(\boldsymbol{x},\hat{\boldsymbol{\Omega}}_2),\hat{\boldsymbol{\Omega}}_2)$ because the distance to the entry point of the DXTRAN region from inside the region is infinite,

$$
\begin{aligned}
\Psi^{\alpha}_{DX}(\boldsymbol{p}) = &\int_{4\pi}\int_{0}^{\infty} f(\boldsymbol{x},\hat{\boldsymbol{\Omega}}\to\hat{\boldsymbol{\Omega}}_1,E\to E_1)\int_{0}^{\min\left\{a_S(\boldsymbol{x},\hat{\boldsymbol{\Omega}}_1),a_{DX}(\boldsymbol{x},\hat{\boldsymbol{\Omega}}_1)-\epsilon\right\}}\exp\Big(-\ell(\boldsymbol{x},\boldsymbol{x}+a\hat{\boldsymbol{\Omega}}_1)\Big)\\
&\times\Big[\mathcal{K}_A(\boldsymbol{x}+a\hat{\boldsymbol{\Omega}}_1,\hat{\boldsymbol{\Omega}}_1,E_1,w,\boldsymbol{p}_2)\bar{s}_A(\boldsymbol{x}+a\hat{\boldsymbol{\Omega}}_1,\hat{\boldsymbol{\Omega}}_1,E_1,w)\\
&+\mathcal{K}'_E(\boldsymbol{x}+a\hat{\boldsymbol{\Omega}}_1,\hat{\boldsymbol{\Omega}}_1,E_1,w,\boldsymbol{p}_3)\Big(\bar{s}_E(\boldsymbol{x}+a\hat{\boldsymbol{\Omega}}_1,\hat{\boldsymbol{\Omega}}_1,E_1,w)+\Psi^{\alpha}_{DX}(\boldsymbol{p}_3)\Big)\\
&+\mathcal{S}(\boldsymbol{x}+a\hat{\boldsymbol{\Omega}}_1,\hat{\boldsymbol{\Omega}}_1,E_1,w,\boldsymbol{p}_4)\Big(\bar{s}_S(\boldsymbol{x}+a\hat{\boldsymbol{\Omega}}_1,\hat{\boldsymbol{\Omega}}_1,E_1,w)+\Psi^{\beta}_{DX}(\boldsymbol{p}_4)\Big)\Big]\,da\,dE_1\,d\Omega_1,\\
&+\int_{\hat{\boldsymbol{\Omega}}_2\in\left\{\hat{\boldsymbol{\Omega}}_{DX}\right\}}\int_{0}^{\infty} f(\boldsymbol{x},\hat{\boldsymbol{\Omega}}\to\hat{\boldsymbol{\Omega}}_2,E\to E_2)\exp\Big(-\ell(\boldsymbol{x},\boldsymbol{x}_{DX}(\boldsymbol{x},\hat{\boldsymbol{\Omega}}_2))\Big)\\
&\times\int_{a_{DX}(\boldsymbol{x},\hat{\boldsymbol{\Omega}}_2)}^{a_{DX}(\boldsymbol{x},\hat{\boldsymbol{\Omega}}_2)+a_S(\boldsymbol{x}_{DX}(\boldsymbol{x},\hat{\boldsymbol{\Omega}}_2),\hat{\boldsymbol{\Omega}}_2)}\exp\Big(-\ell(\boldsymbol{x}_{DX}(\boldsymbol{x},\hat{\boldsymbol{\Omega}}_2),\boldsymbol{x}+a\hat{\boldsymbol{\Omega}}_2)\Big)\\
&\times\Big[\mathcal{K}_A(\boldsymbol{x}+a\hat{\boldsymbol{\Omega}}_2,\hat{\boldsymbol{\Omega}}_2,E_2,w,\boldsymbol{p}_3)\bar{s}_A(\boldsymbol{x}+a\hat{\boldsymbol{\Omega}}_2,\hat{\boldsymbol{\Omega}}_2,E_2,w)\\
&+\mathcal{K}'_E(\boldsymbol{x}+a\hat{\boldsymbol{\Omega}}_2,\hat{\boldsymbol{\Omega}}_2,E_2,w,\boldsymbol{p}_4)\Big(\bar{s}_E(\boldsymbol{x}+a\hat{\boldsymbol{\Omega}}_2,\hat{\boldsymbol{\Omega}}_2,E_2,w)+\Psi^{\alpha}_{DX}(\boldsymbol{p}_4)\Big)\\
&+\mathcal{S}(\boldsymbol{x}+a\hat{\boldsymbol{\Omega}}_2,\hat{\boldsymbol{\Omega}}_2,E_2,w,\boldsymbol{p}_5)\Big(\bar{s}_S(\boldsymbol{x}+a\hat{\boldsymbol{\Omega}}_2,\hat{\boldsymbol{\Omega}}_2,E_2,w)+\Psi^{\beta}_{DX}(\boldsymbol{p}_5)\Big)\Big]\,da\,dE_2\,d\Omega_2.
\end{aligned}
\tag{125}
$$

The integration bounds of the second terms of Eqs. 124 and 125 are identical, as is illustrated in Fig. 4. Combining the two exponential functions in the second term,

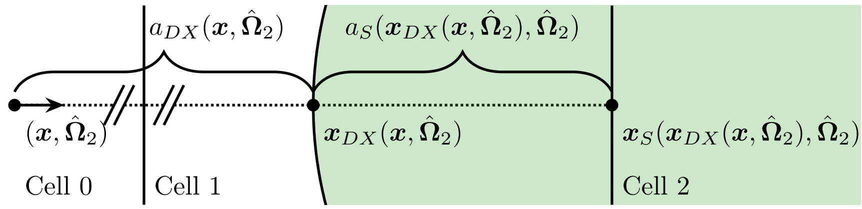

Figure 4: Diagram of the integration path of the second term of Eqs. 124 and 125. Note that an arbitrary number of surfaces could divide cells 0 and 1 or there could be no division.

$$
\begin{aligned}
\Psi^{\alpha}_{DX}(\boldsymbol{p}) = &\int_{4\pi}\int_0^{\infty} f(\boldsymbol{x},\hat{\boldsymbol{\Omega}}\to\hat{\boldsymbol{\Omega}}_1,E\to E_1)\int_0^{\min\left\{a_S(\boldsymbol{x},\hat{\boldsymbol{\Omega}}_1),a_{DX}(\boldsymbol{x},\hat{\boldsymbol{\Omega}}_1)-\epsilon\right\}}\exp\Big(-\ell(\boldsymbol{x},\boldsymbol{x}+a\hat{\boldsymbol{\Omega}}_1)\Big)\\
&\times\Big[\mathcal{K}_A(\boldsymbol{x}+a\hat{\boldsymbol{\Omega}}_1,\hat{\boldsymbol{\Omega}}_1,E_1,w,\boldsymbol{p}_2)\bar{s}_A(\boldsymbol{x}+a\hat{\boldsymbol{\Omega}}_1,\hat{\boldsymbol{\Omega}}_1,E_1,w)\\
&+\mathcal{K}'_E(\boldsymbol{x}+a\hat{\boldsymbol{\Omega}}_1,\hat{\boldsymbol{\Omega}}_1,E_1,w,\boldsymbol{p}_3)\Big(\bar{s}_E(\boldsymbol{x}+a\hat{\boldsymbol{\Omega}}_1,\hat{\boldsymbol{\Omega}}_1,E_1,w)+\Psi^{\alpha}_{DX}(\boldsymbol{p}_3)\Big)\\
&+\mathcal{S}(\boldsymbol{x}+a\hat{\boldsymbol{\Omega}}_1,\hat{\boldsymbol{\Omega}}_1,E_1,w,\boldsymbol{p}_4)\Big(\bar{s}_S(\boldsymbol{x}+a\hat{\boldsymbol{\Omega}}_1,\hat{\boldsymbol{\Omega}}_1,E_1,w)+\Psi^{\beta}_{DX}(\boldsymbol{p}_4)\Big)\Big]dadE_1d\Omega_1,\\
&+\int_{\hat{\boldsymbol{\Omega}}_2\in\left\{\hat{\boldsymbol{\Omega}}_{DX}\right\}}\int_0^{\infty} f(\boldsymbol{x},\hat{\boldsymbol{\Omega}}\to\hat{\boldsymbol{\Omega}}_2,E\to E_2)\\
&\times\int_{a_{DX}(\boldsymbol{x},\hat{\boldsymbol{\Omega}}_2)}^{a_{DX}(\boldsymbol{x},\hat{\boldsymbol{\Omega}}_2)+a_S(\boldsymbol{x}_{DX}(\boldsymbol{x},\hat{\boldsymbol{\Omega}}_2),\hat{\boldsymbol{\Omega}}_2)}\exp\Big(-\ell(\boldsymbol{x},\boldsymbol{x}+a\hat{\boldsymbol{\Omega}}_2)\Big)\\
&\times\Big[\mathcal{K}_A(\boldsymbol{x}+a\hat{\boldsymbol{\Omega}}_2,\hat{\boldsymbol{\Omega}}_2,E_2,w,\boldsymbol{p}_3)\bar{s}_A(\boldsymbol{x}+a\hat{\boldsymbol{\Omega}}_2,\hat{\boldsymbol{\Omega}}_2,E_2,w)\\
&+\mathcal{K}'_E(\boldsymbol{x}+a\hat{\boldsymbol{\Omega}}_2,\hat{\boldsymbol{\Omega}}_2,E_2,w,\boldsymbol{p}_4)\Big(\bar{s}_E(\boldsymbol{x}+a\hat{\boldsymbol{\Omega}}_2,\hat{\boldsymbol{\Omega}}_2,E_2,w)+\Psi^{\alpha}_{DX}(\boldsymbol{p}_4)\Big)\\
&+\mathcal{S}(\boldsymbol{x}+a\hat{\boldsymbol{\Omega}}_2,\hat{\boldsymbol{\Omega}}_2,E_2,w,\boldsymbol{p}_5)\Big(\bar{s}_S(\boldsymbol{x}+a\hat{\boldsymbol{\Omega}}_2,\hat{\boldsymbol{\Omega}}_2,E_2,w)+\Psi^{\beta}_{DX}(\boldsymbol{p}_5)\Big)\Big]dadE_2d\Omega_2.
\end{aligned}
\tag{126}
$$

To break up the min{} function in the first term, define two subsets of $\{\hat{\boldsymbol{\Omega}}_{DX}\}$: the set of directions that intersect with the DXTRAN region before the surface bounding the current cell $\{\hat{\boldsymbol{\Omega}}^{\text{inside}}_{DX}\}$ and the set of angles that intersect the DXTRAN region after the surface bounding the current cell $\{\hat{\boldsymbol{\Omega}}^{\text{outside}}_{DX}\}$. Applying these definition to Eq. 126,

$$
\Psi^{\alpha}_{DX}(\boldsymbol{p}) = X_1+X_2+X_3+X_4+X_5,
\tag{127a}
$$

where

$$
\begin{aligned}
X_1 = &\int_{\hat{\boldsymbol{\Omega}}_1\in\left\{\hat{\boldsymbol{\Omega}}^{\text{inside}}_{DX}\right\}}\int_0^{\infty} f(\boldsymbol{x},\hat{\boldsymbol{\Omega}}\to\hat{\boldsymbol{\Omega}}_1,E\to E_1)\int_0^{a_{DX}(\boldsymbol{x},\hat{\boldsymbol{\Omega}}_1)-\epsilon}\exp\Big(-\ell(\boldsymbol{x},\boldsymbol{x}+a\hat{\boldsymbol{\Omega}}_1)\Big)\\
&\times\Big[\mathcal{K}_A(\boldsymbol{x}+a\hat{\boldsymbol{\Omega}}_1,\hat{\boldsymbol{\Omega}}_1,E_1,w,\boldsymbol{p}_2)\bar{s}_A(\boldsymbol{x}+a\hat{\boldsymbol{\Omega}}_1,\hat{\boldsymbol{\Omega}}_1,E_1,w)\\
&+\mathcal{K}'_E(\boldsymbol{x}+a\hat{\boldsymbol{\Omega}}_1,\hat{\boldsymbol{\Omega}}_1,E_1,w,\boldsymbol{p}_3)\Big(\bar{s}_E(\boldsymbol{x}+a\hat{\boldsymbol{\Omega}}_1,\hat{\boldsymbol{\Omega}}_1,E_1,w)+\Psi^{\alpha}_{DX}(\boldsymbol{p}_3)\Big)\\
&+\mathcal{S}(\boldsymbol{x}+a\hat{\boldsymbol{\Omega}}_1,\hat{\boldsymbol{\Omega}}_1,E_1,w,\boldsymbol{p}_4)\Big(\bar{s}_S(\boldsymbol{x}+a\hat{\boldsymbol{\Omega}}_1,\hat{\boldsymbol{\Omega}}_1,E_1,w)+\Psi^{\beta}_{DX}(\boldsymbol{p}_4)\Big)\Big]dadE_1d\Omega_1,
\end{aligned}
\tag{127b}
$$

$$
\begin{aligned}
X_2 = &\int_{\hat{\boldsymbol{\Omega}}_1\in\left\{\hat{\boldsymbol{\Omega}}^{\text{outside}}_{DX}\right\}}\int_0^{\infty} f(\boldsymbol{x},\hat{\boldsymbol{\Omega}}\to\hat{\boldsymbol{\Omega}}_1,E\to E_1)\int_0^{a_S(\boldsymbol{x},\hat{\boldsymbol{\Omega}}_1)}\exp\Big(-\ell(\boldsymbol{x},\boldsymbol{x}+a\hat{\boldsymbol{\Omega}}_1)\Big)\\
&\times\Big[\mathcal{K}_A(\boldsymbol{x}+a\hat{\boldsymbol{\Omega}}_1,\hat{\boldsymbol{\Omega}}_1,E_1,w,\boldsymbol{p}_2)\bar{s}_A(\boldsymbol{x}+a\hat{\boldsymbol{\Omega}}_1,\hat{\boldsymbol{\Omega}}_1,E_1,w)\\
&+\mathcal{K}'_E(\boldsymbol{x}+a\hat{\boldsymbol{\Omega}}_1,\hat{\boldsymbol{\Omega}}_1,E_1,w,\boldsymbol{p}_3)\Big(\bar{s}_E(\boldsymbol{x}+a\hat{\boldsymbol{\Omega}}_1,\hat{\boldsymbol{\Omega}}_1,E_1,w)+\Psi^{\alpha}_{DX}(\boldsymbol{p}_3)\Big)\\
&+\mathcal{S}(\boldsymbol{x}+a\hat{\boldsymbol{\Omega}}_1,\hat{\boldsymbol{\Omega}}_1,E_1,w,\boldsymbol{p}_4)\Big(\bar{s}_S(\boldsymbol{x}+a\hat{\boldsymbol{\Omega}}_1,\hat{\boldsymbol{\Omega}}_1,E_1,w)+\Psi^{\beta}_{DX}(\boldsymbol{p}_4)\Big)\Big]dadE_1d\Omega_1,
\end{aligned}
\tag{127c}
$$

$$
\begin{aligned}
X_3 = &\int_{\hat{\mathbf{\Omega}}_1 \notin \{\hat{\mathbf{\Omega}}_{DX}\}} \int_0^\infty f(\boldsymbol{x}, \hat{\mathbf{\Omega}} \to \hat{\mathbf{\Omega}}_1, E \to E_1) \int_0^{a_S(\boldsymbol{x}, \hat{\mathbf{\Omega}}_1)} \exp\Big(-\ell(\boldsymbol{x}, \boldsymbol{x} + a\hat{\mathbf{\Omega}}_1)\Big) \\
&\times \Big[\mathcal{K}_A(\boldsymbol{x} + a\hat{\mathbf{\Omega}}_1, \hat{\mathbf{\Omega}}_1, E_1, w, \boldsymbol{p}_2)\bar{s}_A(\boldsymbol{x} + a\hat{\mathbf{\Omega}}_1, \hat{\mathbf{\Omega}}_1, E_1, w) \\
&+ \mathcal{K}'_E(\boldsymbol{x} + a\hat{\mathbf{\Omega}}_1, \hat{\mathbf{\Omega}}_1, E_1, w, \boldsymbol{p}_3)\Big(\bar{s}_E(\boldsymbol{x} + a\hat{\mathbf{\Omega}}_1, \hat{\mathbf{\Omega}}_1, E_1, w) + \Psi^\alpha_{DX}(\boldsymbol{p}_3)\Big) \\
&+ \mathcal{S}(\boldsymbol{x} + a\hat{\mathbf{\Omega}}_1, \hat{\mathbf{\Omega}}_1, E_1, w, \boldsymbol{p}_4)\Big(\bar{s}_S(\boldsymbol{x} + a\hat{\mathbf{\Omega}}_1, \hat{\mathbf{\Omega}}_1, E_1, w) + \Psi^\beta_{DX}(\boldsymbol{p}_4)\Big)\Big] da dE_1 d\Omega_1,
\end{aligned} \tag{127d}
$$

$$
\begin{aligned}
X_4 = &\int_{\hat{\mathbf{\Omega}}_2 \in \{\hat{\mathbf{\Omega}}^{\text{inside}}_{DX}\}} \int_0^\infty f(\boldsymbol{x}, \hat{\mathbf{\Omega}} \to \hat{\mathbf{\Omega}}_2, E \to E_2) \int_{a_{DX}(\boldsymbol{x}, \hat{\mathbf{\Omega}}_2)}^{a_S(\boldsymbol{x}, \hat{\mathbf{\Omega}}_2)} \exp\Big(-\ell(\boldsymbol{x}, \boldsymbol{x} + a\hat{\mathbf{\Omega}}_2)\Big) \\
&\times \Big[\mathcal{K}_A(\boldsymbol{x} + a\hat{\mathbf{\Omega}}_2, \hat{\mathbf{\Omega}}_2, E_2, w, \boldsymbol{p}_3)\bar{s}_A(\boldsymbol{x} + a\hat{\mathbf{\Omega}}_2, \hat{\mathbf{\Omega}}_2, E_2, w) \\
&+ \mathcal{K}'_E(\boldsymbol{x} + a\hat{\mathbf{\Omega}}_2, \hat{\mathbf{\Omega}}_2, E_2, w, \boldsymbol{p}_4)\Big(\bar{s}_E(\boldsymbol{x} + a\hat{\mathbf{\Omega}}_2, \hat{\mathbf{\Omega}}_2, E_2, w) + \Psi^\alpha_{DX}(\boldsymbol{p}_4)\Big) \\
&+ \mathcal{S}(\boldsymbol{x} + a\hat{\mathbf{\Omega}}_2, \hat{\mathbf{\Omega}}_2, E_2, w, \boldsymbol{p}_5)\Big(\bar{s}_S(\boldsymbol{x} + a\hat{\mathbf{\Omega}}_2, \hat{\mathbf{\Omega}}_2, E_2, w) + \Psi^\beta_{DX}(\boldsymbol{p}_5)\Big)\Big] da dE_2 d\Omega_2,
\end{aligned} \tag{127e}
$$

and

$$
\begin{aligned}
X_5 = &\int_{\hat{\mathbf{\Omega}}_2 \in \{\hat{\mathbf{\Omega}}^{\text{outside}}_{DX}\}} \int_0^\infty f(\boldsymbol{x}, \hat{\mathbf{\Omega}} \to \hat{\mathbf{\Omega}}_2, E \to E_2) \\
&\times \int_{a_{DX}(\boldsymbol{x}, \hat{\mathbf{\Omega}}_2)}^{a_{DX}(\boldsymbol{x}, \hat{\mathbf{\Omega}}_2) + a_S(\boldsymbol{x}_{DX}(\boldsymbol{x}, \hat{\mathbf{\Omega}}_2), \hat{\mathbf{\Omega}}_2)} \exp\Big(-\ell(\boldsymbol{x}, \boldsymbol{x} + a\hat{\mathbf{\Omega}}_2)\Big) \\
&\times \Big[\mathcal{K}_A(\boldsymbol{x} + a\hat{\mathbf{\Omega}}_2, \hat{\mathbf{\Omega}}_2, E_2, w, \boldsymbol{p}_3)\bar{s}_A(\boldsymbol{x} + a\hat{\mathbf{\Omega}}_2, \hat{\mathbf{\Omega}}_2, E_2, w) \\
&+ \mathcal{K}'_E(\boldsymbol{x} + a\hat{\mathbf{\Omega}}_2, \hat{\mathbf{\Omega}}_2, E_2, w, \boldsymbol{p}_4)\Big(\bar{s}_E(\boldsymbol{x} + a\hat{\mathbf{\Omega}}_2, \hat{\mathbf{\Omega}}_2, E_2, w) + \Psi^\alpha_{DX}(\boldsymbol{p}_4)\Big) \\
&+ \mathcal{S}(\boldsymbol{x} + a\hat{\mathbf{\Omega}}_2, \hat{\mathbf{\Omega}}_2, E_2, w, \boldsymbol{p}_5)\Big(\bar{s}_S(\boldsymbol{x} + a\hat{\mathbf{\Omega}}_2, \hat{\mathbf{\Omega}}_2, E_2, w) + \Psi^\beta_{DX}(\boldsymbol{p}_5)\Big)\Big] da dE_2 d\Omega_2.
\end{aligned} \tag{127f}
$$

Note that the upper bound of the integration over a in Eq. 127e is changed from Eq. 126 to an equivalent form using the restriction to directions in $\{\hat{\mathbf{\Omega}}^{\text{inside}}_{DX}\}$. A visualization of a system divided into these terms is given in Fig. 5. Note that both green colors correspond to the set of directions $\{\hat{\mathbf{\Omega}}^{\text{inside}}_{DX}\}$ and both purple colors correspond to the set of directions $\{\hat{\mathbf{\Omega}}^{\text{outside}}_{DX}\}$. Combining the integrations over a in terms X_1 and X_4 gives

$$
\begin{aligned}
X_{1,4} = &\int_{\hat{\mathbf{\Omega}}_1 \in \{\hat{\mathbf{\Omega}}^{\text{inside}}_{DX}\}} \int_0^\infty f(\boldsymbol{x}, \hat{\mathbf{\Omega}} \to \hat{\mathbf{\Omega}}_1, E \to E_1) \int_0^{a_S(\boldsymbol{x}, \hat{\mathbf{\Omega}}_1)} \exp\Big(-\ell(\boldsymbol{x}, \boldsymbol{x} + a\hat{\mathbf{\Omega}}_1)\Big) \\
&\times \Big[\mathcal{K}_A(\boldsymbol{x} + a\hat{\mathbf{\Omega}}_1, \hat{\mathbf{\Omega}}_1, E_1, w, \boldsymbol{p}_2)\bar{s}_A(\boldsymbol{x} + a\hat{\mathbf{\Omega}}_1, \hat{\mathbf{\Omega}}_1, E_1, w) \\
&+ \mathcal{K}'_E(\boldsymbol{x} + a\hat{\mathbf{\Omega}}_1, \hat{\mathbf{\Omega}}_1, E_1, w, \boldsymbol{p}_3)\Big(\bar{s}_E(\boldsymbol{x} + a\hat{\mathbf{\Omega}}_1, \hat{\mathbf{\Omega}}_1, E_1, w) + \Psi^\alpha_{DX}(\boldsymbol{p}_3)\Big) \\
&+ \mathcal{S}(\boldsymbol{x} + a\hat{\mathbf{\Omega}}_1, \hat{\mathbf{\Omega}}_1, E_1, w, \boldsymbol{p}_4)\Big(\bar{s}_S(\boldsymbol{x} + a\hat{\mathbf{\Omega}}_1, \hat{\mathbf{\Omega}}_1, E_1, w) + \Psi^\beta_{DX}(\boldsymbol{p}_4)\Big)\Big] da dE_1 d\Omega_1.
\end{aligned} \tag{128}
$$

To reduce Eq. 105 to Eq. 111 exactly, temporarily assume that the DXTRAN technique is not played at later collisions. This means that later collisions do not create DXTRAN particles and that particles exiting those collisions are not truncated if they enter a DXTRAN region and is denoted as “Assumption 1”. This assumption changes Eq. 105 at later collisions to

$$
\Psi^\alpha_{DX}(\boldsymbol{p}) = \int f(\boldsymbol{x}, \hat{\mathbf{\Omega}} \to \hat{\mathbf{\Omega}}_1, E \to E_1)\Psi^\beta_0(\boldsymbol{p}_1)\delta(\boldsymbol{x}_1 - \boldsymbol{x})\delta(w_1 - w)d\boldsymbol{p}_1 = \Psi^\alpha_0(\boldsymbol{p}) \mid \text{Assumption 1}, \tag{129}
$$

so Eq. 106 following the DXTRAN collision becomes

$$
\begin{aligned}
\Psi^\beta_{DX}(\boldsymbol{p}) = &\mathcal{T}_{DX}(\boldsymbol{p}, \boldsymbol{p}_1)\mathcal{K}_A(\boldsymbol{p}_1, \boldsymbol{p}_2)\bar{s}_A(\boldsymbol{p}_1) \\
&+ \mathcal{T}_{DX}(\boldsymbol{p}, \boldsymbol{p}_1)\mathcal{K}'_E(\boldsymbol{p}_1, \boldsymbol{p}_3)(\bar{s}_E(\boldsymbol{p}_1) + \Psi^\alpha_0(\boldsymbol{p}_3)) \\
&+ \mathcal{T}_{DX}(\boldsymbol{p}, \boldsymbol{p}_4)\mathcal{S}(\boldsymbol{p}_4, \boldsymbol{p}_5)\Big(\bar{s}_S(\boldsymbol{p}_4) + \Psi^\beta_{DX}(\boldsymbol{p}_5)\Big) \mid \text{Assumption 1}.
\end{aligned} \tag{130}
$$

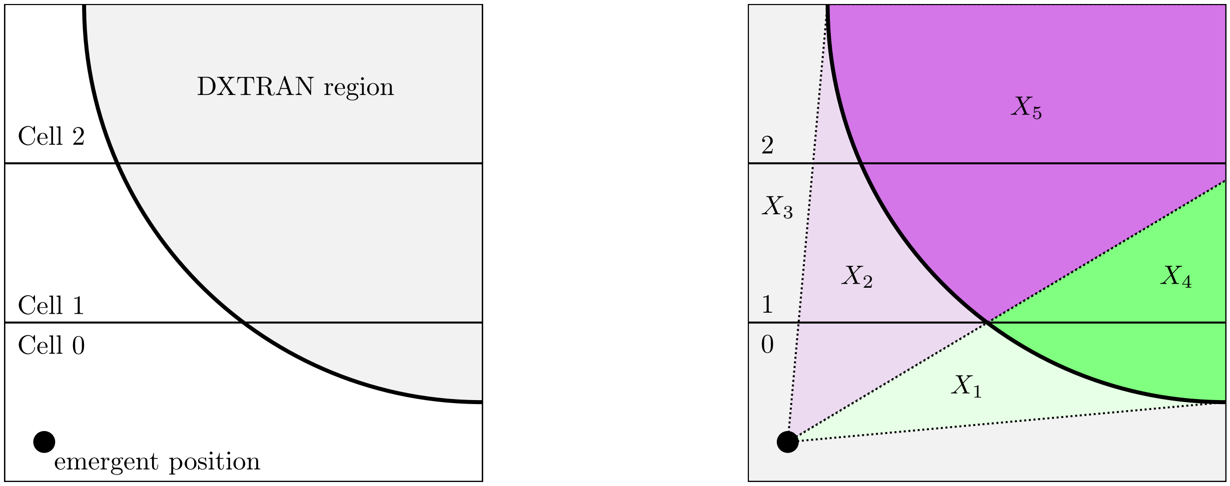

(a) Schematic of simulation geometry.

(b) Simulation geometry with regions color coded.

Figure 5: Representative arrangement of Monte Carlo geometry cells and an overlapping DXTRAN region, with the right figure regions corresponding to Eqs. 127b–127f relative to a particle emerging from the source or an emissive collision at the indicated position.

With this assumption, only non-DXTRAN particles streaming towards the DXTRAN region are truncated because Eq. 195 cannot be satisfied without undergoing another collision, in which case the DXTRAN technique is no longer in play. This means that for DXTRAN particles or particles not streaming towards the DXTRAN region Eq. 130 becomes

$$\begin{aligned}\Psi^{\beta}_{DX}(\boldsymbol{p}) &= \mathcal{T}(\boldsymbol{p},\boldsymbol{p}_1)\mathcal{K}_A(\boldsymbol{p}_1,\boldsymbol{p}_2)\bar{s}_A(\boldsymbol{p}_1) \\ &\quad + \mathcal{T}(\boldsymbol{p},\boldsymbol{p}_1)\mathcal{K}'_E(\boldsymbol{p}_1,\boldsymbol{p}_3)(\bar{s}_E(\boldsymbol{p}_1) + \Psi^{\alpha}_0(\boldsymbol{p}_3)) \\ &\quad + \mathcal{T}(\boldsymbol{p},\boldsymbol{p}_5)\mathcal{S}(\boldsymbol{p}_4,\boldsymbol{p}_5)\Big(\bar{s}_S(\boldsymbol{p}_4) + \Psi^{\beta}_{DX}(\boldsymbol{p}_5)\Big), \\ \Psi^{\beta}_{DX}(\boldsymbol{p}) &= \Psi^{\beta}_0(\boldsymbol{p}) \mid \text{Assumption 1.}\end{aligned} \tag{131}$$

Note that the expanded form of Ψ^{β}_{DX} in Eq. 131 is identical to Eq.112, justifying the equality. In the following intermediate equations, "Assumption 1" is dropped for ease of notation. Because DXTRAN particles are those crossing the cell surface, both Eq. 131 and Eq. 129 can be inserted into Eq. 128,

$$\begin{aligned}X_{1,4} = &\int_{\hat{\boldsymbol{\Omega}}_1 \in \left\{\hat{\boldsymbol{\Omega}}^{\text{inside}}_{DX}\right\}} \int_0^{\infty} f(\boldsymbol{x},\hat{\boldsymbol{\Omega}} \to \hat{\boldsymbol{\Omega}}_1, E \to E_1) \int_0^{a_S(\boldsymbol{x},\hat{\boldsymbol{\Omega}}_1)} \exp\Big(-\ell(\boldsymbol{x},\boldsymbol{x}+a\hat{\boldsymbol{\Omega}}_1)\Big) \\ &\times \Big[\mathcal{K}_A(\boldsymbol{x}+a\hat{\boldsymbol{\Omega}}_1,\hat{\boldsymbol{\Omega}}_1,E_1,w,\boldsymbol{p}_2)\bar{s}_A(\boldsymbol{x}+a\hat{\boldsymbol{\Omega}}_1,\hat{\boldsymbol{\Omega}}_1,E_1,w) \\ &+ \mathcal{K}'_E(\boldsymbol{x}+a\hat{\boldsymbol{\Omega}}_1,\hat{\boldsymbol{\Omega}}_1,E_1,w,\boldsymbol{p}_3)\Big(\bar{s}_E(\boldsymbol{x}+a\hat{\boldsymbol{\Omega}}_1,\hat{\boldsymbol{\Omega}}_1,E_1,w) + \Psi^{\alpha}_0(\boldsymbol{p}_3)\Big) \\ &+ \mathcal{S}(\boldsymbol{x}+a\hat{\boldsymbol{\Omega}}_1,\hat{\boldsymbol{\Omega}}_1,E_1,w,\boldsymbol{p}_4)\Big(\bar{s}_S(\boldsymbol{x}+a\hat{\boldsymbol{\Omega}}_1,\hat{\boldsymbol{\Omega}}_1,E_1,w) + \Psi^{\beta}_0(\boldsymbol{p}_4)\Big)\Big] da dE_1 d\Omega_1.\end{aligned} \tag{132}$$

Because the only directions considered are not directed towards the DXTRAN region, both Eq. 131 and Eq. 129 can also be inserted into Eq. 127d,

$$\begin{aligned}
X_3 = &\int_{\hat{\boldsymbol{\Omega}}_1 \notin \{\hat{\boldsymbol{\Omega}}_{DX}\}} \int_0^\infty f(\boldsymbol{x}, \hat{\boldsymbol{\Omega}} \to \hat{\boldsymbol{\Omega}}_1, E \to E_1) \int_0^{a_S(\boldsymbol{x},\hat{\boldsymbol{\Omega}}_1)} \exp\Big(-\ell(\boldsymbol{x}, \boldsymbol{x} + a\hat{\boldsymbol{\Omega}}_1)\Big) \\
&\times \Big[\mathcal{K}_A(\boldsymbol{x} + a\hat{\boldsymbol{\Omega}}_1, \hat{\boldsymbol{\Omega}}_1, E_1, w, \boldsymbol{p}_2)\bar{s}_A(\boldsymbol{x} + a\hat{\boldsymbol{\Omega}}_1, \hat{\boldsymbol{\Omega}}_1, E_1, w) \\
&+ \mathcal{K}'_E(\boldsymbol{x} + a\hat{\boldsymbol{\Omega}}_1, \hat{\boldsymbol{\Omega}}_1, E_1, w, \boldsymbol{p}_3)\Big(\bar{s}_E(\boldsymbol{x} + a\hat{\boldsymbol{\Omega}}_1, \hat{\boldsymbol{\Omega}}_1, E_1, w) + \Psi_0^\alpha(\boldsymbol{p}_3)\Big) \\
&+ \mathcal{S}(\boldsymbol{x} + a\hat{\boldsymbol{\Omega}}_1, \hat{\boldsymbol{\Omega}}_1, E_1, w, \boldsymbol{p}_4)\Big(\bar{s}_S(\boldsymbol{x} + a\hat{\boldsymbol{\Omega}}_1, \hat{\boldsymbol{\Omega}}_1, E_1, w) + \Psi_0^\beta(\boldsymbol{p}_4)\Big)\Big] da dE_1 d\Omega_1.
\end{aligned} \tag{133}$$

Adding Eqs. 127c and 127f and inserting Eqs. 129 and 131,

$$\begin{aligned}
X_{2,5} = &\int_{\hat{\boldsymbol{\Omega}}_1 \in \{\hat{\boldsymbol{\Omega}}_{DX}^{\text{outside}}\}} \int_0^\infty f(\boldsymbol{x}, \hat{\boldsymbol{\Omega}} \to \hat{\boldsymbol{\Omega}}_1, E \to E_1) \int_0^{a_S(\boldsymbol{x},\hat{\boldsymbol{\Omega}}_1)} \exp\Big(-\ell(\boldsymbol{x}, \boldsymbol{x} + a\hat{\boldsymbol{\Omega}}_1)\Big) \\
&\times \Big[\mathcal{K}_A(\boldsymbol{x} + a\hat{\boldsymbol{\Omega}}_1, \hat{\boldsymbol{\Omega}}_1, E_1, w, \boldsymbol{p}_2)\bar{s}_A(\boldsymbol{x} + a\hat{\boldsymbol{\Omega}}_1, \hat{\boldsymbol{\Omega}}_1, E_1, w) \\
&+ \mathcal{K}'_E(\boldsymbol{x} + a\hat{\boldsymbol{\Omega}}_1, \hat{\boldsymbol{\Omega}}_1, E_1, w, \boldsymbol{p}_3)\Big(\bar{s}_E(\boldsymbol{x} + a\hat{\boldsymbol{\Omega}}_1, \hat{\boldsymbol{\Omega}}_1, E_1, w) + \Psi_0^\alpha(\boldsymbol{p}_3)\Big) \\
&+ \mathcal{S}(\boldsymbol{x} + a\hat{\boldsymbol{\Omega}}_1, \hat{\boldsymbol{\Omega}}_1, E_1, w, \boldsymbol{p}_4)\Big(\bar{s}_S(\boldsymbol{x} + a\hat{\boldsymbol{\Omega}}_1, \hat{\boldsymbol{\Omega}}_1, E_1, w) + \Psi_{DX}^\beta(\boldsymbol{p}_4)\Big)\Big] da dE_1 d\Omega_1 \\
&+ \int_{\hat{\boldsymbol{\Omega}}_2 \in \{\hat{\boldsymbol{\Omega}}_{DX}^{\text{outside}}\}} \int_0^\infty f(\boldsymbol{x}, \hat{\boldsymbol{\Omega}} \to \hat{\boldsymbol{\Omega}}_2, E \to E_2) \\
&\times \int_{a_{DX}(\boldsymbol{x},\hat{\boldsymbol{\Omega}}_2)}^{a_{DX}(\boldsymbol{x},\hat{\boldsymbol{\Omega}}_2)+a_S(\boldsymbol{x}_{DX}(\boldsymbol{x},\hat{\boldsymbol{\Omega}}_2),\hat{\boldsymbol{\Omega}}_2)} \exp\Big(-\ell(\boldsymbol{x}, \boldsymbol{x} + a\hat{\boldsymbol{\Omega}}_2)\Big) \\
&\times \Big[\mathcal{K}_A(\boldsymbol{x} + a\hat{\boldsymbol{\Omega}}_2, \hat{\boldsymbol{\Omega}}_2, E_2, w, \boldsymbol{p}_3)\bar{s}_A(\boldsymbol{x} + a\hat{\boldsymbol{\Omega}}_2, \hat{\boldsymbol{\Omega}}_2, E_2, w) \\
&+ \mathcal{K}'_E(\boldsymbol{x} + a\hat{\boldsymbol{\Omega}}_2, \hat{\boldsymbol{\Omega}}_2, E_2, w, \boldsymbol{p}_4)\Big(\bar{s}_E(\boldsymbol{x} + a\hat{\boldsymbol{\Omega}}_2, \hat{\boldsymbol{\Omega}}_2, E_2, w) + \Psi_0^\alpha(\boldsymbol{p}_4)\Big) \\
&+ \mathcal{S}(\boldsymbol{x} + a\hat{\boldsymbol{\Omega}}_2, \hat{\boldsymbol{\Omega}}_2, E_2, w, \boldsymbol{p}_5)\Big(\bar{s}_S(\boldsymbol{x} + a\hat{\boldsymbol{\Omega}}_2, \hat{\boldsymbol{\Omega}}_2, E_2, w) + \Psi_0^\beta(\boldsymbol{p}_5)\Big)\Big] da dE_2 d\Omega_2.
\end{aligned} \tag{134}$$

Note that transport of a non-DXTRAN particle following a surface does not satisfy Eq. 131, resulting in Ψ_{DX}^β remaining in Eq. 134. To reduce Eq. 134 to only analog terms it is shown in Appendix B.2 that

$$\begin{aligned}
&\int_{\hat{\boldsymbol{\Omega}}_1 \in \{\hat{\boldsymbol{\Omega}}_{DX}^{\text{outside}}\}} \int_0^\infty f(\boldsymbol{x}, \hat{\boldsymbol{\Omega}} \to \hat{\boldsymbol{\Omega}}_1, E \to E_1) \int_0^{a_S(\boldsymbol{x},\hat{\boldsymbol{\Omega}}_1)} \exp\Big(-\ell(\boldsymbol{x}, \boldsymbol{x} + a\hat{\boldsymbol{\Omega}}_1)\Big) \\
&\qquad \times \mathcal{S}(\boldsymbol{x} + a\hat{\boldsymbol{\Omega}}_1, \hat{\boldsymbol{\Omega}}_1, E_1, w, \boldsymbol{p}_4)\Psi_{DX}^\beta(\boldsymbol{p}_4) da dE_1 d\Omega_1 \\
&+ \int_{\hat{\boldsymbol{\Omega}}_2 \in \{\hat{\boldsymbol{\Omega}}_{DX}^{\text{outside}}\}} \int_0^\infty f(\boldsymbol{x}, \hat{\boldsymbol{\Omega}} \to \hat{\boldsymbol{\Omega}}_2, E \to E_2) \int_{a_{DX}(\boldsymbol{x},\hat{\boldsymbol{\Omega}}_2)}^{a_{DX}(\boldsymbol{x},\hat{\boldsymbol{\Omega}}_2)+a_S(\boldsymbol{x}_{DX}(\boldsymbol{x},\hat{\boldsymbol{\Omega}}_2),\hat{\boldsymbol{\Omega}}_2)} \exp\Big(-\ell(\boldsymbol{x}, \boldsymbol{x} + a\hat{\boldsymbol{\Omega}}_2)\Big) \\
&\qquad \times \Big[\mathcal{K}_A(\boldsymbol{x} + a\hat{\boldsymbol{\Omega}}_2, \hat{\boldsymbol{\Omega}}_2, E_2, w, \boldsymbol{p}_3)\bar{s}_A(\boldsymbol{x} + a\hat{\boldsymbol{\Omega}}_2, \hat{\boldsymbol{\Omega}}_2, E_2, w) \\
&\qquad + \mathcal{K}'_E(\boldsymbol{x} + a\hat{\boldsymbol{\Omega}}_2, \hat{\boldsymbol{\Omega}}_2, E_2, w, \boldsymbol{p}_4)\Big(\bar{s}_E(\boldsymbol{x} + a\hat{\boldsymbol{\Omega}}_2, \hat{\boldsymbol{\Omega}}_2, E_2, w) + \Psi_0^\alpha(\boldsymbol{p}_4)\Big) \\
&\qquad + \mathcal{S}(\boldsymbol{x} + a\hat{\boldsymbol{\Omega}}_2, \hat{\boldsymbol{\Omega}}_2, E_2, w, \boldsymbol{p}_5)\Big(\bar{s}_S(\boldsymbol{x} + a\hat{\boldsymbol{\Omega}}_2, \hat{\boldsymbol{\Omega}}_2, E_2, w) + \Psi_0^\beta(\boldsymbol{p}_5)\Big)\Big] da dE_2 d\Omega_2 \\
&= \int_{\hat{\boldsymbol{\Omega}}_1 \in \{\hat{\boldsymbol{\Omega}}_{DX}^{\text{outside}}\}} \int_0^\infty f(\boldsymbol{x}, \hat{\boldsymbol{\Omega}} \to \hat{\boldsymbol{\Omega}}_1, E \to E_1) \int_0^{a_S(\boldsymbol{x},\hat{\boldsymbol{\Omega}}_1)} \exp\Big(-\ell(\boldsymbol{x}, \boldsymbol{x} + a\hat{\boldsymbol{\Omega}}_1)\Big) \\
&\qquad \times \mathcal{S}(\boldsymbol{x} + a\hat{\boldsymbol{\Omega}}_1, \hat{\boldsymbol{\Omega}}_1, E_1, w, \boldsymbol{p}_4)\Psi_0^\beta(\boldsymbol{p}_4).
\end{aligned} \tag{135}$$

Eq. 135 may be interpreted as equating flight to the cell boundary followed by transport disallowing travel into the DXTRAN region plus the simulation of a DXTRAN particle with flight to the cell boundary followed by analog transport. Inserting Eq. 135 into Eq. 134 yields

$$\begin{aligned} X_{2,5} = &\int_{\hat{\boldsymbol{\Omega}}_1 \in \left\{\hat{\boldsymbol{\Omega}}_{DX}^{\text{outside}}\right\}} \int_0^\infty f(\boldsymbol{x}, \hat{\boldsymbol{\Omega}} \to \hat{\boldsymbol{\Omega}}_1, E \to E_1) \int_0^{a_S(\boldsymbol{x}, \hat{\boldsymbol{\Omega}}_1)} \exp\Big(-\ell(\boldsymbol{x}, \boldsymbol{x} + a\hat{\boldsymbol{\Omega}}_1)\Big) \\ &\times \Big[\mathcal{K}_A(\boldsymbol{x} + a\hat{\boldsymbol{\Omega}}_1, \hat{\boldsymbol{\Omega}}_1, E_1, w, \boldsymbol{p}_2)\bar{s}_A(\boldsymbol{x} + a\hat{\boldsymbol{\Omega}}_1, \hat{\boldsymbol{\Omega}}_1, E_1, w) \\ &+ \mathcal{K}'_E(\boldsymbol{x} + a\hat{\boldsymbol{\Omega}}_1, \hat{\boldsymbol{\Omega}}_1, E_1, w, \boldsymbol{p}_3)\Big(\bar{s}_E(\boldsymbol{x} + a\hat{\boldsymbol{\Omega}}_1, \hat{\boldsymbol{\Omega}}_1, E_1, w) + \Psi_0^\alpha(\boldsymbol{p}_3)\Big) \\ &+ \mathcal{S}(\boldsymbol{x} + a\hat{\boldsymbol{\Omega}}_1, \hat{\boldsymbol{\Omega}}_1, E_1, w, \boldsymbol{p}_4)\Big(\bar{s}_S(\boldsymbol{x} + a\hat{\boldsymbol{\Omega}}_1, \hat{\boldsymbol{\Omega}}_1, E_1, w) + \Psi_0^\beta(\boldsymbol{p}_4)\Big)\Big] da dE_1 d\Omega_1. \end{aligned} \tag{136}$$

Finally, combining Eqs. 132, 133, and 136 yields

$$\begin{aligned} \Psi_{DX}^\alpha(\boldsymbol{p}) = &\int_{4\pi} \int_0^\infty f(\boldsymbol{x}, \hat{\boldsymbol{\Omega}} \to \hat{\boldsymbol{\Omega}}_1, E \to E_1) \int_0^{a_S(\boldsymbol{x}, \hat{\boldsymbol{\Omega}}_1)} \exp\Big(-\ell(\boldsymbol{x}, \boldsymbol{x} + a\hat{\boldsymbol{\Omega}}_1)\Big) \\ &\times \Big[\mathcal{K}_A(\boldsymbol{x} + a\hat{\boldsymbol{\Omega}}_1, \hat{\boldsymbol{\Omega}}_1, E_1, w, \boldsymbol{p}_2)\bar{s}_A(\boldsymbol{x} + a\hat{\boldsymbol{\Omega}}_1, \hat{\boldsymbol{\Omega}}_1, E_1, w) \\ &+ \mathcal{K}'_E(\boldsymbol{x} + a\hat{\boldsymbol{\Omega}}_1, \hat{\boldsymbol{\Omega}}_1, E_1, w, \boldsymbol{p}_3)\Big(\bar{s}_E(\boldsymbol{x} + a\hat{\boldsymbol{\Omega}}_1, \hat{\boldsymbol{\Omega}}_1, E_1, w) + \Psi_0^\alpha(\boldsymbol{p}_3)\Big) \\ &+ \mathcal{S}(\boldsymbol{x} + a\hat{\boldsymbol{\Omega}}_1, \hat{\boldsymbol{\Omega}}_1, E_1, w, \boldsymbol{p}_4)\Big(\bar{s}_S(\boldsymbol{x} + a\hat{\boldsymbol{\Omega}}_1, \hat{\boldsymbol{\Omega}}_1, E_1, w) + \Psi_0^\beta(\boldsymbol{p}_4)\Big)\Big] da dE_1 d\Omega_1, \\ &\boldsymbol{x} \notin \{\boldsymbol{x}_{DX}\} \mid \text{Assumption 1.} \end{aligned} \tag{137}$$

Using Eq. 118 and Eq. 123, Eq. 137 reduces to

$$\Psi_{DX}^\alpha(\boldsymbol{p}) = \Psi_0^\alpha(\boldsymbol{p}),\ \boldsymbol{x} \notin \{\boldsymbol{x}_{DX}\} \mid \text{Assumption 1.} \tag{138}$$

For the case of $\boldsymbol{x} \in \{\boldsymbol{x}_{DX}\}$, Eq. 105 becomes

$$\Psi_{DX}^\alpha(\boldsymbol{p}) = \int f(\boldsymbol{x}, \hat{\boldsymbol{\Omega}} \to \hat{\boldsymbol{\Omega}}_1, E \to E_1)\Psi_{DX}^\beta(\boldsymbol{p}_1)\delta(\boldsymbol{x}_1 - \boldsymbol{x})\delta(w_1 - w)d\boldsymbol{p}_1,\ \boldsymbol{x} \in \{\boldsymbol{x}_{DX}\} \tag{139}$$

because Eq. 193 goes to zero inside the DXTRAN region. For the same case, Eq. 106 becomes

$$\begin{aligned} \Psi_{DX}^\beta(\boldsymbol{p}) = &\mathcal{T}(\boldsymbol{p}, \boldsymbol{p}_1)\mathcal{K}_A(\boldsymbol{p}_1, \boldsymbol{p}_2)\bar{s}_A(\boldsymbol{p}_1) \\ &+ \mathcal{T}(\boldsymbol{p}, \boldsymbol{p}_1)\mathcal{K}'_E(\boldsymbol{p}_1, \boldsymbol{p}_3)(\bar{s}_E(\boldsymbol{p}_1) + \Psi_{DX}^\alpha(\boldsymbol{p}_3)) \\ &+ \mathcal{T}(\boldsymbol{p}, \boldsymbol{p}_5)\mathcal{S}(\boldsymbol{p}_4, \boldsymbol{p}_5)\Big(\bar{s}_S(\boldsymbol{p}_4) + \Psi_{DX}^\beta(\boldsymbol{p}_5)\Big),\ \boldsymbol{x} \in \{\boldsymbol{x}_{DX}\} \end{aligned} \tag{140}$$

because Eq. 195 can never be satisfied inside the DXTRAN region. Recognize that Eqs. 139 and 140 are identical to Eqs. 111 and 112 so transport inside the DXTRAN region is identical to analog.

It has been shown by Eqs. 139 and 140 that transport with the DXTRAN variance-reduction technique is identical to analog transport when inside the DXTRAN region. Because transport is carried out identically, the technique is fair. For the case of transport outside of the DXTRAN region, Eq. 138 shows that the first moment of the score contributed by the history is identical to the analog moment when analyzing the particle history directly following particle construction or scattering. Because the first moment of the score contribution is unaltered by the technique, it does not bias estimates of quantities of interest and is fair when played in isolation. Recall that Eq. 138 is derived with the assumption that the technique is not in play at later collisions, allowing the use of the analog moment for later collisions in Eq. 131. Because the technique is proven to be fair, the use of the analog moment for later collisions is justified without assumption, so Eq. 138 may stand alone and the general statement

$$\Psi_{DX}^\alpha(\boldsymbol{p}) = \Psi_0^\alpha(\boldsymbol{p}) \tag{141}$$

holds for all phase spaces.

6 Proof that the Combined Forced-Collision and DXTRAN Techniques are Unbiased

The combined variance-reduction techniques are shown to be fair by reducing the combined-technique HSME to the DXTRAN HSME. Because the DXTRAN HSME is shown to be equivalent to the analog HSME in Sec. 5, reducing the combined-technique HSME to it demonstrates an unbiased first score moment. The combined-technique HSME is analyzed separately for the cases of forced collisions either specified or not so that forced-collision operators can be expanded into case-specific definitions. Note that the combined-technique HSME in the case where the forced collisions are not specified is different from the DXTRAN HSME because the particle may travel to a region where forced collisions are specified.

6.1 Forced Collisions Not Specified

Phase spaces (i.e., cells in the MCNP code) without forced collisions specified are governed by Eq. 54. Note that the only difference between Eq. 54 and the DXTRAN HSME given by Eq. 52 and proven to be fair in Sec. 5 is the recursion with $\Psi_{FC,DX}$ rather than $\Psi^{DX}_{FC,DX}$ following a surface crossing. This difference accounts for the possibility of a particle crossing a surface and entering a phase space where forced collisions are specified. Temporarily assuming that the combined-technique HSME is equivalent to the DXTRAN HSME in phase spaces where forced collisions are specified, Eq. 54 becomes

$$\begin{aligned}\Psi^{DX}_{FC,DX}(\boldsymbol{p}) = {} & \mathcal{T}_{DX}(\boldsymbol{p},\boldsymbol{p}_1)\mathcal{K}_A(\boldsymbol{p}_1,\boldsymbol{p}_2)\bar{s}_A(\boldsymbol{p}_1) \\ & + \mathcal{T}_{DX}(\boldsymbol{p},\boldsymbol{p}_1)\mathcal{K}_E(\boldsymbol{p}_1,\boldsymbol{p}_3)\big(\bar{s}_E(\boldsymbol{p}_1) + \Psi^{DX}_{FC,DX}(\boldsymbol{p}_3)\big) \\ & + \mathcal{T}_{DX}(\boldsymbol{p},\boldsymbol{p}_4)\mathcal{S}(\boldsymbol{p}_4,\boldsymbol{p}_5)(\bar{s}_S(\boldsymbol{p}_4) + \Psi_{DX}(\boldsymbol{p}_5)) \\ & + \mathcal{T}_{DX}(\boldsymbol{p},\boldsymbol{p}_1)\mathcal{K}_E(\boldsymbol{p}_1,\boldsymbol{p}_3)\mathcal{B}_{DX}(\boldsymbol{p}_1,\boldsymbol{p}_6)\Psi^{DX}_{FC,DX}(\boldsymbol{p}_6),\end{aligned} \tag{142}$$

which is equivalent to the DXTRAN HSME. In other words, if the combined technique is shown to be equivalent to the DXTRAN technique where forced collisions are specified, then the combined technique is also known to be equivalent in the phase spaces where forced collisions are not specified by Eq. 142. Because the combined-technique HSME is defined for two recursively interdependent cases, this temporary assumption must be made for one before the other can be shown to be equivalent. Here, the assumption is made for the simpler of the two cases. The assumed equivalence of the combined-technique HSME to the DXTRAN HSME where forced collisions are specified is shown in Sec. 6.2. The general equivalence of the combined-technique HSME to the DXTRAN HSME proves an unbiased technique because the fairness of the DXTRAN technique is shown in Sec. 5.

6.2 Forced Collisions Specified

When forced collisions are specified, the combined-technique HSME takes the form of Eq. 60. To reduce this form to the DXTRAN HSME, the forced-collision operators are expanded into case-specific definitions. This expansion is done for two cases, the streaming path intersecting a DXTRAN region before the next surface and vice versa. The expanded form for both cases is then shown to be equivalent to the DXTRAN HSME. This process is essentially converting the flight-to-collision and flight-to-transmission operators with the corresponding weight adjustments into the DXTRAN free-flight transmission operator. Again, because the DXTRAN HSME is shown is be unbiased in Sec. 5, reducing the combined-technique HSME to it proves that it is also unbiased.

6.2.1 Expansion for the Case of the DXTRAN Region Next in the Streaming Path

In this case, the next surface intersected by the particle's trajectory is the surface of the DXTRAN region. Note that a particle traveling inside the DXTRAN region does not consider intersections with the bounding surface of the DXTRAN region. For forced-collision transport operators, this means that $\|\boldsymbol{x} - \boldsymbol{x}_S\| > \|\boldsymbol{x} - \boldsymbol{x}_{DX}\|$

is true, so the flight-to-collision and flight-to-transmission operators in Eq. 60 can be expanded using the second cases of Eqs. 191 and 192. Writing the combined-technique HSME with forced collisions specified with terms conveniently separated,

$$\begin{aligned}\Psi_{FC,DX}(\boldsymbol{p}) = {} & \mathcal{B}_c(\boldsymbol{p},\boldsymbol{p}_1)\mathcal{K}_A(\boldsymbol{p}_1,\boldsymbol{p}_2)\bar{s}_A(\boldsymbol{p}_1) \\ & + \mathcal{B}_c(\boldsymbol{p},\boldsymbol{p}_1)\mathcal{K}_E(\boldsymbol{p}_1,\boldsymbol{p}_3)\big(\bar{s}_E(\boldsymbol{p}_1) + \Psi^{DX}_{FC,DX}(\boldsymbol{p}_3)\big) \\ & + \mathcal{B}_c(\boldsymbol{p},\boldsymbol{p}_1)(\mathcal{K}_A(\boldsymbol{p}_1,\boldsymbol{p}_2) + \mathcal{K}_E(\boldsymbol{p}_1,\boldsymbol{p}_3)) \\ & \times \mathcal{B}_t(\boldsymbol{p},\boldsymbol{p}_4)\mathcal{S}(\boldsymbol{p}_4,\boldsymbol{p}_5)(\bar{s}_S(\boldsymbol{p}_4) + \Psi_{FC,DX}(\boldsymbol{p}_5)) \\ & + \mathcal{B}_c(\boldsymbol{p},\boldsymbol{p}_1)\mathcal{K}_E(\boldsymbol{p}_1,\boldsymbol{p}_3)\mathcal{B}_{DX}(\boldsymbol{p}_1,\boldsymbol{p}_6)\Psi^{DX}_{FC,DX}(\boldsymbol{p}_6),\ \boldsymbol{p} \in \{\boldsymbol{p}_{FC}\}.\end{aligned} \tag{143}$$

The forced-collision operators are now expanded on a term by term basis with $\boldsymbol{p} \in \{\boldsymbol{p}_{FC}\}$ temporarily dropped for ease of notation.

In the first term of Eq. 143, expanding the flight-to-collision operator using Eq. 191 and the average score contribution using Eq. 62 yields

$$\begin{aligned}\text{Term}_1 = {} & \int_{\boldsymbol{x}\in\{\boldsymbol{x}_\Gamma \cap \neg \boldsymbol{x}_{DX}\}} \int_{4\pi} \int_0^\infty \int_{-\infty}^\infty \frac{\exp(-\ell(\boldsymbol{x},\boldsymbol{x}_1))}{1-\exp(-\ell(\boldsymbol{x},\boldsymbol{x}_{DX}(\boldsymbol{x},\hat{\boldsymbol{\Omega}})))} \delta(\hat{\boldsymbol{\Omega}}_1 - \hat{\boldsymbol{\Omega}})\delta(E_1 - E)\delta(w_1 - w_c) \\ & \times \mathcal{K}_A(\boldsymbol{p}_1,\boldsymbol{p}_2) w_1 m_A(\boldsymbol{r}_1) dw_1 dE_1 d\Omega_1 dx_1.\end{aligned} \tag{144}$$

Evaluating the integral over weight and changing the starting weight of the absorptive collision operator because it is arbitrary as is apparent in Eq. 189,

$$\begin{aligned}\text{Term}_1 = {} & \int_{\boldsymbol{x}\in\{\boldsymbol{x}_\Gamma \cap \neg \boldsymbol{x}_{DX}\}} \int_{4\pi} \int_0^\infty \frac{\exp(-\ell(\boldsymbol{x},\boldsymbol{x}_1))}{1-\exp(-\ell(\boldsymbol{x},\boldsymbol{x}_{DX}(\boldsymbol{x},\hat{\boldsymbol{\Omega}})))} \delta(\hat{\boldsymbol{\Omega}}_1 - \hat{\boldsymbol{\Omega}})\delta(E_1 - E) \\ & \times \mathcal{K}_A(\boldsymbol{r}_1, w, \boldsymbol{p}_2) w_c m_A(\boldsymbol{r}_1) dE_1 d\Omega_1 dx_1.\end{aligned} \tag{145}$$

As noted in Eq. 191, $\boldsymbol{x}_{DX}$ should be used in Eq. 3 rather than $\boldsymbol{x}_S$ when using this definition of the flight-to-collision operator. Combining Eqs. 3 and 5 after making this substitution results in

$$w_c = w_0(1-\exp(-\ell(\boldsymbol{x},\boldsymbol{x}_{DX}(\boldsymbol{x},\hat{\boldsymbol{\Omega}})))). \tag{146}$$

Inserting Eq. 146 into Eq. 145 and simplifying,

$$\begin{aligned}\text{Term}_1 = {} & \int_{\boldsymbol{x}\in\{\boldsymbol{x}_\Gamma \cap \neg \boldsymbol{x}_{DX}\}} \int_{4\pi} \int_0^\infty \exp(-\ell(\boldsymbol{x},\boldsymbol{x}_1))\delta(\hat{\boldsymbol{\Omega}}_1 - \hat{\boldsymbol{\Omega}})\delta(E_1 - E) \\ & \times \mathcal{K}_A(\boldsymbol{r}_1, w, \boldsymbol{p}_2) w \cancelto{1}{\frac{1-\exp(-\ell(\boldsymbol{x},\boldsymbol{x}_{DX}(\boldsymbol{x},\hat{\boldsymbol{\Omega}})))}{1-\exp(-\ell(\boldsymbol{x},\boldsymbol{x}_{DX}(\boldsymbol{x},\hat{\boldsymbol{\Omega}})))}} m_A(\boldsymbol{r}_1) dE_1 d\Omega_1 dx_1.\end{aligned} \tag{147}$$

Eq. 147 is equivalent to integrating over all possible weights with support only for the weight w using a Dirac delta and again using Eq. 62 such that

$$\begin{aligned}\text{Term}_1 = {} & \int_{\boldsymbol{x}\in\{\boldsymbol{x}_\Gamma \cap \neg \boldsymbol{x}_{DX}\}} \int_{4\pi} \int_0^\infty \int_{-\infty}^\infty \exp(-\ell(\boldsymbol{x},\boldsymbol{x}_1))\delta(\hat{\boldsymbol{\Omega}}_1 - \hat{\boldsymbol{\Omega}})\delta(E_1 - E)\delta(w_1 - w) \\ & \times \mathcal{K}_A(\boldsymbol{p}_1,\boldsymbol{p}_2)\bar{s}_A(\boldsymbol{p}_1) dw_1 dE_1 d\Omega_1 dx_1.\end{aligned} \tag{148}$$

In the second term of Eq. 143, expanding the flight-to-collision operator using Eq. 191, the average score contribution using Eq. 62, and the emissive collision operator using Eq. 190 yields

$$\begin{aligned}\text{Term}_2 = {} & \int_{\boldsymbol{x}\in\{\boldsymbol{x}_\Gamma \cap \neg \boldsymbol{x}_{DX}\}} \int_{4\pi} \int_0^\infty \int_{-\infty}^\infty \frac{\exp(-\ell(\boldsymbol{x},\boldsymbol{x}_1))}{1-\exp(-\ell(\boldsymbol{x},\boldsymbol{x}_{DX}(\boldsymbol{x},\hat{\boldsymbol{\Omega}})))} \delta(\hat{\boldsymbol{\Omega}}_1 - \hat{\boldsymbol{\Omega}})\delta(E_1 - E)\delta(w_1 - w_c) \\ & \times \iiiint \Sigma_s(\boldsymbol{x}_1, \hat{\boldsymbol{\Omega}}_1 \to \hat{\boldsymbol{\Omega}}_3, E_1 \to E_3)\delta(\boldsymbol{x}_3 - \boldsymbol{x}_1)\delta(w_3 - w_1)\big(w_1 m_E(\boldsymbol{r}_1) + \Psi^{DX}_{FC,DX}(\boldsymbol{p}_3)\big) \\ & \times dw_3 dE_3 d\Omega_3 dx_3 dw_1 dE_1 d\Omega_1 dx_1.\end{aligned} \tag{149}$$

Evaluating the integrations over weight,

$$\begin{aligned}\text{Term}_2 = &\int_{\boldsymbol{x}\in\{\boldsymbol{x}_\Gamma\cap\neg\boldsymbol{x}_{DX}\}}\int_{4\pi}\int_0^\infty \frac{\exp(-\ell(\boldsymbol{x},\boldsymbol{x}_1))}{1-\exp(-\ell(\boldsymbol{x},\boldsymbol{x}_{DX}(\boldsymbol{x},\hat{\boldsymbol{\Omega}})))}\delta(\hat{\boldsymbol{\Omega}}_1-\hat{\boldsymbol{\Omega}})\delta(E_1-E)\\ &\times\iiint \Sigma_s(\boldsymbol{x}_1,\hat{\boldsymbol{\Omega}}_1\to\hat{\boldsymbol{\Omega}}_3,E_1\to E_3)\delta(\boldsymbol{x}_3-\boldsymbol{x}_1)\big(w_c m_E(\boldsymbol{r}_1)+\Psi_{FC,DX}^{DX}(\boldsymbol{r}_3,w_c)\big)\\ &\times dE_3 d\Omega_3 dx_3 dE_1 d\Omega_1 dx_1.\end{aligned}\tag{150}$$

Using the separability of weight and score moment in weight-independent techniques $\Psi(\boldsymbol{r},cw)=c\Psi(\boldsymbol{r},w)$ [7] and the value of w_c given in Eq. 146,

$$\begin{aligned}\text{Term}_2 = &\int_{\boldsymbol{x}\in\{\boldsymbol{x}_\Gamma\cap\neg\boldsymbol{x}_{DX}\}}\int_{4\pi}\int_0^\infty \exp(-\ell(\boldsymbol{x},\boldsymbol{x}_1))\delta(\hat{\boldsymbol{\Omega}}_1-\hat{\boldsymbol{\Omega}})\delta(E_1-E)\\ &\times\iiint \Sigma_s(\boldsymbol{x}_1,\hat{\boldsymbol{\Omega}}_1\to\hat{\boldsymbol{\Omega}}_3,E_1\to E_3)\delta(\boldsymbol{x}_3-\boldsymbol{x}_1)\cancelto{1}{\frac{1-\exp(-\ell(\boldsymbol{x},\boldsymbol{x}_{DX}(\boldsymbol{x},\hat{\boldsymbol{\Omega}})))}{1-\exp(-\ell(\boldsymbol{x},\boldsymbol{x}_{DX}(\boldsymbol{x},\hat{\boldsymbol{\Omega}})))}}\\ &\times\big(w m_E(\boldsymbol{r}_1)+\Psi_{FC,DX}^{DX}(\boldsymbol{r}_3,w)\big)dE_3 d\Omega_3 dx_3 dE_1 d\Omega_1 dx_1.\end{aligned}\tag{151}$$

Eq. 151 is equivalent to integrating over all weight with support only for weight w using Dirac delta functions such that

$$\begin{aligned}\text{Term}_2 = &\int_{\boldsymbol{x}\in\{\boldsymbol{x}_\Gamma\cap\neg\boldsymbol{x}_{DX}\}}\int_{4\pi}\int_0^\infty\int_{-\infty}^\infty \exp(-\ell(\boldsymbol{x},\boldsymbol{x}_1))\delta(\hat{\boldsymbol{\Omega}}_1-\hat{\boldsymbol{\Omega}})\delta(E_1-E)\delta(w_1-w)\\ &\times\iiiint \Sigma_s(\boldsymbol{x}_1,\hat{\boldsymbol{\Omega}}_1\to\hat{\boldsymbol{\Omega}}_3,E_1\to E_3)\delta(\boldsymbol{x}_3-\boldsymbol{x}_1)\delta(w_3-w_1)\big(w_1 m_E(\boldsymbol{r}_1)+\Psi_{FC,DX}^{DX}(\boldsymbol{p}_3)\big)\\ &\times dw_3 dE_3 d\Omega_3 dx_3 dw_1 dE_1 d\Omega_1 dx_1.\end{aligned}\tag{152}$$

Simplifying the emissive collision operator as $\mathcal{K}_E$ and again using Eq. 62,

$$\begin{aligned}\text{Term}_2 = &\int_{\boldsymbol{x}\in\{\boldsymbol{x}_\Gamma\cap\neg\boldsymbol{x}_{DX}\}}\int_{4\pi}\int_0^\infty\int_{-\infty}^\infty \exp(-\ell(\boldsymbol{x},\boldsymbol{x}_1))\delta(\hat{\boldsymbol{\Omega}}_1-\hat{\boldsymbol{\Omega}})\delta(E_1-E)\delta(w_1-w)\\ &\times\mathcal{K}_E(\boldsymbol{p}_1,\boldsymbol{p}_3)\big(\bar{s}_E(\boldsymbol{p}_1)+\Psi_{FC,DX}^{DX}(\boldsymbol{p}_3)\big)dw_1 dE_1 d\Omega_1 dx_1.\end{aligned}\tag{153}$$

In the third term of Eq. 143, expanding the flight-to-collision operator using Eq. 191 and the average score contribution using Eq. 62 yields

$$\begin{aligned}\text{Term}_3 = &\int_{\boldsymbol{x}\in\{\boldsymbol{x}_\Gamma\cap\neg\boldsymbol{x}_{DX}\}}\int_{4\pi}\int_0^\infty\int_{-\infty}^\infty \frac{\exp(-\ell(\boldsymbol{x},\boldsymbol{x}_1))}{1-\exp(-\ell(\boldsymbol{x},\boldsymbol{x}_{DX}(\boldsymbol{x},\hat{\boldsymbol{\Omega}})))}\delta(\hat{\boldsymbol{\Omega}}_1-\hat{\boldsymbol{\Omega}})\delta(E_1-E)\delta(w_1-w_c)\\ &\times(\mathcal{K}_A(\boldsymbol{p}_1,\boldsymbol{p}_2)+\mathcal{K}_E(\boldsymbol{p}_1,\boldsymbol{p}_3))dw_1 dE_1 d\Omega_1 dx_1 \mathcal{B}_t(\boldsymbol{p},\boldsymbol{p}_4)\mathcal{S}(\boldsymbol{p}_4,\boldsymbol{p}_5)(w_4 m_S(\boldsymbol{r}_4)+\Psi_{FC,DX}(\boldsymbol{p}_5)).\end{aligned}\tag{154}$$

It is shown in Eqs. 83–89 that the integration over $\boldsymbol{p}_1$ for a case nearly identical to that of Eq. 154 results in one. The only difference between the integration in those equations and Eq. 154 is the integration in position over the range $\boldsymbol{x}\in\{\boldsymbol{x}_\Gamma\cap\neg\boldsymbol{x}_{DX}\}$ and the use of $\boldsymbol{x}_{DX}$ in the denominator of the integrand. Applying the steps taken in Eqs. 83–88 to Eq. 154 and assuming a constant total macroscopic cross section Σ_t inside the current cell,

$$\begin{aligned}\text{Term}_3 = &\int_{\boldsymbol{x}\in\{\boldsymbol{x}_\Gamma\cap\neg\boldsymbol{x}_{DX}\}}\frac{\Sigma_t\exp(-\Sigma_t\|\boldsymbol{x}_1-\boldsymbol{x}\|)}{1-\exp(-\Sigma_t\|\boldsymbol{x}_{DX}-\boldsymbol{x}\|)}dx_1\\ &\times\mathcal{B}_t(\boldsymbol{p},\boldsymbol{p}_4)\mathcal{S}(\boldsymbol{p}_4,\boldsymbol{p}_5)(w_4 m_S(\boldsymbol{r}_4)+\Psi_{FC,DX}(\boldsymbol{p}_5)).\end{aligned}\tag{155}$$

The integral identity $\int_0^X \frac{a\cdot\exp(-a\cdot x)}{1-\exp(-a\cdot X)}dx=1$ proven in Appendix B.1 and applied to Eq. 88 can also be applied to Eq. 155 resulting in

$$\text{Term}_3 = \mathcal{B}_t(\boldsymbol{p},\boldsymbol{p}_4)\mathcal{S}(\boldsymbol{p}_4,\boldsymbol{p}_5)(w_4 m_S(\boldsymbol{r}_4)+\Psi_{FC,DX}(\boldsymbol{p}_5)).\tag{156}$$

Expanding the flight-to-transmission operator using Eq. 192,

$$\begin{aligned}\mathrm{Term}_3 = &\iiiint \delta(\boldsymbol{x}_4 - \boldsymbol{x}_{DX}(\boldsymbol{x},\hat{\boldsymbol{\Omega}}))\delta(\hat{\boldsymbol{\Omega}}_4 - \hat{\boldsymbol{\Omega}})\delta(E_4 - E)\delta(w_4 - 0) \\ &\times \mathcal{S}(\boldsymbol{p}_4, \boldsymbol{p}_5)(w_4 m_S(\boldsymbol{r}_4) + \Psi_{FC,DX}(\boldsymbol{p}_5))dw_4 dE_4 d\Omega_4 dx_4.\end{aligned} \tag{157}$$

Evaluating the integration over phase space three,

$$\mathrm{Term}_3 = \mathcal{S}(\boldsymbol{x}_{DX}(\boldsymbol{x},\hat{\boldsymbol{\Omega}}), \hat{\boldsymbol{\Omega}}, E, 0, \boldsymbol{p}_5)\Big(0 \cdot m_S(\boldsymbol{x}_{DX}(\boldsymbol{x},\hat{\boldsymbol{\Omega}}), \hat{\boldsymbol{\Omega}}, E) + \Psi_{FC,DX}(\boldsymbol{p}_5)\Big). \tag{158}$$

Because the surface-crossing operator is being evaluated at a position not on an internal or system boundary, the whole term goes to zero so,

$$\mathrm{Term}_3 = 0. \tag{159}$$

Finally, the fourth term of Eq. 143 is considered. Note that modified particle weights are denoted throughout simply as w_{bias}, where the subscript denotes the type of modification to the particle weight. In this term, the particle weight is modified by both variance-reduction techniques. To more clearly denote which weight is being considered by each technique, modified particle weights are given here as $w_{\text{bias}}(w_{\text{original}})$, where the original weight is that of the particle prior to the modification from a variance-reduction technique. Expanding the flight-to-collision operator using Eq. 191, the emissive collision operator with Eq. 190, the flight-to-DXTRAN operator with Eq. 193, and the average score contribution using Eq. 62 yields

$$\begin{aligned}\mathrm{Term}_4 = &\int_{\boldsymbol{x}\in\{\boldsymbol{x}_\Gamma \cap \neg \boldsymbol{x}_{DX}\}} \int_{4\pi} \int_0^\infty \int_{-\infty}^\infty \frac{\exp(-\ell(\boldsymbol{x},\boldsymbol{x}_1))}{1-\exp(-\ell(\boldsymbol{x},\boldsymbol{x}_{DX}(\boldsymbol{x},\hat{\boldsymbol{\Omega}})))}\delta(\hat{\boldsymbol{\Omega}}_1 - \hat{\boldsymbol{\Omega}})\delta(E_1 - E) \\ &\times \delta(w_1 - w_c(w)) \iiiint \Sigma_s(\boldsymbol{x}_1, \hat{\boldsymbol{\Omega}}_1 \to \hat{\boldsymbol{\Omega}}_3, E_1 \to E_3)\delta(\boldsymbol{x}_3 - \boldsymbol{x}_1)\delta(w_3 - w_1) \\ &\times \iiiint \mathbb{1}(\boldsymbol{x}_1 \notin \{\boldsymbol{x}_{DX}\})\delta\Big(\boldsymbol{x}_6 - \boldsymbol{x}_{DX}(\boldsymbol{x}_1, \hat{\boldsymbol{\Omega}}_6)\Big) f_{DX}(\boldsymbol{x}_1, \hat{\boldsymbol{\Omega}}_1 \to \hat{\boldsymbol{\Omega}}_6, E_1 \to E_6) \\ &\times \delta(w_6 - w_{DX}(w_1))\Psi^{DX}_{FC,DX}(\boldsymbol{p}_6) dw_6 dE_6 d\Omega_6 dx_6 dw_3 dE_3 d\Omega_3 dx_3 dw_1 dE_1 d\Omega_1 dx_1.\end{aligned} \tag{160}$$

Evaluating the integration over the weight dimensions,

$$\begin{aligned}\mathrm{Term}_4 = &\int_{\boldsymbol{x}\in\{\boldsymbol{x}_\Gamma \cap \neg \boldsymbol{x}_{DX}\}} \int_{4\pi} \int_0^\infty \frac{\exp(-\ell(\boldsymbol{x},\boldsymbol{x}_1))}{1-\exp(-\ell(\boldsymbol{x},\boldsymbol{x}_{DX}(\boldsymbol{x},\hat{\boldsymbol{\Omega}})))}\delta(\hat{\boldsymbol{\Omega}}_1 - \hat{\boldsymbol{\Omega}})\delta(E_1 - E) \\ &\times \iiint \Sigma_s(\boldsymbol{x}_1, \hat{\boldsymbol{\Omega}}_1 \to \hat{\boldsymbol{\Omega}}_3, E_1 \to E_3)\delta(\boldsymbol{x}_3 - \boldsymbol{x}_1) \\ &\times \iiint \mathbb{1}(\boldsymbol{x}_1 \notin \{\boldsymbol{x}_{DX}\})\delta\Big(\boldsymbol{x}_6 - \boldsymbol{x}_{DX}(\boldsymbol{x}_1, \hat{\boldsymbol{\Omega}}_6)\Big) f_{DX}(\boldsymbol{x}_1, \hat{\boldsymbol{\Omega}}_1 \to \hat{\boldsymbol{\Omega}}_6, E_1 \to E_6) \\ &\times \Psi^{DX}_{FC,DX}(\boldsymbol{r}_6, w_{DX}(w_c(w))) dE_6 d\Omega_6 dx_6 dE_3 d\Omega_3 dx_3 dE_1 d\Omega_1 dx_1.\end{aligned} \tag{161}$$

Expanding the $w_{DX}(w_c(w))$ weight term using Eqs. 6 and 146,

$$\begin{aligned}\mathrm{Term}_4 = &\int_{\boldsymbol{x}\in\{\boldsymbol{x}_\Gamma \cap \neg \boldsymbol{x}_{DX}\}} \int_{4\pi} \int_0^\infty \frac{\exp(-\ell(\boldsymbol{x},\boldsymbol{x}_1))}{1-\exp(-\ell(\boldsymbol{x},\boldsymbol{x}_{DX}(\boldsymbol{x},\hat{\boldsymbol{\Omega}})))}\delta(\hat{\boldsymbol{\Omega}}_1 - \hat{\boldsymbol{\Omega}})\delta(E_1 - E) \\ &\times \iiint \Sigma_s(\boldsymbol{x}_1, \hat{\boldsymbol{\Omega}}_1 \to \hat{\boldsymbol{\Omega}}_3, E_1 \to E_3)\delta(\boldsymbol{x}_3 - \boldsymbol{x}_1) \\ &\times \iiint \mathbb{1}(\boldsymbol{x}_1 \notin \{\boldsymbol{x}_{DX}\})\delta\Big(\boldsymbol{x}_6 - \boldsymbol{x}_{DX}(\boldsymbol{x}_1, \hat{\boldsymbol{\Omega}}_6)\Big) f_{DX}(\boldsymbol{x}_1, \hat{\boldsymbol{\Omega}}_1 \to \hat{\boldsymbol{\Omega}}_6, E_1 \to E_6) \\ &\times \Psi^{DX}_{FC,DX}(\boldsymbol{r}_6, w_{DX}(w)(1-\exp(-\ell(\boldsymbol{x},\boldsymbol{x}_{DX}(\boldsymbol{x},\hat{\boldsymbol{\Omega}}))))) dE_6 d\Omega_6 dx_6 dE_3 d\Omega_3 dx_3 dE_1 d\Omega_1 dx_1.\end{aligned} \tag{162}$$

Using the separability of weight and score moment in weight-independent techniques $\Psi(\boldsymbol{r}, cw) = c\Psi(\boldsymbol{r}, w)$

and simplifying,

$$
\begin{aligned}
\text{Term}_4 = &\int_{\boldsymbol{x}\in\{\boldsymbol{x}_\Gamma \cap \neg \boldsymbol{x}_{DX}\}} \int_{4\pi} \int_0^\infty \exp(-\ell(\boldsymbol{x},\boldsymbol{x}_1))\delta(\hat{\boldsymbol{\Omega}}_1 - \hat{\boldsymbol{\Omega}})\delta(E_1 - E) \\
&\times \iiint \Sigma_s(\boldsymbol{x}_1, \hat{\boldsymbol{\Omega}}_1 \to \hat{\boldsymbol{\Omega}}_3, E_1 \to E_3)\delta(\boldsymbol{x}_3 - \boldsymbol{x}_1) \\
&\times \iiint \mathbb{1}(\boldsymbol{x}_1 \notin \{\boldsymbol{x}_{DX}\})\delta\Big(\boldsymbol{x}_6 - \boldsymbol{x}_{DX}(\boldsymbol{x}_1, \hat{\boldsymbol{\Omega}}_6)\Big) f_{DX}(\boldsymbol{x}_1, \hat{\boldsymbol{\Omega}}_1 \to \hat{\boldsymbol{\Omega}}_6, E_1 \to E_6) \\
&\times \cancelto{1}{\frac{1-\exp(-\ell(\boldsymbol{x},\boldsymbol{x}_{DX}(\boldsymbol{x},\hat{\boldsymbol{\Omega}})))}{1-\exp(-\ell(\boldsymbol{x},\boldsymbol{x}_{DX}(\boldsymbol{x},\hat{\boldsymbol{\Omega}})))}} \Psi^{DX}_{FC,DX}(\boldsymbol{r}_6, w_{DX}(w)) dE_6 d\Omega_6 dx_6 dE_3 d\Omega_3 dx_3 dE_1 d\Omega_1 dx_1.
\end{aligned}
\tag{163}
$$

Eq. 163 is equivalent to integrating over all possible weight with support restricted to a weight of $w_{DX}(w)$ using Dirac delta functions such that

$$
\begin{aligned}
\text{Term}_4 = &\int_{\boldsymbol{x}\in\{\boldsymbol{x}_\Gamma \cap \neg \boldsymbol{x}_{DX}\}} \int_{4\pi} \int_0^\infty \int_{-\infty}^{\infty} \exp(-\ell(\boldsymbol{x},\boldsymbol{x}_1))\delta(\hat{\boldsymbol{\Omega}}_1 - \hat{\boldsymbol{\Omega}})\delta(E_1 - E)\delta(w_1 - w) \\
&\times \iiiint \Sigma_s(\boldsymbol{x}_1, \hat{\boldsymbol{\Omega}}_1 \to \hat{\boldsymbol{\Omega}}_3, E_1 \to E_3)\delta(\boldsymbol{x}_3 - \boldsymbol{x}_1)\delta(w_3 - w_1) \\
&\times \iiiint \mathbb{1}(\boldsymbol{x}_1 \notin \{\boldsymbol{x}_{DX}\})\delta\Big(\boldsymbol{x}_6 - \boldsymbol{x}_{DX}(\boldsymbol{x}_1, \hat{\boldsymbol{\Omega}}_6)\Big) f_{DX}(\boldsymbol{x}_1, \hat{\boldsymbol{\Omega}}_1 \to \hat{\boldsymbol{\Omega}}_6, E_1 \to E_6) \\
&\times \delta(w_6 - w_{DX}(w_1)) \Psi^{DX}_{FC,DX}(\boldsymbol{p}_6) dw_6 dE_6 d\Omega_6 dx_6 dw_3 dE_3 d\Omega_3 dx_3 dw_1 dE_1 d\Omega_1 dx_1.
\end{aligned}
\tag{164}
$$

Recognizing the emissive collision and flight-to-DXTRAN operators,

$$
\begin{aligned}
\text{Term}_4 = &\int_{\boldsymbol{x}\in\{\boldsymbol{x}_\Gamma \cap \neg \boldsymbol{x}_{DX}\}} \int_{4\pi} \int_0^\infty \int_{-\infty}^{\infty} \exp(-\ell(\boldsymbol{x},\boldsymbol{x}_1))\delta(\hat{\boldsymbol{\Omega}}_1 - \hat{\boldsymbol{\Omega}})\delta(E_1 - E)\delta(w_1 - w) \\
&\times \mathcal{K}_E(\boldsymbol{p}_1, \boldsymbol{p}_3)\mathcal{B}_{DX}(\boldsymbol{p}_1, \boldsymbol{p}_6)\Psi^{DX}_{FC,DX}(\boldsymbol{p}_6) dw_1 dE_1 d\Omega_1 dx_1.
\end{aligned}
\tag{165}
$$

Note that the integration over $\boldsymbol{p}_1$ of the first, second, and fourth terms of Eq. 143 (given by Eqs. 148, 153, and 165) is identical and that the third term (given by Eq. 159) is zero. Therefore, Eq. 143 can be written for the case of the particle streaming path intersecting the DXTRAN region before a cell surface as,

$$
\begin{aligned}
\Psi_{FC,DX}(\boldsymbol{p}) = &\int_{\boldsymbol{x}\in\{\boldsymbol{x}_\Gamma \cap \neg \boldsymbol{x}_{DX}\}} \int_{4\pi} \int_0^\infty \int_{-\infty}^{\infty} \exp(-\ell(\boldsymbol{x},\boldsymbol{x}_1))\delta(\hat{\boldsymbol{\Omega}}_1 - \hat{\boldsymbol{\Omega}})\delta(E_1 - E)\delta(w_1 - w) \\
&\times \Bigg(\mathcal{K}_A(\boldsymbol{p}_1, \boldsymbol{p}_2)\bar{s}_A(\boldsymbol{p}_1) \\
&+ \mathcal{K}_E(\boldsymbol{p}_1, \boldsymbol{p}_3)\big(\bar{s}_E(\boldsymbol{p}_1) + \Psi^{DX}_{FC,DX}(\boldsymbol{p}_3)\big) \\
&+ 0 \\
&+ \mathcal{K}_E(\boldsymbol{p}_1, \boldsymbol{p}_3)\mathcal{B}_{DX}(\boldsymbol{p}_1, \boldsymbol{p}_6)\Psi^{DX}_{FC,DX}(\boldsymbol{p}_6)\Bigg) dw_1 dE_1 d\Omega_1 dx_1, \ \boldsymbol{p} \in \{\boldsymbol{p}_{FC}\}.
\end{aligned}
\tag{166}
$$

6.2.2 Expansion for the Case of a Cell Surface Next in the Streaming Path

In this case, the next surface intersected by the particle streaming path is a part of the computational geometry, not the surface of the DXTRAN region. For forced-collision transport operators, this means that $\|\boldsymbol{x} - \boldsymbol{x}_S\| < \|\boldsymbol{x} - \boldsymbol{x}_{DX}\|$ is true, so the flight-to-collision and flight-to-transmission operators in Eq. 60 can be expanded using the first cases of Eqs. 191 and 192. Again, The forced-collision operators in Eq. 143 are expanded on a term by term basis with $\boldsymbol{p} \in \{\boldsymbol{p}_{FC}\}$ omitted for ease of notation. Because a similar process is used in this section as in Sec. 6.2.1, some steps are omitted to avoid undue redundancy.

In the first term of Eq. 143, expanding the flight-to-collision operator using Eq. 191 and the average score contribution using Eq. 62 yields

$$\begin{aligned}\text{Term}_1 = &\int_{\boldsymbol{x}\in\{\boldsymbol{x}_\Gamma\}}\int_{4\pi}\int_0^\infty\int_{-\infty}^\infty \frac{\exp(-\ell(\boldsymbol{x},\boldsymbol{x}_1))}{1-\exp(-\ell(\boldsymbol{x},\boldsymbol{x}_S(\boldsymbol{x},\hat{\boldsymbol{\Omega}})))}\delta(\hat{\boldsymbol{\Omega}}_1-\hat{\boldsymbol{\Omega}})\delta(E_1-E)\delta(w_1-w_c)\\ &\times \mathcal{K}_A(\boldsymbol{p}_1,\boldsymbol{p}_2)w_1 m_A(\boldsymbol{r}_1)dw_1 dE_1 d\Omega_1 dx_1.\end{aligned} \tag{167}$$

Note that Eq. 167 and Eq. 144 differ because the flight-to-collision operator definition depends on the first surface intersected by the particle streaming path. Taking the identical steps to those in Eqs. 145–148 except inserting Eq. 73 for w_c,

$$\begin{aligned}\text{Term}_1 = &\int_{\boldsymbol{x}\in\{\boldsymbol{x}_\Gamma\}}\int_{4\pi}\int_0^\infty\int_{-\infty}^\infty \exp(-\ell(\boldsymbol{x},\boldsymbol{x}_1))\delta(\hat{\boldsymbol{\Omega}}_1-\hat{\boldsymbol{\Omega}})\delta(E_1-E)\delta(w_1-w)\\ &\times \mathcal{K}_A(\boldsymbol{p}_1,\boldsymbol{p}_2)\bar{s}_A(\boldsymbol{p}_1)dw_1 dE_1 d\Omega_1 dx_1.\end{aligned} \tag{168}$$

In the second term of Eq. 143, expanding the flight-to-collision operator using Eq. 191, the average score contribution using Eq. 62, and the emissive collision operator using Eq. 190 yields

$$\begin{aligned}\text{Term}_2 = &\int_{\boldsymbol{x}\in\{\boldsymbol{x}_\Gamma\}}\int_{4\pi}\int_0^\infty\int_{-\infty}^\infty \frac{\exp(-\ell(\boldsymbol{x},\boldsymbol{x}_1))}{1-\exp(-\ell(\boldsymbol{x},\boldsymbol{x}_S(\boldsymbol{x},\hat{\boldsymbol{\Omega}})))}\delta(\hat{\boldsymbol{\Omega}}_1-\hat{\boldsymbol{\Omega}})\delta(E_1-E)\delta(w_1-w_c)\\ &\times \iiiint \Sigma_s(\boldsymbol{x}_1,\hat{\boldsymbol{\Omega}}_1\to\hat{\boldsymbol{\Omega}}_3,E_1\to E_3)\delta(\boldsymbol{x}_3-\boldsymbol{x}_1)\delta(w_3-w_1)\big(w_1 m_E(\boldsymbol{r}_1)+\Psi_{FC,DX}^{DX}(\boldsymbol{p}_3)\big)\\ &\times dw_3 dE_3 d\Omega_3 dx_3 dw_1 dE_1 d\Omega_1 dx_1.\end{aligned} \tag{169}$$

Repeating the steps taken in Eqs. 150–153 except using Eq. 73 for w_c yields

$$\begin{aligned}\text{Term}_2 = &\int_{\boldsymbol{x}\in\{\boldsymbol{x}_\Gamma\}}\int_{4\pi}\int_0^\infty\int_{-\infty}^\infty \exp(-\ell(\boldsymbol{x},\boldsymbol{x}_1))\delta(\hat{\boldsymbol{\Omega}}_1-\hat{\boldsymbol{\Omega}})\delta(E_1-E)\delta(w_1-w)\\ &\times \mathcal{K}_E(\boldsymbol{p}_1,\boldsymbol{p}_3)\big(\bar{s}_E(\boldsymbol{p}_1)+\Psi_{FC,DX}^{DX}(\boldsymbol{p}_3)\big)dw_1 dE_1 d\Omega_1 dx_1.\end{aligned} \tag{170}$$

In the third term of Eq. 143, expanding the flight-to-collision operator using Eq. 191 and the average score contribution using Eq. 62 yields

$$\begin{aligned}\text{Term}_3 = &\int_{\boldsymbol{x}\in\{\boldsymbol{x}_\Gamma\}}\int_{4\pi}\int_0^\infty\int_{-\infty}^\infty \frac{\exp(-\ell(\boldsymbol{x},\boldsymbol{x}_1))}{1-\exp(-\ell(\boldsymbol{x},\boldsymbol{x}_S(\boldsymbol{x},\hat{\boldsymbol{\Omega}})))}\delta(\hat{\boldsymbol{\Omega}}_1-\hat{\boldsymbol{\Omega}})\delta(E_1-E)\delta(w_1-w_c)\\ &\times (\mathcal{K}_A(\boldsymbol{p}_1,\boldsymbol{p}_2)+\mathcal{K}_E(\boldsymbol{p}_1,\boldsymbol{p}_3))dw_1 dE_1 d\Omega_1 dx_1 \mathcal{B}_t(\boldsymbol{p},\boldsymbol{p}_4)\mathcal{S}(\boldsymbol{p}_4,\boldsymbol{p}_5)(w_4 m_S(\boldsymbol{r}_4)+\Psi_{FC,DX}(\boldsymbol{p}_5)).\end{aligned} \tag{171}$$

It is shown in Eqs. 83–89 that this integration over $\boldsymbol{p}_1$ results in one. Using this,

$$\text{Term}_3 = \mathcal{B}_t(\boldsymbol{p},\boldsymbol{p}_4)\mathcal{S}(\boldsymbol{p}_4,\boldsymbol{p}_5)(w_4 m_S(\boldsymbol{r}_4)+\Psi_{FC,DX}(\boldsymbol{p}_5)). \tag{172}$$

Expanding the flight-to-transmission operator with Eq. 192 and the surface-crossing operator with Eq. 188,

$$\begin{aligned}\text{Term}_3 = &\iiiint \delta(\boldsymbol{x}_4-\boldsymbol{x}_S(\boldsymbol{x},\hat{\boldsymbol{\Omega}}))\delta(\hat{\boldsymbol{\Omega}}_4-\hat{\boldsymbol{\Omega}})\delta(E_4-E)\delta(w_4-w_t)\\ &\times \iiiint \delta(\boldsymbol{x}_5-\boldsymbol{x}_4)\delta(\hat{\boldsymbol{\Omega}}_5-\hat{\boldsymbol{\Omega}}_4)\delta(E_5-E_4)\delta(w_5-w_4^*)\\ &\times (w_4 m_S(\boldsymbol{r}_4)+\Psi_{FC,DX}(\boldsymbol{p}_5))dw_5 dE_5 d\Omega_5 dx_5 dw_4 dE_4 d\Omega_4 dx_4,\end{aligned} \tag{173}$$

where w_4^* is either w_4 or 0 depending on whether the surface being crossed is an internal or boundary surface as specified in Eq. 188. Evaluating the integrations over weight,

$$\begin{aligned}\text{Term}_3 = &\iiint \delta(\boldsymbol{x}_4-\boldsymbol{x}_S(\boldsymbol{x},\hat{\boldsymbol{\Omega}}))\delta(\hat{\boldsymbol{\Omega}}_4-\hat{\boldsymbol{\Omega}})\delta(E_4-E)\\ &\times \iiint \delta(\boldsymbol{x}_5-\boldsymbol{x}_4)\delta(\hat{\boldsymbol{\Omega}}_5-\hat{\boldsymbol{\Omega}}_4)\delta(E_5-E_4)\\ &\times (w_t m_S(\boldsymbol{r}_4)+\psi_{FC,DX}(\boldsymbol{r}_5,w_t^*))dE_5 d\Omega_5 dx_5 dE_4 d\Omega_4 dx_4,\end{aligned} \tag{174}$$

where w_t^* is either w_t due to the Dirac delta functions in weight or 0. Note that the separability of weight and score moment in weight-independent techniques $\Psi(\boldsymbol{r}, cw) = c\Psi(\boldsymbol{r}, w)$ implies that $\Psi_{FC,DX}(\boldsymbol{r}_4, w_t^*)$ is either $\Psi_{FC,DX}(\boldsymbol{r}_4, w_t)$ or 0. This means that Eq. 3 can be used to pull the weight modification out of the sum of the average score and HSME,

$$\begin{aligned}\text{Term}_3 = &\iiint \exp\Big(-\ell(\boldsymbol{x}, \boldsymbol{x}_S(\boldsymbol{x}, \hat{\boldsymbol{\Omega}}))\Big)\delta(\boldsymbol{x}_4 - \boldsymbol{x}_S(\boldsymbol{x}, \hat{\boldsymbol{\Omega}}))\delta(\hat{\boldsymbol{\Omega}}_4 - \hat{\boldsymbol{\Omega}})\delta(E_4 - E)\\ &\times \iiint \delta(\boldsymbol{x}_5 - \boldsymbol{x}_4)\delta(\hat{\boldsymbol{\Omega}}_5 - \hat{\boldsymbol{\Omega}}_4)\delta(E_5 - E_4)\\ &\times (w m_S(\boldsymbol{r}_4) + \Psi_{FC,DX}(\boldsymbol{r}_5, w^*))dE_5 d\Omega_5 dx_5 dE_4 d\Omega_4 dx_4,\end{aligned} \tag{175}$$

where w^* is either w or 0. Eq. 175 is equivalent to integrating over the weight dimension with support only for weight w using Dirac delta functions such that

$$\begin{aligned}\text{Term}_3 = &\iiiint \exp\Big(-\ell(\boldsymbol{x}, \boldsymbol{x}_S(\boldsymbol{x}, \hat{\boldsymbol{\Omega}}))\Big)\delta(\hat{\boldsymbol{\Omega}}_4 - \hat{\boldsymbol{\Omega}})\delta(E_4 - E)\delta(w_4 - w)\\ &\times \delta(\boldsymbol{x}_4 - \boldsymbol{x}_S(\boldsymbol{x}, \hat{\boldsymbol{\Omega}})) \iiiint \delta(\boldsymbol{x}_5 - \boldsymbol{x}_4)\delta(\hat{\boldsymbol{\Omega}}_5 - \hat{\boldsymbol{\Omega}}_4)\delta(E_5 - E_4)\delta(w_5 - w_4^*)\\ &\times (w_4 m_S(\boldsymbol{r}_4) + \Psi_{FC,DX}(\boldsymbol{p}_5))dw_5 dE_5 d\Omega_5 dx_5 dw_4 dE_4 d\Omega_4 dx_4.\end{aligned} \tag{176}$$

Recognizing the surface-crossing operator,

$$\begin{aligned}\text{Term}_3 = &\iiiint \exp\Big(-\ell(\boldsymbol{x}, \boldsymbol{x}_S(\boldsymbol{x}, \hat{\boldsymbol{\Omega}}))\Big)\delta(\hat{\boldsymbol{\Omega}}_4 - \hat{\boldsymbol{\Omega}})\delta(E_4 - E)\delta(w_4 - w)\\ &\times \delta(\boldsymbol{x}_4 - \boldsymbol{x}_S(\boldsymbol{x}, \hat{\boldsymbol{\Omega}}))\mathcal{S}(\boldsymbol{p}_4, \boldsymbol{p}_5)(w_4 m_S(\boldsymbol{r}_4) + \Psi_{FC,DX}(\boldsymbol{p}_5))dw_4 dE_4 d\Omega_4 dx_4.\end{aligned} \tag{177}$$

Adding explicit integration bounds, removing the Dirac delta function over position that is redundant with the surface-crossing operator, changing $\boldsymbol{x}_S$ to $\boldsymbol{x}_4$ in the exponential function because they are equivalent due to the surface-crossing operator, and using Eq. 62,

$$\begin{aligned}\text{Term}_3 = &\int_{\boldsymbol{x}\in\{\boldsymbol{x}_\Gamma\}} \int_{4\pi} \int_0^\infty \int_{-\infty}^\infty \exp\Big(-\ell(\boldsymbol{x}, \boldsymbol{x}_4(\boldsymbol{x}, \hat{\boldsymbol{\Omega}}))\Big)\delta(\hat{\boldsymbol{\Omega}}_4 - \hat{\boldsymbol{\Omega}})\delta(E_4 - E)\delta(w_4 - w)\\ &\times \mathcal{S}(\boldsymbol{p}_4, \boldsymbol{p}_5)(\bar{s}_S(\boldsymbol{p}_4) + \Psi_{FC,DX}(\boldsymbol{p}_5))dw_4 dE_4 d\Omega_4 dx_4.\end{aligned} \tag{178}$$

In the fourth term of Eq. 143, expanding the flight-to-collision operator using Eq. 191, the emissive collision operator with Eq. 190, the flight-to-DXTRAN operator with Eq. 193, and the average score contribution using Eq. 62 yields

$$\begin{aligned}\text{Term}_4 = &\int_{\boldsymbol{x}\in\{\boldsymbol{x}_\Gamma\}} \int_{4\pi} \int_0^\infty \int_{-\infty}^\infty \frac{\exp(-\ell(\boldsymbol{x}, \boldsymbol{x}_1))}{1 - \exp(-\ell(\boldsymbol{x}, \boldsymbol{x}_S(\boldsymbol{x}, \hat{\boldsymbol{\Omega}})))}\delta(\hat{\boldsymbol{\Omega}}_1 - \hat{\boldsymbol{\Omega}})\delta(E_1 - E)\\ &\times \delta(w_1 - w_c(w)) \iiiint \Sigma_s(\boldsymbol{x}_1, \hat{\boldsymbol{\Omega}}_1 \to \hat{\boldsymbol{\Omega}}_3, E_1 \to E_3)\delta(\boldsymbol{x}_3 - \boldsymbol{x}_1)\delta(w_3 - w_1)\\ &\times \iiiint \mathbb{1}(\boldsymbol{x}_1 \notin \{\boldsymbol{x}_{DX}\})\delta\Big(\boldsymbol{x}_6 - \boldsymbol{x}_{DX}(\boldsymbol{x}_1, \hat{\boldsymbol{\Omega}}_6)\Big) f_{DX}(\boldsymbol{x}_1, \hat{\boldsymbol{\Omega}}_1 \to \hat{\boldsymbol{\Omega}}_6, E_1 \to E_6)\\ &\times \delta(w_6 - w_{DX}(w_1))\Psi_{FC,DX}^{DX}(\boldsymbol{p}_6)dw_6 dE_6 d\Omega_6 dx_6 dw_3 dE_3 d\Omega_3 dx_3 dw_1 dE_1 d\Omega_1 dx_1.\end{aligned} \tag{179}$$

Repeating the steps taken in Eqs. 161–165 on Eq. 179 except using Eq. 73 for w_c yields

$$\begin{aligned}\text{Term}_4 = &\int_{\boldsymbol{x}\in\{\boldsymbol{x}_\Gamma\}} \int_{4\pi} \int_0^\infty \int_{-\infty}^\infty \exp(-\ell(\boldsymbol{x}, \boldsymbol{x}_1))\delta(\hat{\boldsymbol{\Omega}}_1 - \hat{\boldsymbol{\Omega}})\delta(E_1 - E)\delta(w_1 - w)\\ &\times \mathcal{K}_E(\boldsymbol{p}_1, \boldsymbol{p}_3)\mathcal{B}_{DX}(\boldsymbol{p}_1, \boldsymbol{p}_6)\Psi_{FC,DX}^{DX}(\boldsymbol{p}_6)dw_1 dE_1 d\Omega_1 dx_1.\end{aligned} \tag{180}$$

Finally, combining the integrations for all terms given in Eqs. 168, 170, 178, and 180 results in the combined-technique HSME for the case of the particle streaming path intersecting a cell surface before the DXTRAN region,

$$\Psi_{FC,DX}(\boldsymbol{p}) = \int_{\boldsymbol{x}\in\{\boldsymbol{x}_\Gamma\}} \int_{4\pi} \int_0^\infty \int_{-\infty}^\infty \exp(-\ell(\boldsymbol{x},\boldsymbol{x}_1))\delta(\hat{\boldsymbol{\Omega}}_1 - \hat{\boldsymbol{\Omega}})\delta(E_1 - E)\delta(w_1 - w)$$
$$\times \Big(\mathcal{K}_A(\boldsymbol{p}_1,\boldsymbol{p}_2)\bar{s}_A(\boldsymbol{p}_1)$$
$$+ \mathcal{K}_E(\boldsymbol{p}_1,\boldsymbol{p}_3)\big(\bar{s}_E(\boldsymbol{p}_1) + \Psi^{DX}_{FC,DX}(\boldsymbol{p}_3)\big)$$
$$+ \mathcal{S}(\boldsymbol{p}_1,\boldsymbol{p}_5)(\bar{s}_S(\boldsymbol{p}_1) + \Psi_{FC,DX}(\boldsymbol{p}_5))$$
$$+ \mathcal{K}_E(\boldsymbol{p}_1,\boldsymbol{p}_3)\mathcal{B}_{DX}(\boldsymbol{p}_1,\boldsymbol{p}_6)\Psi^{DX}_{FC,DX}(\boldsymbol{p}_6)\Big) dw_1 dE_1 d\Omega_1 dx_1,\ \boldsymbol{p}\in\{\boldsymbol{p}_{FC}\}. \tag{181}$$

6.2.3 Equivalence of the Combined Cases to the DXTRAN Technique

With the forced-collision operators expanded for both cases, the equivalence with the DXTRAN transport operator can be shown. The case of a particle traveling toward a DXTRAN region and intersecting it before a cell surface is described in Sec. 6.2.1. This case satisfies the first three considerations of the truncation function of the DXTRAN free-flight operator given in Eq. 195. The fourth consideration of the truncation function is satisfied for all positions that lay inside the DXTRAN region. The definition of the DXTRAN free-flight transmission operator given in Eq. 194 requires that the particle is killed for all phase spaces which completely satisfy the truncation function. This is done exactly in the integration over position of the combined-technique HSME for this case given in Eq. 166 by excluding positions inside the DXTRAN region, $\boldsymbol{x}\in\{\boldsymbol{x}_\Gamma \cap \neg\boldsymbol{x}_{DX}\}$. The HSME may then be written as

$$\Psi_{FC,DX}(\boldsymbol{p}) = \mathcal{T}_{DX}(\boldsymbol{p},\boldsymbol{p}_1)\Big(\mathcal{K}_A(\boldsymbol{p}_1,\boldsymbol{p}_2)\bar{s}_A(\boldsymbol{p}_1)$$
$$+ \mathcal{K}_E(\boldsymbol{p}_1,\boldsymbol{p}_3)\big(\bar{s}_E(\boldsymbol{p}_1) + \Psi^{DX}_{FC,DX}(\boldsymbol{p}_3)\big)$$
$$+ 0$$
$$+ \mathcal{K}_E(\boldsymbol{p}_1,\boldsymbol{p}_3)\mathcal{B}_{DX}(\boldsymbol{p}_1,\boldsymbol{p}_6)\Psi^{DX}_{FC,DX}(\boldsymbol{p}_6)\Big),\ \boldsymbol{p}\in\{\boldsymbol{p}_{FC}\}\,|\,\text{Case 1}, \tag{182}$$

where Case 1 denotes the assumptions about the particle streaming path made in Sec. 6.2.1. Similarly, because the DXTRAN free-flight operator kills the particle before reaching a cell surface in this case, the third term may be replaced with the surface-crossing operator without losing equality because it will never be non-zero on this range of positions so,

$$\Psi_{FC,DX}(\boldsymbol{p}) = \mathcal{T}_{DX}(\boldsymbol{p},\boldsymbol{p}_1)\Big(\mathcal{K}_A(\boldsymbol{p}_1,\boldsymbol{p}_2)\bar{s}_A(\boldsymbol{p}_1)$$
$$+ \mathcal{K}_E(\boldsymbol{p}_1,\boldsymbol{p}_3)\big(\bar{s}_E(\boldsymbol{p}_1) + \Psi^{DX}_{FC,DX}(\boldsymbol{p}_3)\big)$$
$$+ \mathcal{S}(\boldsymbol{p}_1,\boldsymbol{p}_5)\big(\bar{s}_S(\boldsymbol{p}_5) + \Psi^{DX}_{FC,DX}(\boldsymbol{p}_5)\big)$$
$$+ \mathcal{K}_E(\boldsymbol{p}_1,\boldsymbol{p}_3)\mathcal{B}_{DX}(\boldsymbol{p}_1,\boldsymbol{p}_6)\Psi^{DX}_{FC,DX}(\boldsymbol{p}_6)\Big),\ \boldsymbol{p}\in\{\boldsymbol{p}_{FC}\}\,|\,\text{Case 1}. \tag{183}$$

In the opposite case presented in Sec. 6.2.2, the second and fourth considerations of the truncation operator are never satisfied together because the particle streaming path intersects a cell surface before the DXTRAN region. Because the truncation function is never satisfied, the DXTRAN free-flight transmission operator takes the form of the analog free-flight transmission operator, which is identical to the expanded form of combined-technique HSME for this case given by Eq. 181. The HSME may then be written as

$$\Psi_{FC,DX}(\boldsymbol{p}) = \mathcal{T}_{DX}(\boldsymbol{p},\boldsymbol{p}_1)\Big(\mathcal{K}_A(\boldsymbol{p}_1,\boldsymbol{p}_2)\bar{s}_A(\boldsymbol{p}_1)$$
$$+ \mathcal{K}_E(\boldsymbol{p}_1,\boldsymbol{p}_3)\big(\bar{s}_E(\boldsymbol{p}_1) + \Psi^{DX}_{FC,DX}(\boldsymbol{p}_3)\big)$$
$$+ \mathcal{S}(\boldsymbol{p}_1,\boldsymbol{p}_5)\big(\bar{s}_S(\boldsymbol{p}_5) + \Psi^{DX}_{FC,DX}(\boldsymbol{p}_5)\big)$$
$$+ \mathcal{K}_E(\boldsymbol{p}_1,\boldsymbol{p}_3)\mathcal{B}_{DX}(\boldsymbol{p}_1,\boldsymbol{p}_6)\Psi^{DX}_{FC,DX}(\boldsymbol{p}_6)\Big),\ \boldsymbol{p}\in\{\boldsymbol{p}_{FC}\}\,|\,\text{Case 2}, \tag{184}$$

where Case 2 denotes the assumptions about the particle streaming path made in Sec. 6.2.2. Note that Eqs. 183 and 184 show that the combined-technique HSME takes identical forms for each disjoint case, so it may be written generally as

$$
\begin{aligned}
\Psi_{FC,DX}(\boldsymbol{p}) = {} & \mathcal{T}_{DX}(\boldsymbol{p},\boldsymbol{p}_1)\mathcal{K}_A(\boldsymbol{p}_1,\boldsymbol{p}_2)\bar{s}_A(\boldsymbol{p}_1) \\
& + \mathcal{T}_{DX}(\boldsymbol{p},\boldsymbol{p}_1)\mathcal{K}_E(\boldsymbol{p}_1,\boldsymbol{p}_3)\big(\bar{s}_E(\boldsymbol{p}_1) + \Psi^{DX}_{FC,DX}(\boldsymbol{p}_3)\big) \\
& + \mathcal{T}_{DX}(\boldsymbol{p},\boldsymbol{p}_4)\mathcal{S}(\boldsymbol{p}_4,\boldsymbol{p}_5)\big(\bar{s}_S(\boldsymbol{p}_4) + \Psi^{DX}_{FC,DX}(\boldsymbol{p}_5)\big) \\
& + \mathcal{T}_{DX}(\boldsymbol{p},\boldsymbol{p}_1)\mathcal{K}_E(\boldsymbol{p}_1,\boldsymbol{p}_3)\mathcal{B}_{DX}(\boldsymbol{p}_1,\boldsymbol{p}_6)\Psi^{DX}_{FC,DX}(\boldsymbol{p}_6),\ \boldsymbol{p} \in \{\boldsymbol{p}_{FC}\}.
\end{aligned}
\tag{185}
$$

The combined-technique HSME in a phase space where forced collisions are specified given in Eq. 185 is identical to the DXTRAN HSME except that it is recursive with $\Psi^{DX}_{FC,DX}$ rather than itself. Recall that Eq. 142 shows that $\Psi^{DX}_{FC,DX}$ is equivalent to the DXTRAN HSME. Considered together, Eqs. 142 and 186 show that the combined-techniques HSME is equivalent to the DXTRAN HSME for all phase spaces,

$$
\Psi_{FC,DX}(\boldsymbol{p}) = \Psi_{DX}(\boldsymbol{p}). \tag{186}
$$

Because the DXTRAN HSME is shown to be equivalent to the analog HSME in Sec. 5, Eq. 186 proves that the combined-technique HSME is similarly equivalent to the analog HSME and no scoring bias is expected.

7 Conclusions

Starting from the definitions of the forced-collision, DXTRAN, and combined forced-collision and DXTRAN variance-reduction techniques, this report provides proof that the these techniques do not bias Monte Carlo particle transport. This is done by first deriving the History Score Probability Density Function (HSPDF), a function that governs the probability of a particle at some phase space contributing a given combined score to all tallies when simulated to the end of its history, for analog transport and each variance-reduction technique. Then, first History Score Moment Equations (HSMEs), functions that govern the expected combined score to all tallies from simulating a particle at some phase space to the end of its history, are found by calculating the first score moment of each HSPDF. Finally, through a series of manipulations with care taken to show all necessary detail to follow the derivation exactly, each HSME is shown to be equivalent to the other. Because the HSMEs for transport with variance-reduction techniques in use are shown to reduce to the analog HSME, it is shown that the expected score to tallies in these simulations is unaltered by the techniques. Demonstration of an unaltered expected score is proof that these techniques do not bias Monte Carlo simulation results.

For simplicity, a non-multiplying medium and specific variance-reduction technique methodologies are assumed. If suspicious results from simulations employing these techniques are obtained where these assumptions are violated, future work may extend this proof to relax simplifying assumptions. In addition to providing rigorous proof that these techniques may be safely employed by Monte Carlo simulation code users, the authors hope that the derivation provided here sheds light on the nature of these techniques, what makes them fair, and how they may be correctly implemented in more cases than are explicitly detailed here for future researchers in the area.

References

1. S. Chucas and M. Grimstone, "The Acceleration Techniques in the Monte Carlo Code MCBEND," in *8th International Conference on Radiation Shielding*, Arlington, TX, USA, 1994, pp. 1–9.

2. X-5 Monte Carlo Team, "MCNP - A General Monte Carlo N-Particle Transport Code, Version 5 Volume I: Overview and Theory," Los Alamos National Laboratory, Los Alamos, NM, Tech. Rep. LA-UR-03-1987, Apr. 2003. [Online]. Available: https://laws.lanl.gov/vhosts/mcnp.lanl.gov/pdf_files/la-ur-03-1987.pdf

3. R. J. Juzaitis, "Minimizing the Cost of Splitting in Monte Carlo Radiation Transport Simulation," Ph.D. Thesis, University of Virginia, Oct. 1980, LA-8546-T. [Online]. Available: https://doi.org/10.2172/6753224

4. C. J. Solomon, "Discrete-Ordinates Cost Optimization of Weight-Dependent Variance Reduction Techniques for Monte Carlo Neutral Particle Transport," Ph.D. Thesis, Kansas State University, Dec. 2010. [Online]. Available: http://hdl.handle.net/2097/7014

5. J. A. Kulesza, "Cost-optimized Automated Variance Reduction for Highly Angle-dependent Radiation Transport Analyses," Ph.D. Thesis, University of Michigan, 2018. [Online]. Available: http://hdl.handle.net/2027.42/147541

6. B. C. Kiedrowski, J. A. Kulesza, C. J. Solomon, "Discrete Ordinates Prediction of the Forced-Collision Variance Reduction Technique in Slab Geometry," in *Proc. 2019 ANS Math. and Comp. Div.*, Aug. 2019.

7. T. E. Booth and E. D. Cashwell, "Analysis of Error in Monte Carlo Transport Calculations," *Nuclear Science and Engineering*, vol. 71, no. 2, pp. 128–142, 1979. [Online]. Available: https://doi.org/10.13182/NSE79-A20404

A Operator Definitions

The mathematical definitions of all operators used in this derivation are given in this appendix.

A.1 Free-Flight Transmission Operator

The free-flight transmission operator is

$$\mathcal{T}(\boldsymbol{p},\boldsymbol{p}') = \int_{\boldsymbol{x}\in\{\boldsymbol{x}_\Gamma\}} \int_{4\pi} \int_0^\infty \int_{-\infty}^\infty \exp(-\ell(\boldsymbol{x},\boldsymbol{x}'))\delta(\hat{\boldsymbol{\Omega}}' - \hat{\boldsymbol{\Omega}})\delta(E'-E)\delta(w'-w)dw'dE'd\Omega'dx', \tag{187}$$

where $\ell(\boldsymbol{x},\boldsymbol{x}')$ is the optical thickness between $\boldsymbol{x}$ and $\boldsymbol{x}'$ defined in Eq. 4 and $\{\boldsymbol{x}_\Gamma\}$ is the set of points on the ray from $\boldsymbol{x}$ along $\hat{\boldsymbol{\Omega}}'$ in the current cell. This operator governs the transmission of particles without a collision or surface crossing from $\boldsymbol{x}$ to $\boldsymbol{x}'$ by enforcing that all dimensions of the phase space other than the particle position remain the same and by accounting for the probability of free flight.

A.2 Surface-Crossing Operator

The surface-crossing operator is

$$\mathcal{S}(\boldsymbol{p},\boldsymbol{p}') = \begin{cases} \iiiint \delta(\boldsymbol{x}'-\boldsymbol{x})\delta(\hat{\boldsymbol{\Omega}}' - \hat{\boldsymbol{\Omega}})\delta(E'-E)\delta(w'-w)dw'dE'd\Omega'dx', & \boldsymbol{x}\in\{\boldsymbol{x}_{\text{Internal Surfaces}}\}, \\ \iiiint \delta(\boldsymbol{x}'-\boldsymbol{x})\delta(\hat{\boldsymbol{\Omega}}' - \hat{\boldsymbol{\Omega}})\delta(E'-E)\delta(w'-0)dw'dE'd\Omega'dx', & \boldsymbol{x}\in\{\boldsymbol{x}_{\text{Boundary Surfaces}}\}, \\ 0, & \text{otherwise}, \end{cases} \tag{188}$$

where $\{\boldsymbol{x}_{\text{Internal Surfaces}}\}$ is the set of all points that lay on the internal surfaces of the system and $\{\boldsymbol{x}_{\text{Boundary Surfaces}}\}$ is the set of all points that lay on the boundary surfaces of the system. This operator governs particles crossing a cell surface at position $\boldsymbol{x}$. Because the cell that the particle currently resides in is not included in the phase space defined herein, crossing a surface does not alter the particle phase space unless the surface crossed is a boundary of the system, in which case the particle is killed as denoted by a statistical weight of zero. Note that this operator may be modified to take on different roles in the presence of variance-reduction techniques not considered here such as when importance splitting is applied at boundaries between cells.

A.3 Absorptive Collision Operator

The absorptive collision operator is

$$\mathcal{K}_A(\boldsymbol{p},\boldsymbol{p}') = \iiiint \Sigma_a(\boldsymbol{x},E)\delta(\boldsymbol{x}'-\boldsymbol{x})\delta(\hat{\boldsymbol{\Omega}}' - \hat{\boldsymbol{\Omega}})\delta(E'-E)\delta(w'-0)dw'dE'd\Omega'dx', \tag{189}$$

where Σ_a is the macroscopic absorption cross section. This operator governs particles undergoing an absorptive collision at phase space $\boldsymbol{p}$ and emerging in phase space $\boldsymbol{p}'$. Because an absorption kills a particle in this work, the only phase space considered is that of the incident particle with a statistical weight of zero.

A.4 Emissive Collision Operator

The emissive collision operator is

$$\mathcal{K}_E(\boldsymbol{p},\boldsymbol{p}') = \iiiint \Sigma_s(\boldsymbol{x},\hat{\boldsymbol{\Omega}}\to\hat{\boldsymbol{\Omega}}',E\to E')\delta(\boldsymbol{x}'-\boldsymbol{x})\delta(w'-w)dw'dE'd\Omega'dx', \tag{190}$$

where $\Sigma_s(\boldsymbol{x},\hat{\boldsymbol{\Omega}}\to\hat{\boldsymbol{\Omega}}',E\to E')$ is the macroscopic double-differential scattering cross section. This operator governs particles undergoing an emissive collision at phase space $\boldsymbol{p}$ and emerging in a new phase space $\boldsymbol{p}'$ by enforcing that the position and weight of the particle does not change and accounting for the probability of emerging in a given direction with a given energy.

A.5 Flight-to-Collision Operator

The flight-to-collision operator is

$$\mathcal{B}_c(\boldsymbol{p},\boldsymbol{p}') = \begin{cases} \int \dfrac{\exp(-\ell(\boldsymbol{x},\boldsymbol{x}'))}{1-\exp(-\ell(\boldsymbol{x},\boldsymbol{x}_S(\boldsymbol{x},\hat{\boldsymbol{\Omega}})))}\delta(\hat{\boldsymbol{\Omega}}'-\hat{\boldsymbol{\Omega}})\delta(E'-E)\delta(w'-w_c)d\boldsymbol{p}', & \begin{bmatrix} \|\boldsymbol{x}-\boldsymbol{x}_S\| < \|\boldsymbol{x}-\boldsymbol{x}_{DX}\| \\ \text{and} \\ x' \in \{\boldsymbol{x}_\Gamma\} \end{bmatrix}, \\ \int \dfrac{\exp(-\ell(\boldsymbol{x},\boldsymbol{x}'))}{1-\exp(-\ell(\boldsymbol{x},\boldsymbol{x}_{DX}(\boldsymbol{x},\hat{\boldsymbol{\Omega}})))}\delta(\hat{\boldsymbol{\Omega}}'-\hat{\boldsymbol{\Omega}})\delta(E'-E)\delta(w'-w_c)d\boldsymbol{p}', & \begin{bmatrix} \|\boldsymbol{x}-\boldsymbol{x}_S\| > \|\boldsymbol{x}-\boldsymbol{x}_{DX}\|, \\ \boldsymbol{x}' \in \{\boldsymbol{x}_\Gamma\}, \text{ and} \\ \boldsymbol{x}' \notin \{\boldsymbol{x}_{DX}\} \end{bmatrix}, \\ 0, & \text{otherwise}, \end{cases} \tag{191}$$

where the collided weight w_c and surface position $\boldsymbol{x}_S$ are defined in Eq. 5, the DXTRAN-entering position $\boldsymbol{x}_{DX}$ is defined in Eq. 6, $\{\boldsymbol{x}_\Gamma\}$ is defined in Eq. 187, and $\{\boldsymbol{x}_{DX}\}$ is defined in Eq. 193. In the second case of Eq. 191, $\boldsymbol{x}_{DX}$ should be used in Eq. 3 rather than $\boldsymbol{x}_S$ because it is the extent of the truncated exponential distribution being sampled. This operator governs the transmission of a portion of the statistical weight of a particle to a collision before reaching either the boundary of the current cell or the DXTRAN region depending on which is intersected first by the streaming path.

A.6 Flight-to-Transmission Operator

The flight-to-transmission operator is

$$\mathcal{B}_t(\boldsymbol{p},\boldsymbol{p}') = \begin{cases} \int \delta(\boldsymbol{x}'-\boldsymbol{x}_S(\boldsymbol{x},\hat{\boldsymbol{\Omega}}))\delta(\hat{\boldsymbol{\Omega}}'-\hat{\boldsymbol{\Omega}})\delta(E'-E)\delta(w'-w_t)d\boldsymbol{p}', & \begin{bmatrix} \|\boldsymbol{x}-\boldsymbol{x}_S\| < \|\boldsymbol{x}-\boldsymbol{x}_{DX}\| \\ \text{and} \\ \boldsymbol{x}' \in \{\boldsymbol{x}_\Gamma\} \end{bmatrix}, \\ \int \delta(\boldsymbol{x}'-\boldsymbol{x}_{DX}(\boldsymbol{x},\hat{\boldsymbol{\Omega}}))\delta(\hat{\boldsymbol{\Omega}}'-\hat{\boldsymbol{\Omega}})\delta(E'-E)\delta(w'-0)d\boldsymbol{p}', & \begin{bmatrix} \|\boldsymbol{x}-\boldsymbol{x}_S\| > \|\boldsymbol{x}-\boldsymbol{x}_{DX}\| \\ \text{and} \\ \boldsymbol{x}' \in \{\boldsymbol{x}_\Gamma\} \end{bmatrix}, \\ 0, & \text{otherwise}, \end{cases} \tag{192}$$

where the transmitted weight w_t and surface position $\boldsymbol{x}_S$ are defined in Eq. 3, $\{\boldsymbol{x}_\Gamma\}$ is defined in Eq. 187, and the DXTRAN-entering position $\boldsymbol{x}_{DX}$ is defined in Eq. 6. This operator governs the transmission of a portion of the statistical weight of a particle to either the boundary of the current cell or to the DXTRAN region depending on which is intersected first when traveling along the current direction of flight. If the weight is transmitted to the DXTRAN region the particle is killed.

A.7 Flight-to-DXTRAN Operator

Adapted from Ref. [5, Sec. 3.7.1], the flight-to-DXTRAN operator is

$$\begin{aligned} \mathcal{B}_{DX}(\boldsymbol{p},\boldsymbol{p}') = \int & \mathbb{1}(\boldsymbol{x} \notin \{\boldsymbol{x}_{DX}\})\delta\Big(\boldsymbol{x}'-\boldsymbol{x}_{DX}(\boldsymbol{x},\hat{\boldsymbol{\Omega}}')\Big) \\ & \times f_{DX}(\boldsymbol{x},\hat{\boldsymbol{\Omega}} \to \hat{\boldsymbol{\Omega}}', E \to E')\delta(w'-w_{DX})d\boldsymbol{p}', \end{aligned} \tag{193}$$

where $\mathbb{1}$ is the indicator function; $\{\boldsymbol{x}_{DX}\}$ is the set of all points in the DXTRAN region; and the DXTRAN-entering position $\boldsymbol{x}_{DX}(\boldsymbol{x},\hat{\boldsymbol{\Omega}}')$, DXTRAN emergence PDF $f_{DX}(\boldsymbol{x},\hat{\boldsymbol{\Omega}} \to \hat{\boldsymbol{\Omega}}', E \to E')$, and DXTRAN weight w_{DX} are defined in Eq. 6. This operator governs the creation of a particle on the surface of the DXTRAN region by enforcing that the weight is created according to Eq. 6 on the surface of the DXTRAN region and accounting for the biased probability of emerging towards the DXTRAN region with a given direction and energy. Note that this operator integrates to unity over its full domain because it consists of probability distribution functions in all dimensions.

A.8 DXTRAN Free-Flight Transmission Operator

Adapted from Ref. [5, Sec. 3.7.2], the DXTRAN free-flight transmission operator is

$$\mathcal{T}_{DX}(\boldsymbol{p},\boldsymbol{p}') = \begin{cases} \int \exp\Big(-\ell(\boldsymbol{x},\boldsymbol{x}_{DX}(\boldsymbol{x},\hat{\boldsymbol{\Omega}}'))\Big)\delta(\hat{\boldsymbol{\Omega}}'-\hat{\boldsymbol{\Omega}})\delta(E'-E)\delta(w'-0)d\boldsymbol{p}', & \mathbb{1}(\text{truncate}), \\ \mathcal{T}(\boldsymbol{p},\boldsymbol{p}'), & \text{otherwise}, \end{cases} \tag{194}$$

where

$$\mathbb{1}(\text{truncate}) = \begin{bmatrix} \boldsymbol{x} \notin \{\boldsymbol{x}_{DX}\}, \\ \boldsymbol{x}' \in \{\boldsymbol{x}_\Gamma\}, \\ \frac{\boldsymbol{x}'-\boldsymbol{x}}{\|\boldsymbol{x}'-\boldsymbol{x}\|}\cdot\frac{\boldsymbol{g}-\boldsymbol{x}}{\|\boldsymbol{g}-\boldsymbol{x}\|} = 1, \text{ and} \\ \|\boldsymbol{x}'-\boldsymbol{x}\| \geq \|\boldsymbol{g}-\boldsymbol{x}\| \end{bmatrix}, \exists\, \boldsymbol{g} \in \{\boldsymbol{x}_{DX}\}, \tag{195}$$

where $\ell(\boldsymbol{x},\boldsymbol{x}_{DX})$ is the optical thickness defined in Eq. 5, $\{\boldsymbol{x}_{DX}\}$ is defined in Eq. 193, and $\{\boldsymbol{x}_\Gamma\}$ and $\mathcal{T}$ are given by Eq. 187. This operator governs the free flight of particles in much the same way as the free-flight transmission operator $\mathcal{T}$ except that particles are killed if they arrive at the surface of the DXTRAN region as enforced by the Dirac delta function on w' if $\mathbb{1}$(truncate) is satisfied.

B Useful Equivalences

B.1 Truncated Exponential Integration to Unity

A truncated exponential distribution defined for a range starting at zero is given by

$$f(x) = \frac{a\cdot\exp(-a\cdot x)}{1-\exp(-a\cdot X)},\ 0 \leq x \leq X. \tag{196}$$

The result of the integration of this distribution over the entire range of x is one. This is shown starting with the definition of the distribution,

$$\int_0^X f(x)dx = \int_0^X \frac{a\cdot\exp(-a\cdot x)}{1-\exp(-a\cdot X)}dx. \tag{197}$$

Pulling out constants,

$$\int_0^X f(x)dx = \frac{a}{1-\exp(-a\cdot X)}\int_0^X \exp(-a\cdot x)dx. \tag{198}$$

Taking the antiderivative of the integrand,

$$\int_0^X f(x)dx = \frac{a}{1-\exp(-a\cdot X)}\left[-\frac{1}{a}\exp(-a\cdot x)\right]\Bigg|_0^X. \tag{199}$$

Evaluating the antiderivative at the bounds of integration,

$$\int_0^X f(x)dx = \frac{a}{1-\exp(-a\cdot X)}\left[-\frac{1}{a}\exp(-a\cdot X)+\frac{1}{a}\right]. \tag{200}$$

Simplifying yields the final result of integration to unity,

$$\int_0^X f(x)dx = 1. \tag{201}$$

B.2 Equivalence of DXTRAN and Analog Transport Past a Cell Surface

The equivalence of transport with the DXTRAN variance-reduction technique in play to analog transport in phase space past the boundary of the current cell traveling towards a DXTRAN region, stated formally in Eq. 135, is proven here. First, the terms concerning transport past the bounding surface of the current cell are isolated from Eq. 134, which governs DXTRAN transport in directions pointed towards the DXTRAN region, and the definition of the surface-crossing operator given in Eq. 188 is applied,

$$
\begin{aligned}
X_{2,5}^{\text{partial},0} = &\int_{\hat{\boldsymbol{\Omega}}_1 \in \left\{\hat{\boldsymbol{\Omega}}_{DX}^{\text{outside},0}\right\}} \int_0^\infty f(\boldsymbol{x}, \hat{\boldsymbol{\Omega}} \to \hat{\boldsymbol{\Omega}}_1, E \to E_1) \exp(-\ell(\boldsymbol{x}, \boldsymbol{x}_1)) \Psi_{DX}^{\beta}(\boldsymbol{x}_1, \hat{\boldsymbol{\Omega}}_1, E_1, w) dE_1 d\Omega_1 \\
&+ \int_{\hat{\boldsymbol{\Omega}}_2 \in \left\{\hat{\boldsymbol{\Omega}}_{DX}^{\text{outside},0}\right\}} \int_0^\infty f(\boldsymbol{x}, \hat{\boldsymbol{\Omega}} \to \hat{\boldsymbol{\Omega}}_2, E \to E_2) \\
&\times \int_{a_{DX}(\boldsymbol{x}, \hat{\boldsymbol{\Omega}}_2)}^{a_{DX}(\boldsymbol{x}, \hat{\boldsymbol{\Omega}}_2) + a_S(\boldsymbol{x}_{DX}(\boldsymbol{x}, \hat{\boldsymbol{\Omega}}_2), \hat{\boldsymbol{\Omega}}_2)} \exp\Big(-\ell(\boldsymbol{x}, \boldsymbol{x} + a\hat{\boldsymbol{\Omega}}_2)\Big) \\
&\times \Big[\mathcal{K}_A(\boldsymbol{x} + a\hat{\boldsymbol{\Omega}}_2, \hat{\boldsymbol{\Omega}}_2, E_2, w, \boldsymbol{p}_3) \bar{s}_A(\boldsymbol{x} + a\hat{\boldsymbol{\Omega}}_2, \hat{\boldsymbol{\Omega}}_2, E_2, w) \\
&+ \mathcal{K}_E'(\boldsymbol{x} + a\hat{\boldsymbol{\Omega}}_2, \hat{\boldsymbol{\Omega}}_2, E_2, w, \boldsymbol{p}_4) \Big(\bar{s}_E(\boldsymbol{x} + a\hat{\boldsymbol{\Omega}}_2, \hat{\boldsymbol{\Omega}}_2, E_2, w) + \Psi_0^{\alpha}(\boldsymbol{p}_4)\Big) \\
&+ \mathcal{S}(\boldsymbol{x} + a\hat{\boldsymbol{\Omega}}_2, \hat{\boldsymbol{\Omega}}_2, E_2, w, \boldsymbol{p}_5) \Big(\bar{s}_S(\boldsymbol{x} + a\hat{\boldsymbol{\Omega}}_2, \hat{\boldsymbol{\Omega}}_2, E_2, w) + \Psi_0^{\beta}(\boldsymbol{p}_5)\Big)\Big] da dE_2 d\Omega_2,
\end{aligned}
\tag{202}
$$

where $\boldsymbol{x}_1 = \boldsymbol{x} + a_S(\boldsymbol{x}, \hat{\boldsymbol{\Omega}}_1)\hat{\boldsymbol{\Omega}}_1$ and the superscript 0 is used to denote that this is the term for the cell 0 cells away from $\boldsymbol{x}$, i.e., the current cell. Note that a superscript 0 is used in other sections to denote analog transport and is being redefined for this proof while a subscript 0 is still used to denote analog transport. Next, expand $\Psi_{DX}^{\beta}(\boldsymbol{x}_1, \hat{\boldsymbol{\Omega}}_1, E_1, w)$ with Eq. 115,

$$
\begin{aligned}
X_{2,5}^{\text{partial},0} = &\int_{\hat{\boldsymbol{\Omega}}_1 \in \left\{\hat{\boldsymbol{\Omega}}_{DX}^{\text{outside},0}\right\}} \int_0^\infty f(\boldsymbol{x}, \hat{\boldsymbol{\Omega}} \to \hat{\boldsymbol{\Omega}}_1, E \to E_1) \exp(-\ell(\boldsymbol{x}, \boldsymbol{x}_1)) \\
&\times \int_0^{\min\left\{a_S(\boldsymbol{x}_1, \hat{\boldsymbol{\Omega}}_1), a_{DX}(\boldsymbol{x}_1, \hat{\boldsymbol{\Omega}}_1) - \epsilon\right\}} \exp\Big(-\ell(\boldsymbol{x}_1, \boldsymbol{x}_1 + a\hat{\boldsymbol{\Omega}}_1)\Big) \\
&\times \Big[\mathcal{K}_A(\boldsymbol{x}_1 + a\hat{\boldsymbol{\Omega}}_1, \hat{\boldsymbol{\Omega}}_1, E_1, w, \boldsymbol{p}_2) \bar{s}_A(\boldsymbol{x} + a\hat{\boldsymbol{\Omega}}_1, \hat{\boldsymbol{\Omega}}_1, E_1, w) \\
&+ \mathcal{K}_E'(\boldsymbol{x}_1 + a\hat{\boldsymbol{\Omega}}_1, \hat{\boldsymbol{\Omega}}_1, E_1, w, \boldsymbol{p}_3) \Big(\bar{s}_E(\boldsymbol{x}_1 + a\hat{\boldsymbol{\Omega}}_1, \hat{\boldsymbol{\Omega}}_1, E_1, w) + \Psi_{DX}^{\alpha}(\boldsymbol{p}_3)\Big) \\
&+ \mathcal{S}(\boldsymbol{x}_1 + a\hat{\boldsymbol{\Omega}}_1, \hat{\boldsymbol{\Omega}}_1, E_1, w, \boldsymbol{p}_4) \Big(\bar{s}_S(\boldsymbol{x}_1 + a\hat{\boldsymbol{\Omega}}_1, \hat{\boldsymbol{\Omega}}_1, E_1, w) + \Psi_{DX}^{\beta}(\boldsymbol{p}_4)\Big)\Big] da dE_1 d\Omega_1, \\
&+ \int_{\hat{\boldsymbol{\Omega}}_2 \in \left\{\hat{\boldsymbol{\Omega}}_{DX}^{\text{outside},0}\right\}} \int_0^\infty f(\boldsymbol{x}, \hat{\boldsymbol{\Omega}} \to \hat{\boldsymbol{\Omega}}_2, E \to E_2) \\
&\times \int_{a_{DX}(\boldsymbol{x}, \hat{\boldsymbol{\Omega}}_2)}^{a_{DX}(\boldsymbol{x}, \hat{\boldsymbol{\Omega}}_2) + a_S(\boldsymbol{x}_{DX}(\boldsymbol{x}, \hat{\boldsymbol{\Omega}}_2), \hat{\boldsymbol{\Omega}}_2)} \exp\Big(-\ell(\boldsymbol{x}, \boldsymbol{x} + a\hat{\boldsymbol{\Omega}}_2)\Big) \\
&\times \Big[\mathcal{K}_A(\boldsymbol{x} + a\hat{\boldsymbol{\Omega}}_2, \hat{\boldsymbol{\Omega}}_2, E_2, w, \boldsymbol{p}_3) \bar{s}_A(\boldsymbol{x} + a\hat{\boldsymbol{\Omega}}_2, \hat{\boldsymbol{\Omega}}_2, E_2, w) \\
&+ \mathcal{K}_E'(\boldsymbol{x} + a\hat{\boldsymbol{\Omega}}_2, \hat{\boldsymbol{\Omega}}_2, E_2, w, \boldsymbol{p}_4) \Big(\bar{s}_E(\boldsymbol{x} + a\hat{\boldsymbol{\Omega}}_2, \hat{\boldsymbol{\Omega}}_2, E_2, w) + \Psi_0^{\alpha}(\boldsymbol{p}_4)\Big) \\
&+ \mathcal{S}(\boldsymbol{x} + a\hat{\boldsymbol{\Omega}}_2, \hat{\boldsymbol{\Omega}}_2, E_2, w, \boldsymbol{p}_5) \Big(\bar{s}_S(\boldsymbol{x} + a\hat{\boldsymbol{\Omega}}_2, \hat{\boldsymbol{\Omega}}_2, E_2, w) + \Psi_0^{\beta}(\boldsymbol{p}_5)\Big)\Big] da dE_2 d\Omega_2.
\end{aligned}
\tag{203}
$$

Inserting Eq. 129, breaking up the exponential function in the second term, and changing the bounds of the integration over a in the second term,

$$
\begin{aligned}
X_{2,5}^{\text{partial},0} = &\int_{\hat{\boldsymbol{\Omega}}_1 \in \left\{\hat{\boldsymbol{\Omega}}_{DX}^{\text{outside},0}\right\}} \int_0^\infty f(\boldsymbol{x}, \hat{\boldsymbol{\Omega}} \to \hat{\boldsymbol{\Omega}}_1, E \to E_1) \exp(-\ell(\boldsymbol{x}, \boldsymbol{x}_1)) \\
&\quad \times \int_0^{\min\left\{a_S(\boldsymbol{x}_1, \hat{\boldsymbol{\Omega}}_1), a_{DX}(\boldsymbol{x}_1, \hat{\boldsymbol{\Omega}}_1) - \epsilon\right\}} \exp\Big(-\ell(\boldsymbol{x}_1, \boldsymbol{x}_1 + a\hat{\boldsymbol{\Omega}}_1)\Big) \\
&\quad \Big[\mathcal{K}_A(\boldsymbol{x}_1 + a\hat{\boldsymbol{\Omega}}_1, \hat{\boldsymbol{\Omega}}_1, E_1, w, \boldsymbol{p}_2) \bar{s}_A(\boldsymbol{x} + a\hat{\boldsymbol{\Omega}}_1, \hat{\boldsymbol{\Omega}}_1, E_1, w) \\
&\quad + \mathcal{K}_E'(\boldsymbol{x}_1 + a\hat{\boldsymbol{\Omega}}_1, \hat{\boldsymbol{\Omega}}_1, E_1, w, \boldsymbol{p}_3) \Big(\bar{s}_E(\boldsymbol{x}_1 + a\hat{\boldsymbol{\Omega}}_1, \hat{\boldsymbol{\Omega}}_1, E_1, w) + \Psi_0^\alpha(\boldsymbol{p}_3)\Big) \\
&\quad + \mathcal{S}(\boldsymbol{x}_1 + a\hat{\boldsymbol{\Omega}}_1, \hat{\boldsymbol{\Omega}}_1, E_1, w, \boldsymbol{p}_4) \Big(\bar{s}_S(\boldsymbol{x}_1 + a\hat{\boldsymbol{\Omega}}_1, \hat{\boldsymbol{\Omega}}_1, E_1, w) + \Psi_{DX}^\beta(\boldsymbol{p}_4)\Big)\Big] da dE_1 d\Omega_1, \\
&+ \int_{\hat{\boldsymbol{\Omega}}_2 \in \left\{\hat{\boldsymbol{\Omega}}_{DX}^{\text{outside},0}\right\}} \int_0^\infty f(\boldsymbol{x}, \hat{\boldsymbol{\Omega}} \to \hat{\boldsymbol{\Omega}}_2, E \to E_2) \exp(-\ell(\boldsymbol{x}, \boldsymbol{x}_1)) \\
&\quad \times \int_{a_{DX}(\boldsymbol{x}_1, \hat{\boldsymbol{\Omega}}_2)}^{a_{DX}(\boldsymbol{x}_1, \hat{\boldsymbol{\Omega}}_2) + a_S(\boldsymbol{x}_{DX}(\boldsymbol{x}_1, \hat{\boldsymbol{\Omega}}_2), \hat{\boldsymbol{\Omega}}_2)} \exp\Big(-\ell(\boldsymbol{x}_1, \boldsymbol{x}_1 + a\hat{\boldsymbol{\Omega}}_2)\Big) \\
&\quad \times \Big[\mathcal{K}_A(\boldsymbol{x}_1 + a\hat{\boldsymbol{\Omega}}_2, \hat{\boldsymbol{\Omega}}_2, E_2, w, \boldsymbol{p}_3) \bar{s}_A(\boldsymbol{x}_1 + a\hat{\boldsymbol{\Omega}}_2, \hat{\boldsymbol{\Omega}}_2, E_2, w) \\
&\quad + \mathcal{K}_E'(\boldsymbol{x}_1 + a\hat{\boldsymbol{\Omega}}_2, \hat{\boldsymbol{\Omega}}_2, E_2, w, \boldsymbol{p}_4) \Big(\bar{s}_E(\boldsymbol{x}_1 + a\hat{\boldsymbol{\Omega}}_2, \hat{\boldsymbol{\Omega}}_2, E_2, w) + \Psi_0^\alpha(\boldsymbol{p}_4)\Big) \\
&\quad + \mathcal{S}(\boldsymbol{x}_1 + a\hat{\boldsymbol{\Omega}}_2, \hat{\boldsymbol{\Omega}}_2, E_2, w, \boldsymbol{p}_5) \Big(\bar{s}_S(\boldsymbol{x}_1 + a\hat{\boldsymbol{\Omega}}_2, \hat{\boldsymbol{\Omega}}_2, E_2, w) + \Psi_0^\beta(\boldsymbol{p}_5)\Big)\Big] da dE_2 d\Omega_2.
\end{aligned} \tag{204}
$$

Recall that the subset of direction vectors $\{\hat{\boldsymbol{\Omega}}_{DX}^{\text{outside},0}\}$ is defined for the cell containing position $\boldsymbol{x}$. Inside and outside direction vector subsets of $\{\hat{\boldsymbol{\Omega}}_{DX}^{\text{outside},0}\}$ can also be defined for the cell entered after traveling along $\hat{\boldsymbol{\Omega}} \in \{\hat{\boldsymbol{\Omega}}_{DX}^{\text{outside},0}\}$. The subset of directions that intersect the DXTRAN region before a surface from the cell entered after traveling along $\hat{\boldsymbol{\Omega}} \in \{\hat{\boldsymbol{\Omega}}_{DX}^{\text{outside},0}\}$ is denoted as $\{\hat{\boldsymbol{\Omega}}_{DX}^{\text{inside},1}\}$. Similarly, the subset of directions that does not intersect the DXTRAN region first is denoted as $\{\hat{\boldsymbol{\Omega}}_{DX}^{\text{outside},1}\}$. Using the inside and outside direction subsets of $\{\hat{\boldsymbol{\Omega}}_{DX}^{\text{outside},0}\}$,

$$
X_{2,5}^{\text{partial},0} = Y_1 + Y_2 + Y_3 + Y_4, \tag{205a}
$$

where,

$$
\begin{aligned}
Y_1 = &\int_{\hat{\boldsymbol{\Omega}}_1 \in \left\{\hat{\boldsymbol{\Omega}}_{DX}^{\text{inside},1}\right\}} \int_0^\infty f(\boldsymbol{x}, \hat{\boldsymbol{\Omega}} \to \hat{\boldsymbol{\Omega}}_1, E \to E_1) \exp(-\ell(\boldsymbol{x}, \boldsymbol{x}_1)) \\
&\times \int_0^{a_{DX}(\boldsymbol{x}_1, \hat{\boldsymbol{\Omega}}_1) - \epsilon} \exp\Big(-\ell(\boldsymbol{x}_1, \boldsymbol{x}_1 + a\hat{\boldsymbol{\Omega}}_1)\Big) \\
&\times \Big[\mathcal{K}_A(\boldsymbol{x}_1 + a\hat{\boldsymbol{\Omega}}_1, \hat{\boldsymbol{\Omega}}_1, E_1, w, \boldsymbol{p}_2) \bar{s}_A(\boldsymbol{x}_1 + a\hat{\boldsymbol{\Omega}}_1, \hat{\boldsymbol{\Omega}}_1, E_1, w) \\
&+ \mathcal{K}_E'(\boldsymbol{x}_1 + a\hat{\boldsymbol{\Omega}}_1, \hat{\boldsymbol{\Omega}}_1, E_1, w, \boldsymbol{p}_3) \Big(\bar{s}_E(\boldsymbol{x}_1 + a\hat{\boldsymbol{\Omega}}_1, \hat{\boldsymbol{\Omega}}_1, E_1, w) + \Psi_0^\alpha(\boldsymbol{p}_3)\Big) \\
&+ \mathcal{S}(\boldsymbol{x}_1 + a\hat{\boldsymbol{\Omega}}_1, \hat{\boldsymbol{\Omega}}_1, E_1, w, \boldsymbol{p}_4) \Big(\bar{s}_S(\boldsymbol{x}_1 + a\hat{\boldsymbol{\Omega}}_1, \hat{\boldsymbol{\Omega}}_1, E_1, w) + \Psi_{DX}^\beta(\boldsymbol{p}_4)\Big)\Big] da dE_1 d\Omega_1,
\end{aligned} \tag{205b}
$$

$$
\begin{aligned}
Y_2 = &\int_{\hat{\boldsymbol{\Omega}}_1 \in \left\{\hat{\boldsymbol{\Omega}}_{DX}^{\text{outside},1}\right\}} \int_0^\infty f(\boldsymbol{x}, \hat{\boldsymbol{\Omega}} \to \hat{\boldsymbol{\Omega}}_1, E \to E_1) \exp(-\ell(\boldsymbol{x}, \boldsymbol{x}_1)) \\
&\times \int_0^{a_S(\boldsymbol{x}_1, \hat{\boldsymbol{\Omega}}_1)} \exp\Big(-\ell(\boldsymbol{x}_1, \boldsymbol{x}_1 + a\hat{\boldsymbol{\Omega}}_1)\Big) \\
&\times \Big[\mathcal{K}_A(\boldsymbol{x}_1 + a\hat{\boldsymbol{\Omega}}_1, \hat{\boldsymbol{\Omega}}_1, E_1, w, \boldsymbol{p}_2)\bar{s}_A(\boldsymbol{x}_1 + a\hat{\boldsymbol{\Omega}}_1, \hat{\boldsymbol{\Omega}}_1, E_1, w) \\
&+ \mathcal{K}_E'(\boldsymbol{x}_1 + a\hat{\boldsymbol{\Omega}}_1, \hat{\boldsymbol{\Omega}}_1, E_1, w, \boldsymbol{p}_3)\Big(\bar{s}_E(\boldsymbol{x}_1 + a\hat{\boldsymbol{\Omega}}_1, \hat{\boldsymbol{\Omega}}_1, E_1, w) + \Psi_0^\alpha(\boldsymbol{p}_3)\Big) \\
&+ \mathcal{S}(\boldsymbol{x}_1 + a\hat{\boldsymbol{\Omega}}_1, \hat{\boldsymbol{\Omega}}_1, E_1, w, \boldsymbol{p}_4)\Big(\bar{s}_S(\boldsymbol{x}_1 + a\hat{\boldsymbol{\Omega}}_1, \hat{\boldsymbol{\Omega}}_1, E_1, w) + \Psi_{DX}^\beta(\boldsymbol{p}_4)\Big)\Big] da dE_1 d\Omega_1,
\end{aligned}
\tag{205c}
$$

$$
\begin{aligned}
Y_3 = &\int_{\hat{\boldsymbol{\Omega}}_2 \in \left\{\hat{\boldsymbol{\Omega}}_{DX}^{\text{inside},1}\right\}} \int_0^\infty f(\boldsymbol{x}, \hat{\boldsymbol{\Omega}} \to \hat{\boldsymbol{\Omega}}_2, E \to E_2) \exp(-\ell(\boldsymbol{x}, \boldsymbol{x}_1)) \\
&\times \int_{a_{DX}(\boldsymbol{x}_1, \hat{\boldsymbol{\Omega}}_2)}^{a_S(\boldsymbol{x}_1, \hat{\boldsymbol{\Omega}}_2)} \exp\Big(-\ell(\boldsymbol{x}_1, \boldsymbol{x}_1 + a\hat{\boldsymbol{\Omega}}_2)\Big) \\
&\times \Big[\mathcal{K}_A(\boldsymbol{x}_1 + a\hat{\boldsymbol{\Omega}}_2, \hat{\boldsymbol{\Omega}}_2, E_2, w, \boldsymbol{p}_3)\bar{s}_A(\boldsymbol{x}_1 + a\hat{\boldsymbol{\Omega}}_2, \hat{\boldsymbol{\Omega}}_2, E_2, w) \\
&+ \mathcal{K}_E'(\boldsymbol{x}_1 + a\hat{\boldsymbol{\Omega}}_2, \hat{\boldsymbol{\Omega}}_2, E_2, w, \boldsymbol{p}_4)\Big(\bar{s}_E(\boldsymbol{x}_1 + a\hat{\boldsymbol{\Omega}}_2, \hat{\boldsymbol{\Omega}}_2, E_2, w) + \Psi_0^\alpha(\boldsymbol{p}_4)\Big) \\
&+ \mathcal{S}(\boldsymbol{x}_1 + a\hat{\boldsymbol{\Omega}}_2, \hat{\boldsymbol{\Omega}}_2, E_2, w, \boldsymbol{p}_5)\Big(\bar{s}_S(\boldsymbol{x}_1 + a\hat{\boldsymbol{\Omega}}_2, \hat{\boldsymbol{\Omega}}_2, E_2, w) + \Psi_0^\beta(\boldsymbol{p}_5)\Big)\Big] da dE_2 d\Omega_2,
\end{aligned}
\tag{205d}
$$

and

$$
\begin{aligned}
Y_4 = &\int_{\hat{\boldsymbol{\Omega}}_2 \in \left\{\hat{\boldsymbol{\Omega}}_{DX}^{\text{outside},1}\right\}} \int_0^\infty f(\boldsymbol{x}, \hat{\boldsymbol{\Omega}} \to \hat{\boldsymbol{\Omega}}_2, E \to E_2) \exp(-\ell(\boldsymbol{x}, \boldsymbol{x}_1)) \\
&\times \int_{a_{DX}(\boldsymbol{x}_1, \hat{\boldsymbol{\Omega}}_2)}^{a_{DX}(\boldsymbol{x}_1, \hat{\boldsymbol{\Omega}}_2) + a_S(\boldsymbol{x}_{DX}(\boldsymbol{x}_1, \hat{\boldsymbol{\Omega}}_2), \hat{\boldsymbol{\Omega}}_2)} \exp\Big(-\ell(\boldsymbol{x}_1, \boldsymbol{x}_1 + a\hat{\boldsymbol{\Omega}}_2)\Big) \\
&\times \Big[\mathcal{K}_A(\boldsymbol{x}_1 + a\hat{\boldsymbol{\Omega}}_2, \hat{\boldsymbol{\Omega}}_2, E_2, w, \boldsymbol{p}_3)\bar{s}_A(\boldsymbol{x}_1 + a\hat{\boldsymbol{\Omega}}_2, \hat{\boldsymbol{\Omega}}_2, E_2, w) \\
&+ \mathcal{K}_E'(\boldsymbol{x}_1 + a\hat{\boldsymbol{\Omega}}_2, \hat{\boldsymbol{\Omega}}_2, E_2, w, \boldsymbol{p}_4)\Big(\bar{s}_E(\boldsymbol{x}_1 + a\hat{\boldsymbol{\Omega}}_2, \hat{\boldsymbol{\Omega}}_2, E_2, w) + \Psi_0^\alpha(\boldsymbol{p}_4)\Big) \\
&+ \mathcal{S}(\boldsymbol{x}_1 + a\hat{\boldsymbol{\Omega}}_2, \hat{\boldsymbol{\Omega}}_2, E_2, w, \boldsymbol{p}_5)\Big(\bar{s}_S(\boldsymbol{x}_1 + a\hat{\boldsymbol{\Omega}}_2, \hat{\boldsymbol{\Omega}}_2, E_2, w) + \Psi_0^\beta(\boldsymbol{p}_5)\Big)\Big] da dE_2 d\Omega_2.
\end{aligned}
\tag{205e}
$$

Note that the upper bound of integration over a in Eq. 205d is changed from Eq. 204 to an equivalent form using the restriction to directions in $\{\hat{\boldsymbol{\Omega}}_{DX}^{\text{inside},1}\}$. A visualization of a system divided into these terms is given in Fig. 6. Note that both blue colors correspond to the set of directions $\{\hat{\boldsymbol{\Omega}}_{DX}^{\text{inside},1}\}$ and both red colors correspond to the set of directions $\{\hat{\boldsymbol{\Omega}}_{DX}^{\text{outside},1}\}$. Combining the integration over a in terms Y_1 and Y_3,

$$
\begin{aligned}
X_{2,5}^{\text{partial},0} = &\int_{\hat{\boldsymbol{\Omega}}_1 \in \left\{\hat{\boldsymbol{\Omega}}_{DX}^{\text{inside},1}\right\}} \int_0^\infty f(\boldsymbol{x}, \hat{\boldsymbol{\Omega}} \to \hat{\boldsymbol{\Omega}}_1, E \to E_1) \exp(-\ell(\boldsymbol{x}, \boldsymbol{x}_1)) \\
&\times \int_0^{a_S(\boldsymbol{x}_1, \hat{\boldsymbol{\Omega}}_1)} \exp\Big(-\ell(\boldsymbol{x}_1, \boldsymbol{x}_1 + a\hat{\boldsymbol{\Omega}}_1)\Big) \\
&\times \Big[\mathcal{K}_A(\boldsymbol{x}_1 + a\hat{\boldsymbol{\Omega}}_1, \hat{\boldsymbol{\Omega}}_1, E_1, w, \boldsymbol{p}_2)\bar{s}_A(\boldsymbol{x}_1 + a\hat{\boldsymbol{\Omega}}_1, \hat{\boldsymbol{\Omega}}_1, E_1, w) \\
&+ \mathcal{K}_E'(\boldsymbol{x}_1 + a\hat{\boldsymbol{\Omega}}_1, \hat{\boldsymbol{\Omega}}_1, E_1, w, \boldsymbol{p}_3)\Big(\bar{s}_E(\boldsymbol{x}_1 + a\hat{\boldsymbol{\Omega}}_1, \hat{\boldsymbol{\Omega}}_1, E_1, w) + \Psi_0^\alpha(\boldsymbol{p}_3)\Big) \\
&+ \mathcal{S}(\boldsymbol{x}_1 + a\hat{\boldsymbol{\Omega}}_1, \hat{\boldsymbol{\Omega}}_1, E_1, w, \boldsymbol{p}_4)\Big(\bar{s}_S(\boldsymbol{x}_1 + a\hat{\boldsymbol{\Omega}}_1, \hat{\boldsymbol{\Omega}}_1, E_1, w) + \Psi_0^\beta(\boldsymbol{p}_4)\Big)\Big] da dE_1 d\Omega_1 \\
&+ Y_2 + Y_4.
\end{aligned}
\tag{206}
$$

Eq. 206 is then simplified with Eq. 118,

$$
\begin{aligned}
X_{2,5}^{\text{partial},0} = &\int_{\hat{\boldsymbol{\Omega}}_1 \in \left\{\hat{\boldsymbol{\Omega}}_{DX}^{\text{inside},1}\right\}} \int_0^\infty f(\boldsymbol{x}, \hat{\boldsymbol{\Omega}} \to \hat{\boldsymbol{\Omega}}_1, E \to E_1) \exp(-\ell(\boldsymbol{x}, \boldsymbol{x}_1)) \Psi_0^\beta\Big(\boldsymbol{x}_1, \hat{\boldsymbol{\Omega}}_1, E_1, w\Big) dE_1 d\Omega_1 \\
&+ Y_2 + Y_4.
\end{aligned}
\tag{207}
$$

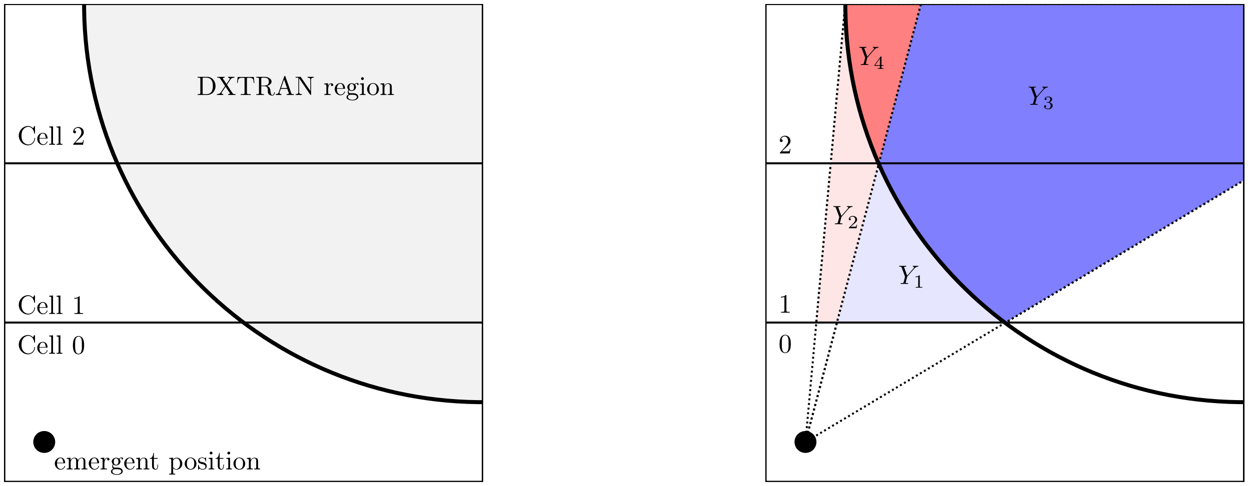

(a) Schematic of simulation geometry.

(b) Simulation geometry with regions color coded.

Figure 6: Representative arrangement of Monte Carlo geometry cells and an overlapping DXTRAN region, with the right figure regions corresponding to Eqs. 205b–205e relative to a particle emerging from the source or an emissive collision at the indicated position.

By the definition of the surface-crossing operator and using the definition of $\boldsymbol{x}_1$, Eq. 207 can be equivalently rewritten as,

$$\begin{aligned} X_{2,5}^{\text{partial},0} = & \int_{\hat{\boldsymbol{\Omega}}_1 \in \left\{\hat{\boldsymbol{\Omega}}_{DX}^{\text{inside},1}\right\}} \int_0^{\infty} f(\boldsymbol{x}, \hat{\boldsymbol{\Omega}} \to \hat{\boldsymbol{\Omega}}_1, E \to E_1) \int_0^{a_S(\boldsymbol{x}, \hat{\boldsymbol{\Omega}}_1)} \exp\Big(-\ell(\boldsymbol{x}, \boldsymbol{x} + a\hat{\boldsymbol{\Omega}}_1)\Big) \\ & \times \mathcal{S}(\boldsymbol{x} + a\hat{\boldsymbol{\Omega}}_1, \hat{\boldsymbol{\Omega}}_1, E_1, w, \boldsymbol{p}_4) \Psi_0^{\beta}(\boldsymbol{p}_4) da dE_1 d\Omega_1 \\ & + Y_2 + Y_4. \end{aligned} \tag{208}$$

Expanding Y_2 and Y_4 with Eqs. 205c and 205e, respectively,

$$
\begin{aligned}
X_{2,5}^{\text{partial},0} = &\int_{\hat{\boldsymbol{\Omega}}_1 \in \left\{\hat{\boldsymbol{\Omega}}_{DX}^{\text{inside},1}\right\}} \int_0^\infty f(\boldsymbol{x}, \hat{\boldsymbol{\Omega}} \to \hat{\boldsymbol{\Omega}}_1, E \to E_1) \int_0^{a_S(\boldsymbol{x},\hat{\boldsymbol{\Omega}}_1)} \exp\Big(-\ell(\boldsymbol{x}, \boldsymbol{x} + a\hat{\boldsymbol{\Omega}}_1)\Big) \\
&\times \mathcal{S}(\boldsymbol{x} + a\hat{\boldsymbol{\Omega}}_1, \hat{\boldsymbol{\Omega}}_1, E_1, w, \boldsymbol{p}_4)\Psi_0^\beta(\boldsymbol{p}_4) da dE_1 d\Omega_1 \\
&+ \int_{\hat{\boldsymbol{\Omega}}_1 \in \left\{\hat{\boldsymbol{\Omega}}_{DX}^{\text{outside},1}\right\}} \int_0^\infty f(\boldsymbol{x}, \hat{\boldsymbol{\Omega}} \to \hat{\boldsymbol{\Omega}}_1, E \to E_1) \exp(-\ell(\boldsymbol{x}, \boldsymbol{x}_1)) \\
&\times \int_0^{a_S(\boldsymbol{x}_1,\hat{\boldsymbol{\Omega}}_1)} \exp\Big(-\ell(\boldsymbol{x}_1, \boldsymbol{x}_1 + a\hat{\boldsymbol{\Omega}}_1)\Big) \\
&\times \Big[\mathcal{K}_A(\boldsymbol{x}_1 + a\hat{\boldsymbol{\Omega}}_1, \hat{\boldsymbol{\Omega}}_1, E_1, w, \boldsymbol{p}_2)\bar{s}_A(\boldsymbol{x}_1 + a\hat{\boldsymbol{\Omega}}_1, \hat{\boldsymbol{\Omega}}_1, E_1, w) \\
&+ \mathcal{K}_E'(\boldsymbol{x}_1 + a\hat{\boldsymbol{\Omega}}_1, \hat{\boldsymbol{\Omega}}_1, E_1, w, \boldsymbol{p}_3)\Big(\bar{s}_E(\boldsymbol{x}_1 + a\hat{\boldsymbol{\Omega}}_1, \hat{\boldsymbol{\Omega}}_1, E_1, w) + \Psi_0^\alpha(\boldsymbol{p}_3)\Big) \\
&+ \mathcal{S}(\boldsymbol{x}_1 + a\hat{\boldsymbol{\Omega}}_1, \hat{\boldsymbol{\Omega}}_1, E_1, w, \boldsymbol{p}_4)\Big(\bar{s}_S(\boldsymbol{x}_1 + a\hat{\boldsymbol{\Omega}}_1, \hat{\boldsymbol{\Omega}}_1, E_1, w)\Big)\Big] da dE_1 d\Omega_1 \\
&+ \int_{\hat{\boldsymbol{\Omega}}_1 \in \left\{\hat{\boldsymbol{\Omega}}_{DX}^{\text{outside},1}\right\}} \int_0^\infty f(\boldsymbol{x}, \hat{\boldsymbol{\Omega}} \to \hat{\boldsymbol{\Omega}}_1, E \to E_1) \int_0^{a_S(\boldsymbol{x},\hat{\boldsymbol{\Omega}}_1)} \exp\Big(-\ell(\boldsymbol{x}, \boldsymbol{x} + a\hat{\boldsymbol{\Omega}}_1)\Big) \\
&\times \mathcal{S}(\boldsymbol{x} + a\hat{\boldsymbol{\Omega}}_1, \hat{\boldsymbol{\Omega}}_1, E_1, w, \boldsymbol{p}_4)\Psi_{DX}^\beta(\boldsymbol{p}_4) da dE_1 d\Omega_1 \\
&+ \int_{\hat{\boldsymbol{\Omega}}_2 \in \left\{\hat{\boldsymbol{\Omega}}_{DX}^{\text{outside},1}\right\}} \int_0^\infty f(\boldsymbol{x}, \hat{\boldsymbol{\Omega}} \to \hat{\boldsymbol{\Omega}}_2, E \to E_2) \\
&\times \int_{a_{DX}(\boldsymbol{x},\hat{\boldsymbol{\Omega}}_2)}^{a_{DX}(\boldsymbol{x},\hat{\boldsymbol{\Omega}}_2) + a_S(\boldsymbol{x}_{DX}(\boldsymbol{x},\hat{\boldsymbol{\Omega}}_2),\hat{\boldsymbol{\Omega}}_2)} \exp\Big(-\ell(\boldsymbol{x}, \boldsymbol{x} + a\hat{\boldsymbol{\Omega}}_2)\Big) \\
&\times \Big[\mathcal{K}_A(\boldsymbol{x} + a\hat{\boldsymbol{\Omega}}_2, \hat{\boldsymbol{\Omega}}_2, E_2, w, \boldsymbol{p}_3)\bar{s}_A(\boldsymbol{x} + a\hat{\boldsymbol{\Omega}}_2, \hat{\boldsymbol{\Omega}}_2, E_2, w) \\
&+ \mathcal{K}_E'(\boldsymbol{x} + a\hat{\boldsymbol{\Omega}}_2, \hat{\boldsymbol{\Omega}}_2, E_2, w, \boldsymbol{p}_4)\Big(\bar{s}_E(\boldsymbol{x} + a\hat{\boldsymbol{\Omega}}_2, \hat{\boldsymbol{\Omega}}_2, E_2, w) + \Psi_0^\alpha(\boldsymbol{p}_4)\Big) \\
&+ \mathcal{S}(\boldsymbol{x} + a\hat{\boldsymbol{\Omega}}_2, \hat{\boldsymbol{\Omega}}_2, E_2, w, \boldsymbol{p}_5)\Big(\bar{s}_S(\boldsymbol{x} + a\hat{\boldsymbol{\Omega}}_2, \hat{\boldsymbol{\Omega}}_2, E_2, w) + \Psi_0^\beta(\boldsymbol{p}_5)\Big)\Big] da dE_2 d\Omega_2.
\end{aligned} \tag{209}
$$

Note that the non-analog terms isolated in Eq. 135 appear in the last two terms of Eq. 209 except they now concern angles that do not intersect the DXTRAN region in the cell containing position $\boldsymbol{x}$ nor in the cell containing position $\boldsymbol{x}_1$. Using this similarity to Eq. 135, Eq. 209 can then be written recursively,

$$
\begin{aligned}
X_{2,5}^{\text{partial},0} = &\int_{\hat{\boldsymbol{\Omega}}_1 \in \left\{\hat{\boldsymbol{\Omega}}_{DX}^{\text{inside},1}\right\}} \int_0^\infty f(\boldsymbol{x}, \hat{\boldsymbol{\Omega}} \to \hat{\boldsymbol{\Omega}}_1, E \to E_1) \int_0^{a_S(\boldsymbol{x},\hat{\boldsymbol{\Omega}}_1)} \exp\Big(-\ell(\boldsymbol{x}, \boldsymbol{x} + a\hat{\boldsymbol{\Omega}}_1)\Big) \\
&\times \mathcal{S}(\boldsymbol{x} + a\hat{\boldsymbol{\Omega}}_1, \hat{\boldsymbol{\Omega}}_1, E_1, w, \boldsymbol{p}_4)\Psi_0^\beta(\boldsymbol{p}_4) da dE_1 d\Omega_1 \\
&+ \int_{\hat{\boldsymbol{\Omega}}_1 \in \left\{\hat{\boldsymbol{\Omega}}_{DX}^{\text{outside},1}\right\}} \int_0^\infty f(\boldsymbol{x}, \hat{\boldsymbol{\Omega}} \to \hat{\boldsymbol{\Omega}}_1, E \to E_1) \exp(-\ell(\boldsymbol{x}, \boldsymbol{x}_1)) \\
&\times \int_0^{a_S(\boldsymbol{x}_1,\hat{\boldsymbol{\Omega}}_1)} \exp\Big(-\ell(\boldsymbol{x}_1, \boldsymbol{x}_1 + a\hat{\boldsymbol{\Omega}}_1)\Big) \\
&\times \Big[\mathcal{K}_A(\boldsymbol{x}_1 + a\hat{\boldsymbol{\Omega}}_1, \hat{\boldsymbol{\Omega}}_1, E_1, w, \boldsymbol{p}_2)\bar{s}_A(\boldsymbol{x}_1 + a\hat{\boldsymbol{\Omega}}_1, \hat{\boldsymbol{\Omega}}_1, E_1, w) \\
&+ \mathcal{K}_E'(\boldsymbol{x}_1 + a\hat{\boldsymbol{\Omega}}_1, \hat{\boldsymbol{\Omega}}_1, E_1, w, \boldsymbol{p}_3)\Big(\bar{s}_E(\boldsymbol{x}_1 + a\hat{\boldsymbol{\Omega}}_1, \hat{\boldsymbol{\Omega}}_1, E_1, w) + \Psi_0^\alpha(\boldsymbol{p}_3)\Big) \\
&+ \mathcal{S}(\boldsymbol{x}_1 + a\hat{\boldsymbol{\Omega}}_1, \hat{\boldsymbol{\Omega}}_1, E_1, w, \boldsymbol{p}_4)\bar{s}_S(\boldsymbol{x}_1 + a\hat{\boldsymbol{\Omega}}_1, \hat{\boldsymbol{\Omega}}_1, E_1, w)\Big] da dE_1 d\Omega_1 \\
&+ X_{2,5}^{\text{partial},1}.
\end{aligned} \tag{210}
$$

The same process of expanding the definition of Ψ_{DX}^β, defining new subsets of angles, and merging terms may be repeated continuously until the set $\{\hat{\boldsymbol{\Omega}}_{DX}^{\text{outside},n+1}\}$ is empty. This situation is shown in cell 2 in Fig. 6.

The set being empty corresponds to the case where all angles being considered intersect with the DXTRAN region inside the cell being considered, the cell of position $\boldsymbol{x}_n$. This must occur eventually because there are a finite number of cells in a given problem. In this base case, Eq. 209 becomes

$$\begin{aligned}X_{2,5}^{\text{partial},n} = &\int_{\hat{\boldsymbol{\Omega}}_1 \in \left\{\hat{\boldsymbol{\Omega}}_{DX}^{\text{inside},n+1}\right\}} \int_0^\infty f(\boldsymbol{x}, \hat{\boldsymbol{\Omega}} \to \hat{\boldsymbol{\Omega}}_1, E \to E_1) \int_0^{a_S(\boldsymbol{x}_n, \hat{\boldsymbol{\Omega}}_1)} \exp\Big(-\ell(\boldsymbol{x}_n, \boldsymbol{x}_n + a\hat{\boldsymbol{\Omega}}_1)\Big) \\ &\times \mathcal{S}(\boldsymbol{x}_n + a\hat{\boldsymbol{\Omega}}_1, \hat{\boldsymbol{\Omega}}_1, E_1, w, \boldsymbol{p}_4)\Psi_0^\beta(\boldsymbol{p}_4) da dE_1 d\Omega_1,\end{aligned} \tag{211a}$$

or

$$\begin{aligned}X_{2,5}^{\text{partial},n} = &\int_{\hat{\boldsymbol{\Omega}}_1 \in \left\{\hat{\boldsymbol{\Omega}}_{DX}^{\text{outside},n}\right\}} \int_0^\infty f(\boldsymbol{x}, \hat{\boldsymbol{\Omega}} \to \hat{\boldsymbol{\Omega}}_1, E \to E_1) \int_0^{a_S(\boldsymbol{x}_n, \hat{\boldsymbol{\Omega}}_1)} \exp\Big(-\ell(\boldsymbol{x}_n, \boldsymbol{x}_n + a\hat{\boldsymbol{\Omega}}_1)\Big) \\ &\times \mathcal{S}(\boldsymbol{x}_n + a\hat{\boldsymbol{\Omega}}_1, \hat{\boldsymbol{\Omega}}_1, E_1, w, \boldsymbol{p}_4)\Psi_0^\beta(\boldsymbol{p}_4) da dE_1 d\Omega_1,\end{aligned} \tag{211b}$$

where $\boldsymbol{x}_n = \boldsymbol{x}_{n-1} + a_S(\boldsymbol{x}_{n-1}, \hat{\boldsymbol{\Omega}}_1)\hat{\boldsymbol{\Omega}}_1$ and $\boldsymbol{x}_0 = \boldsymbol{x}$. Unfolding the recursive dependency using Eq. 211, the case of the cell before the base case becomes

$$\begin{aligned}X_{2,5}^{\text{partial},n-1} = &\int_{\hat{\boldsymbol{\Omega}}_1 \in \left\{\hat{\boldsymbol{\Omega}}_{DX}^{\text{inside},n}\right\}} \int_0^\infty f(\boldsymbol{x}, \hat{\boldsymbol{\Omega}} \to \hat{\boldsymbol{\Omega}}_1, E \to E_1) \\ &\times \int_0^{a_S(\boldsymbol{x}_{n-1}, \hat{\boldsymbol{\Omega}}_1)} \exp\Big(-\ell(\boldsymbol{x}_{n-1}, \boldsymbol{x}_{n-1} + a\hat{\boldsymbol{\Omega}}_1)\Big) \\ &\times \mathcal{S}(\boldsymbol{x}_{n-1} + a\hat{\boldsymbol{\Omega}}_1, \hat{\boldsymbol{\Omega}}_1, E_1, w, \boldsymbol{p}_4)\Psi_0^\beta(\boldsymbol{p}_4) da dE_1 d\Omega_1 \\ &+ \int_{\hat{\boldsymbol{\Omega}}_1 \in \left\{\hat{\boldsymbol{\Omega}}_{DX}^{\text{outside},n}\right\}} \int_0^\infty f(\boldsymbol{x}, \hat{\boldsymbol{\Omega}} \to \hat{\boldsymbol{\Omega}}_1, E \to E_1) \exp(-\ell(\boldsymbol{x}_{n-1}, \boldsymbol{x}_n)) \\ &\times \int_0^{a_S(\boldsymbol{x}_n, \hat{\boldsymbol{\Omega}}_1)} \exp\Big(-\ell(\boldsymbol{x}_n, \boldsymbol{x}_n + a\hat{\boldsymbol{\Omega}}_1)\Big) \\ &\times \Big[\mathcal{K}_A(\boldsymbol{x}_n + a\hat{\boldsymbol{\Omega}}_1, \hat{\boldsymbol{\Omega}}_1, E_1, w, \boldsymbol{p}_2)\bar{s}_A(\boldsymbol{x}_n + a\hat{\boldsymbol{\Omega}}_1, \hat{\boldsymbol{\Omega}}_1, E_1, w) \\ &+ \mathcal{K}_E'(\boldsymbol{x}_n + a\hat{\boldsymbol{\Omega}}_1, \hat{\boldsymbol{\Omega}}_1, E_1, w, \boldsymbol{p}_3)\Big(\bar{s}_E(\boldsymbol{x}_n + a\hat{\boldsymbol{\Omega}}_1, \hat{\boldsymbol{\Omega}}_1, E_1, w) + \Psi_0^\alpha(\boldsymbol{p}_3)\Big) \\ &+ \mathcal{S}(\boldsymbol{x}_n + a\hat{\boldsymbol{\Omega}}_1, \hat{\boldsymbol{\Omega}}_1, E_1, w, \boldsymbol{p}_4)\Big(\bar{s}_S(\boldsymbol{x}_n + a\hat{\boldsymbol{\Omega}}_1, \hat{\boldsymbol{\Omega}}_1, E_1, w) + \Psi_0^\beta(\boldsymbol{p}_4)\Big)\Big] da dE_1 d\Omega_1.\end{aligned} \tag{212}$$

Applying Eq. 118 and the definition of the surface-crossing operator to the second term, Eq. 212 may be reduced to

$$\begin{aligned}X_{2,5}^{\text{partial},n-1} = &\int_{\hat{\boldsymbol{\Omega}}_1 \in \left\{\hat{\boldsymbol{\Omega}}_{DX}^{\text{inside},n}\right\}} \int_0^\infty f(\boldsymbol{x}, \hat{\boldsymbol{\Omega}} \to \hat{\boldsymbol{\Omega}}_1, E \to E_1) \\ &\times \int_0^{a_S(\boldsymbol{x}_{n-1}, \hat{\boldsymbol{\Omega}}_1)} \exp\Big(-\ell(\boldsymbol{x}_{n-1}, \boldsymbol{x}_{n-1} + a\hat{\boldsymbol{\Omega}}_1)\Big) \\ &\times \mathcal{S}(\boldsymbol{x}_{n-1} + a\hat{\boldsymbol{\Omega}}_1, \hat{\boldsymbol{\Omega}}_1, E_1, w, \boldsymbol{p}_4)\Psi_0^\beta(\boldsymbol{p}_4) da dE_1 d\Omega_1 \\ &+ \int_{\hat{\boldsymbol{\Omega}}_1 \in \left\{\hat{\boldsymbol{\Omega}}_{DX}^{\text{outside},n}\right\}} \int_0^\infty f(\boldsymbol{x}, \hat{\boldsymbol{\Omega}} \to \hat{\boldsymbol{\Omega}}_1, E \to E_1) \\ &\times \int_0^{a_S(\boldsymbol{x}_{n-1}, \hat{\boldsymbol{\Omega}}_1)} \exp\Big(-\ell(\boldsymbol{x}_{n-1}, \boldsymbol{x}_{n-1} + a\hat{\boldsymbol{\Omega}}_1)\Big) \\ &\times \mathcal{S}(\boldsymbol{x}_{n-1} + a\hat{\boldsymbol{\Omega}}_1, \hat{\boldsymbol{\Omega}}_1, E_1, w, \boldsymbol{p}_4)\Psi_0^\beta(\boldsymbol{p}_4) da dE_1 d\Omega_1.\end{aligned} \tag{213}$$

Combining the integrals over angle yields

$$
\begin{aligned}
X_{2,5}^{\text{partial},n-1} = \int_{\hat{\boldsymbol{\Omega}}_1 \in \left\{\hat{\boldsymbol{\Omega}}_{DX}^{\text{outside},n-1}\right\}} \int_0^\infty & f(\boldsymbol{x}, \hat{\boldsymbol{\Omega}} \to \hat{\boldsymbol{\Omega}}_1, E \to E_1) \\
\times \int_0^{a_S(\boldsymbol{x}_{n-1}, \hat{\boldsymbol{\Omega}}_1)} & \exp\Big(-\ell(\boldsymbol{x}_{n-1}, \boldsymbol{x}_{n-1} + a\hat{\boldsymbol{\Omega}}_1)\Big) \\
\times\, & \mathcal{S}(\boldsymbol{x}_{n-1} + a\hat{\boldsymbol{\Omega}}_1, \hat{\boldsymbol{\Omega}}_1, E_1, w, \boldsymbol{p}_4)\Psi_0^\beta(\boldsymbol{p}_4) da dE_1 d\Omega_1.
\end{aligned}
\tag{214}
$$

Note that $\{\hat{\boldsymbol{\Omega}}_{DX}^{\text{inside},n}\}$ may be empty, in which case the step from Eq. 213 to Eq. 214 is unaffected. The unfolding of the recursion shown in Eqs. 212–214 is repeated to the case of the first cell considered, proving Eq. 135.